

Aus der Klinik und Poliklinik für  
Orthopädie, Physikalische Medizin und Rehabilitation

Klinik der Ludwig-Maximilians-Universität München

Direktor: Prof. Dr. med. Dipl.-Ing. Volkmar Jansson

**Evaluation of the initial fixation, stress distribution and  
revision of short stem hip arthroplasty: A biomechanical  
study and finite element analysis**

Dissertation

zum Erwerb des Doktorgrades der Medizin  
an der Medizinischen Fakultät der  
Ludwig-Maximilians-Universität zu München

vorgelegt von

Shuanggen Yan

aus

Wuhu

Jahr

2019

**Mit Genehmigung der Medizinischen Fakultät  
der Universität München**

Berichterstatter: Prof. Dr. med. Dipl.-Ing. Volkmar Jansson

Mitberichterstatter: Prof. Dr. Rainer Burgkart  
PD. Dr. Hermann Anetzberger  
PD. Dr. Elias Volkmer

Mitbetreuung durch die  
promovierten Mitarbeiter: PD. Dr. med. Florian Schmidutz, MD, M.Sc.  
Dr. techn. Yan Chevalier

Dekan: Prof. Dr. med. dent. Reinhard Hickel

Tag der mündlichen Prüfung: 17.01. 2019

*To my family*

# Eidesstattliche Versicherung

Yan Shuanggen

---

Name, Vorname

Ich erkläre hiermit an Eides statt,

dass ich die vorliegende Dissertation mit dem Thema

**Evaluation of the initial fixation, stress distribution and revision of short stem hip arthroplasty: A biomechanical study and finite element analysis**

selbständig verfasst, mich außer der angegebenen keiner weiteren Hilfsmittel bedient und alle Erkenntnisse, die aus dem Schrifttum ganz oder annähernd übernommen sind, als solche kenntlich gemacht und nach ihrer Herkunft unter Bezeichnung der Fundstelle einzeln nachgewiesen habe.

Ich erkläre des Weiteren, dass die hier vorgelegte Dissertation nicht in gleicher oder in ähnlicher Form bei einer anderen Stelle zur Erlangung eines akademischen Grades eingereicht wurde.

26.09.2017 München

Shuanggen Yan

---

Ort, Datum

---

Unterschrift Doktorandin/Doktorand

# Table of Contents

<b>1. Introduction .....</b>	<b>1</b>
1.1. Anatomy of the hip joint.....	1
1.2. Osteoarthritis of the hip joint.....	2
1.3. Hip arthroplasty .....	3
1.3.1. Structure of a hip endoprosthesis.....	4
1.3.2. Cemented and Cementless THA.....	5
1.3.3. Conventional and short cementless femoral implants .....	7
1.3.4. Revision total hip arthroplasty .....	10
1.4. Osseous integration of cementless THA.....	12
1.4.1. Primary stability of hip prostheses.....	12
1.4.2. Secondary stability of hip prostheses.....	13
1.5. Load transfer and stress shielding of cementless THA.....	14
1.6. Finite element analysis of total hip arthroplasty.....	18
1.6.1. Primary stability measuring in FEA .....	18
1.6.2. Secondary stability measuring in FEA .....	19
1.6.3. Stress distribution studies of FEA.....	19
<b>2. Aim of the study .....</b>	<b>21</b>
<b>3. Materials and methods .....</b>	<b>22</b>
3.1. Micromotion setup.....	22
3.1.1. Specimen.....	22
3.1.2. Metha short stem prosthesis.....	22
3.1.3. CLS standard stem prosthesis .....	24
3.1.4. Specimen preparation.....	25
3.1.5. Loading procedure .....	27
3.1.6. Measurement of the primary stability under dynamic loading .....	28
3.1.7. Study design of revising SHA with standard THA.....	29
3.1.8. Primary setting (Metha and CLS stem) .....	31
3.1.9. Revision setting (Metha revised by a CLS stem).....	31
3.2. Finite Element Analysis.....	32
3.2.1. CT scanning and 3D model generation.....	33

3.2.2.	Alignment of the Hip Stems .....	34
3.2.3.	Material Properties Assignment.....	35
3.2.4.	Boundary Conditions .....	36
3.2.5.	Calculation of relative interface displacements and stress distribution.....	36
3.3.	Data analysis .....	38
3.4.	Statistics.....	38
<b>4.</b>	<b>Results .....</b>	<b>40</b>
4.1.	Results of biomechanical 3D-Micromotion study.....	40
4.1.1.	Primary setting (Metha short and CLS standard stems) .....	40
4.1.2.	3D-Micromotions in the Revision setting (Metha revised by a CLS stem).....	42
4.2.	Results of FEA study .....	44
4.2.1.	3D relative displacement in the FEA models of primary SHA and THA .....	45
4.2.2.	Comparison of primary stability between FEA and biomechanical setting .....	46
4.2.3.	Cortical stress distribution patterns of native and implanted femurs.....	48
<b>5.</b>	<b>Discussion.....</b>	<b>53</b>
5.1.	3D-Micromotion .....	53
5.2.	FEA study .....	60
5.3.	Comparison of the FE analysis and biomechanical study .....	65
<b>6.</b>	<b>Conclusion.....</b>	<b>67</b>
<b>7.</b>	<b>Summary .....</b>	<b>68</b>
<b>8.</b>	<b>Zusammenfassung.....</b>	<b>70</b>
<b>9.</b>	<b>References .....</b>	<b>72</b>
<b>10.</b>	<b>List of figures .....</b>	<b>90</b>
<b>11.</b>	<b>Abbreviations.....</b>	<b>92</b>
<b>12.</b>	<b>Curriculum Vitae .....</b>	<b>93</b>
<b>13.</b>	<b>Publication .....</b>	<b>95</b>
<b>14.</b>	<b>Acknowledgment.....</b>	<b>96</b>

# 1. Introduction

## 1.1. Anatomy of the hip joint

The hip joint is a spheroidal synovial articulation, formed between the leg and lateral part of the pelvis called acetabulum. The acetabulum is composed of the ilium, ischium, and pubis. The head of the femur is ball-shaped and fits into the acetabulum. In the healthy hip joint, there is a durable layer of articular cartilage between the femoral head and acetabulum, providing a smooth movement and facilitating the transmission of loads with a low friction (Sophia Fox 2009) (Fig. 1).

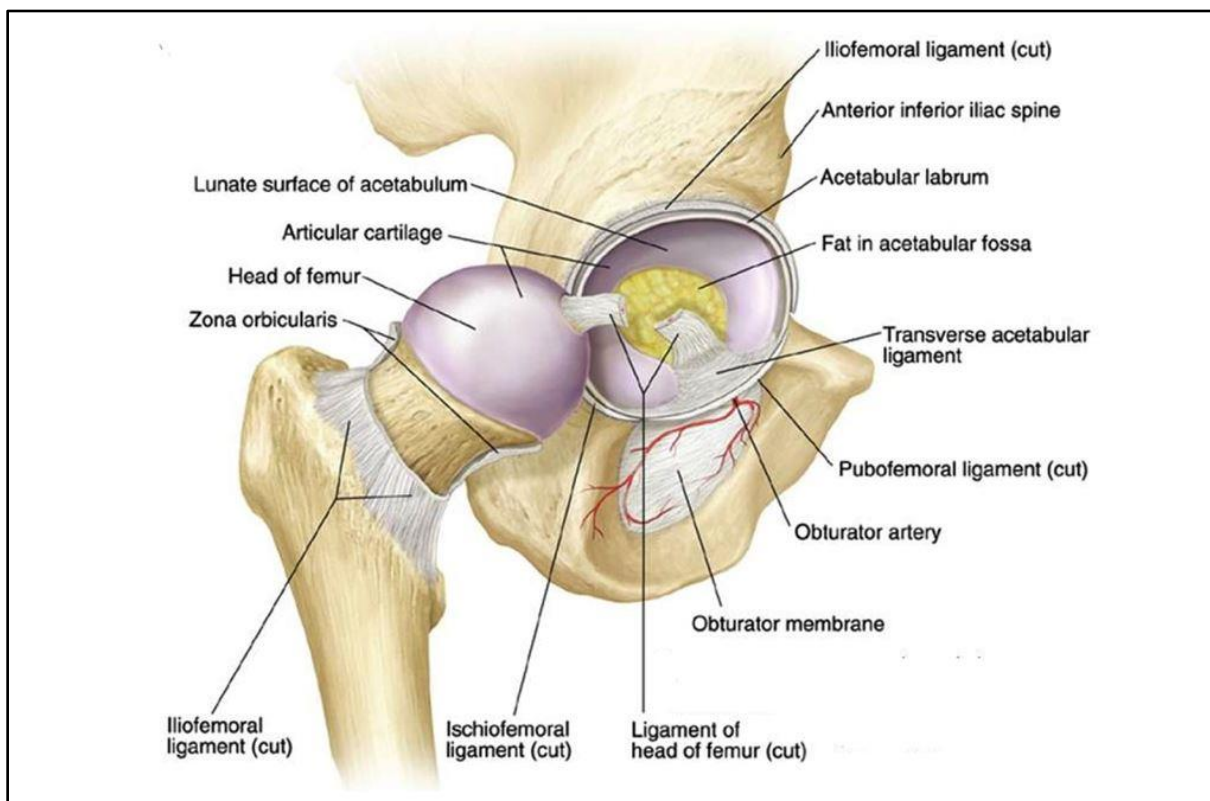


Fig. 1: Schematic drawing of a healthy hip joint (Singh n.d.-a)

Ligaments around the hip, including the iliofemoral, pubofemoral, and ischiofemoral ligaments, connect the ball to the socket and strongly stabilize the joint (Whittle 2003, Claes 2011) (Fig. 2). The joint capsule, consisting of the fibrous membrane and synovial membrane, encloses the femoral head and most of its neck permitting the hip joint to have a high range of movement (SchüNke 2015). The motion of the hip joint is enabled by multiple muscles, which are mainly categorized as gluteal, adductor, iliopsoas, and lateral rotator according to the movement they mediate.

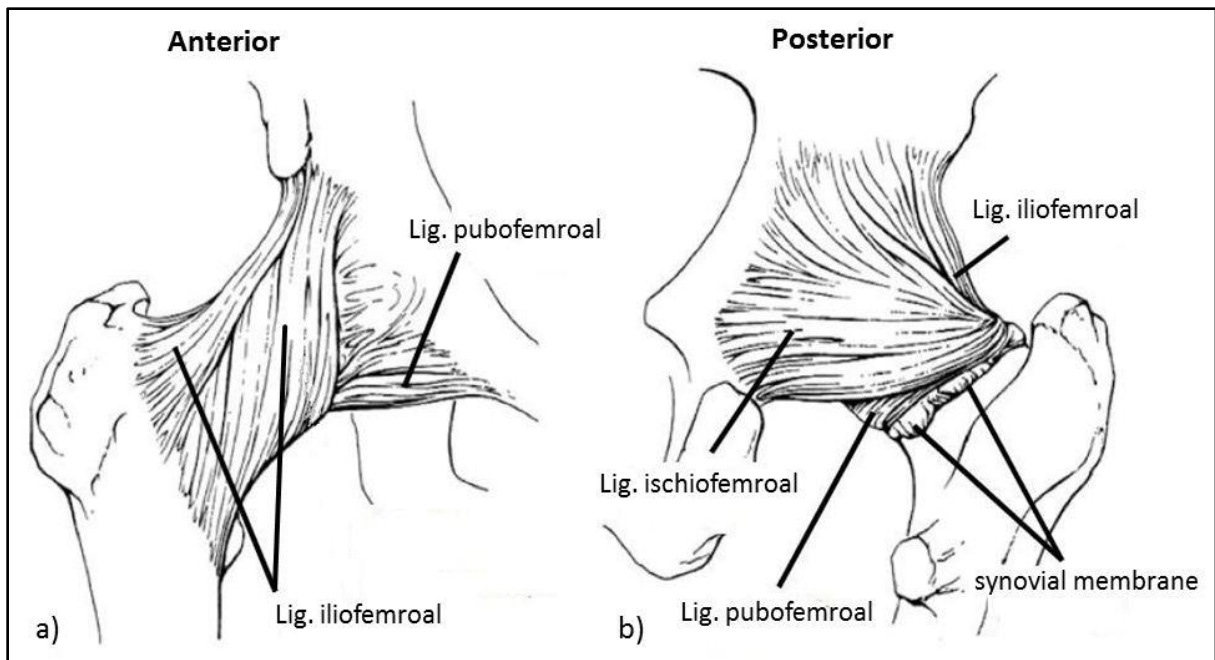


Fig. 2: Schematic drawing of the ligaments around the hip joint (Claes 2011):

- a) Anterior view
- b) Posterior view

## 1.2. Osteoarthritis of the hip joint

Osteoarthritis is the most common chronic joint disease and starts with progressive cartilage degradation. It finally results in the exposure of subchondral bone (Sharma 2013) and also involves the neighboring structures such as bone and muscles (Rasch 2007). It is associated with a narrowed joint space, osteophytes, bone cysts and subchondral sclerosis (Fig. 3). Bone-on-bone friction impairs the function of the hip and the daily living due to hip pain, swelling, and stiffness (Tsertsvadze 2014). Managing the daily living and continuing the lifestyle can be greatly affected by the osteoarthritis of hip (Salaffi 2005, Peeters 2016). Worldwide, osteoarthritis is the most common type of joint disorder and leads to more disabilities than any other diseases in the aged population (Woolf 2012).



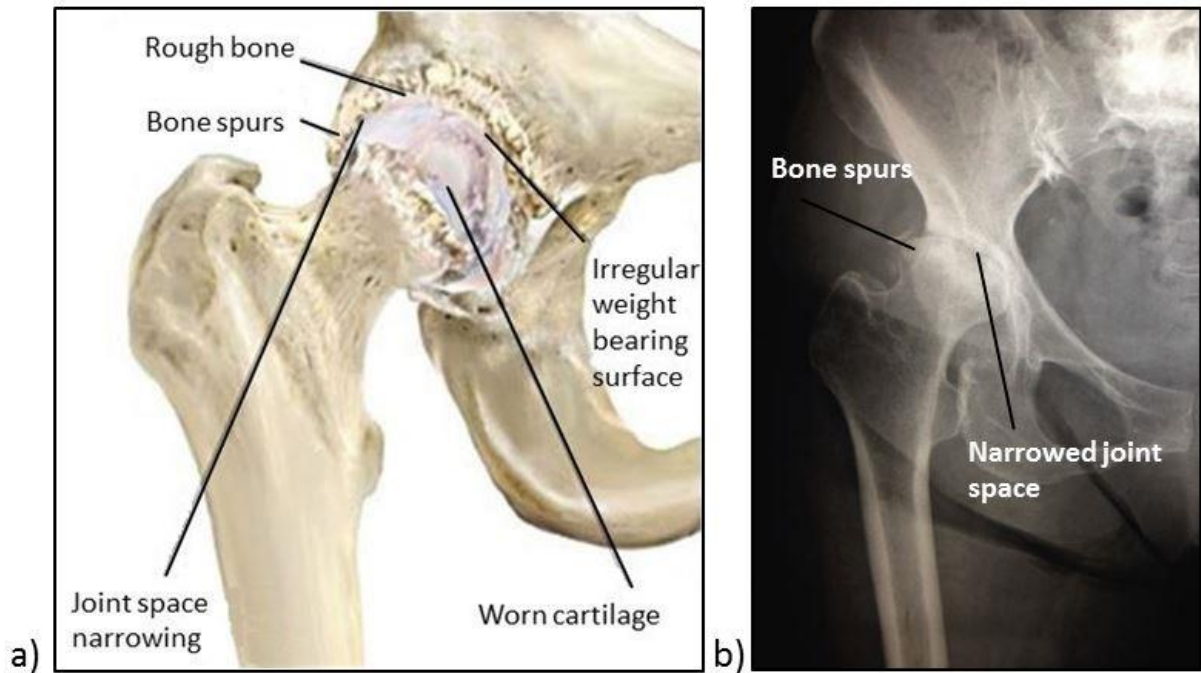


Fig. 3: Graphical illustration of hip joint arthritis:

- a) Schematic drawing (Singh n.d.-b)
- b) Clinical X-ray (Homma 2014)

### 1.3. Hip arthroplasty

Hip arthroplasty is an intervention which replaces a destroyed hip joint by a prosthetic device. Different methods of hip replacement exist and it can be either performed as hemiarthroplasty or total hip arthroplasty (THA). Hemiarthroplasty only replaces the femoral part with a femoral stem and a femoral head, whereas THA replaces both the femoral and acetabular sides with a femoral stem, a femoral head, and an acetabular cup. Hip arthroplasty has developed into an integral part of orthopedics and is one of the most frequent surgical procedures performed in Germany. The number of primary hip replacement procedures in Germany reaches more than 200,000 per year. Besides, hip revision surgery accounts for about 35,000 per year, indicating a high socio-economic impact of this procedure (Statistisches Bundesamt 2005 to 2015) (Fig. 4).

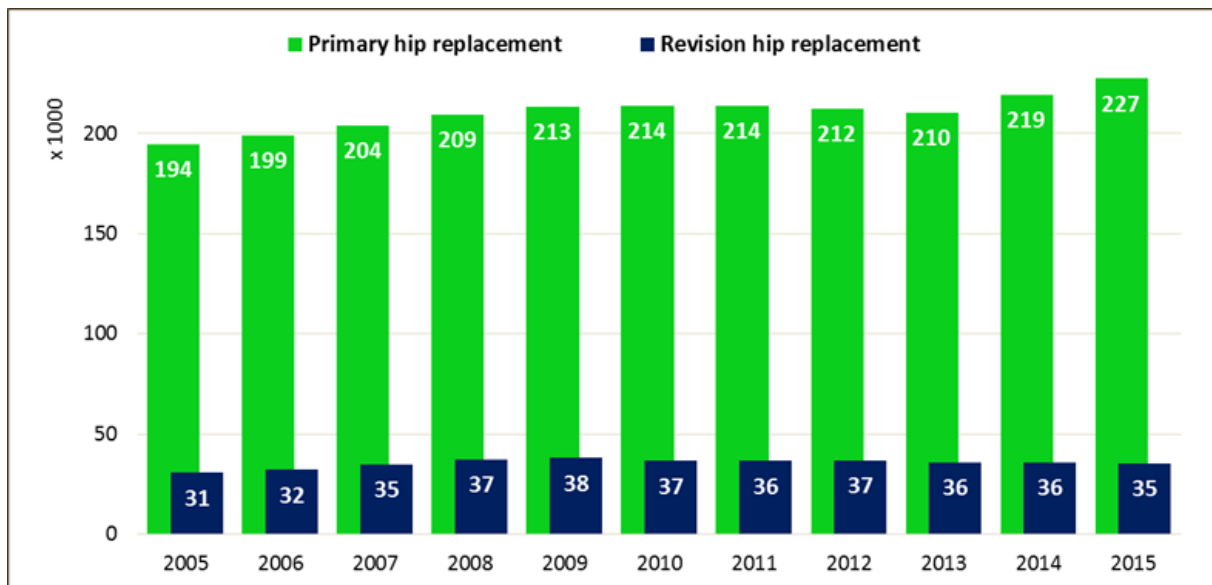


Fig. 4: Number of primary and revision hip replacements in Germany (Statistisches Bundesamt 2005 to 2015)

### 1.3.1. Structure of a hip endoprosthesis

The standard total hip endoprosthesis includes the femoral stem, femoral head, liner (inlay) and acetabular shell (Fig. 5). The femoral stem and head can be either a monoblock or modular in design. In the monoblock design the femoral stem and head merge, while in the modular design, the femoral head is independent and attaches to the stem by a neck adapter. The acetabular part is also either a monoblock design with a one-piece construct, or a modular design including a shell fixed to the pelvis and a separate liner located inside the shell. Thus the inner surface of the liner (polyethylene, ceramic or metal) and the femoral head (metal or ceramic) constitute the bearing surface of the artificial joint.

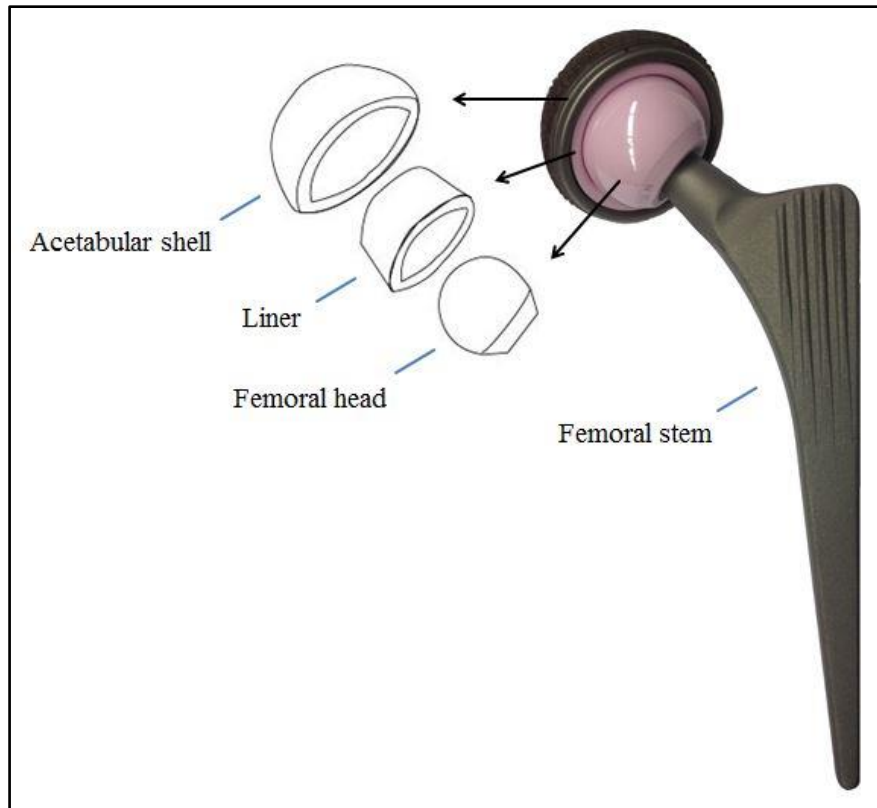


Fig. 5: Modular structure of a standard hip joint endoprosthesis

### 1.3.2. Cemented and Cementless THA

THA has developed over the recent decades to one of the most reliable and successful orthopedic surgeries in advanced stage osteoarthritis or other hip pathologies (Liang 1986, Jonsson and Larsson 1991). This procedure can significantly reduce pain and improve the functional status in patients with serious hip osteoarthritis. It dramatically improves the quality of life of patients (Mcguigan 1995, Ritter 1995, Rissanen 1995) and 85% of patients with THA can expect to have a pain-free function of the hip over a period of 20 years (Schulte 1993).

In the procedure of hip arthroplasty, the hip endoprosthesis must be stably fixed in the bone of a patient. Fixation is obtained by two major fixation methods: cemented and cementless prostheses (Fig. 6). Cemented joint prosthesis uses polymethylmethacrylate (PMMA), a so-called fast-drying “bone cement”, to quickly establish a solid attachment. Polymethylmethacrylate (PMMA) was first introduced by Dr. John Charnley in 1961 (Charnley 1961) and is still widely used for implant fixation (Vaishya 2013).

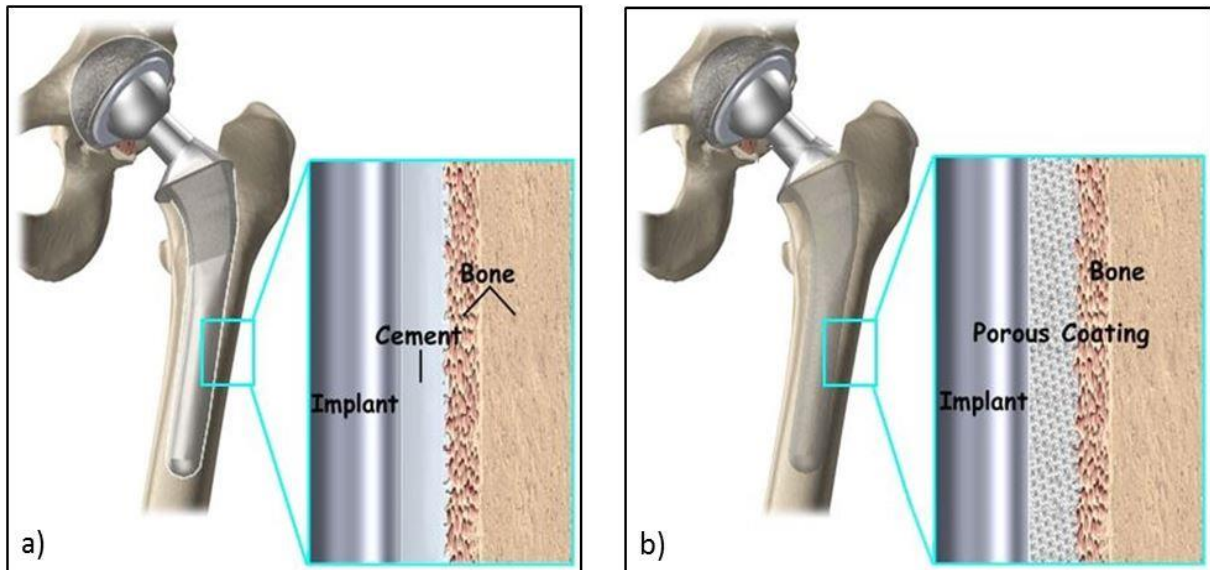


Fig. 6: Graphical illustration (Eorthopod n.d.):

a) Cemented THA (cement = PMMA)

b) Cementless THA which relies on the bone integration of implant

Recently, the cementless joint prosthesis has gained increasing popularity and requires osseous integration to the surface of implant, thus forming a solid attachment over time. Cementless THA has increasingly being used as a fixation method. The cementless femoral stem is typically made from the titanium with various shapes and surfaces. The acquisition of cementless fixation is achieved by the press fitting for the primary stability and by the osseous integration for the secondary stability. The implant surface is commonly roughened by a coating of hydroxyapatite (HA) to stimulate and allow the bone ingrowth. The coating is carried out by osteoinductive and osteoconductive materials, such as titanium alloy or hydroxyapatite. A coated stem design is demonstrated to yield higher osteoconductivity and bone ingrowth rate (Soballe 1990, Soballe 1992).

Furthermore, the combination of cemented and cementless implants e.g. combining a cemented femoral stem and a cementless acetabular shell is possible, and is labelled as hybrid prosthesis. Previous studies have shown an excellent and reliable survival rate of cemented implants in the long-term follow-up (Carstens and Lu 1990, Wroblewski 2007). Similarly, modern cementless fixation concept has shown a comparable survival rate (Hooper 2009, Kim 2011).

The choice of implant fixation in THA with or without cement has been a subject of much controversy. Some authors indicated that the short-term clinical and functional outcomes of cemented femoral fixation might be better than those of cementless femoral fixation. While as

for the long-term follow-up, no significant difference was found between cemented and cementless groups in terms of the survivorship identified by the revision rate, mortality or the complication rate (Ni 2005, Abdulkarim 2013). So far, there is no consensus allowing definitive statement which type of the implant fixation is superior. The optimal type of femoral component depends on the diverse issues such as the patient's age, bone quality, surgical procedures and the surgeon's preference.

### 1.3.3. Conventional and short cementless femoral implants

Recently, another type of implant, the so-called short stem implant, has gained increasing popularity. Such short stem implants hold a shorter stem than the standard stem implants and are supposed to conserve the femoral bone stock and to provide a more physiological load transfer (Fig. 7).

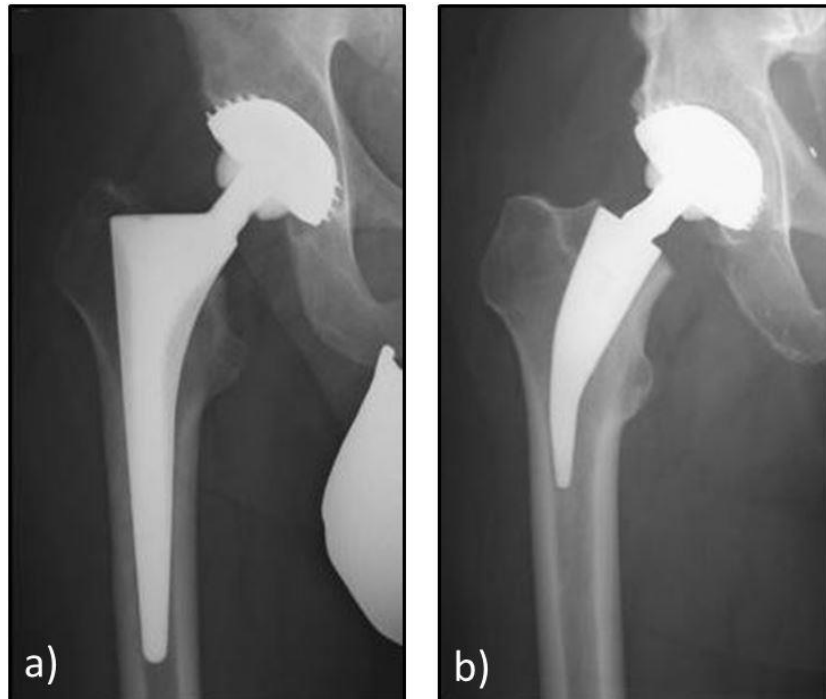


Fig. 7: X-ray images of primary THA (Schmidutz 2012a):

- a) Conventional cementless prosthesis
- b) Short cementless prosthesis

Nevertheless, conventional cementless femoral stems, also called standard stems, provide excellent outcomes reported with long-term follow-up (Bordini 2007, Khanuja 2011) (Fig. 8). Although these conventional implants show excellent results, some undesirable side effects have been observed, such as proximal stress shielding and bone loss in the revision procedures (Brown 2002, Engh 2003, Bugbee 1997, Stukenborg-Colsman 2012).

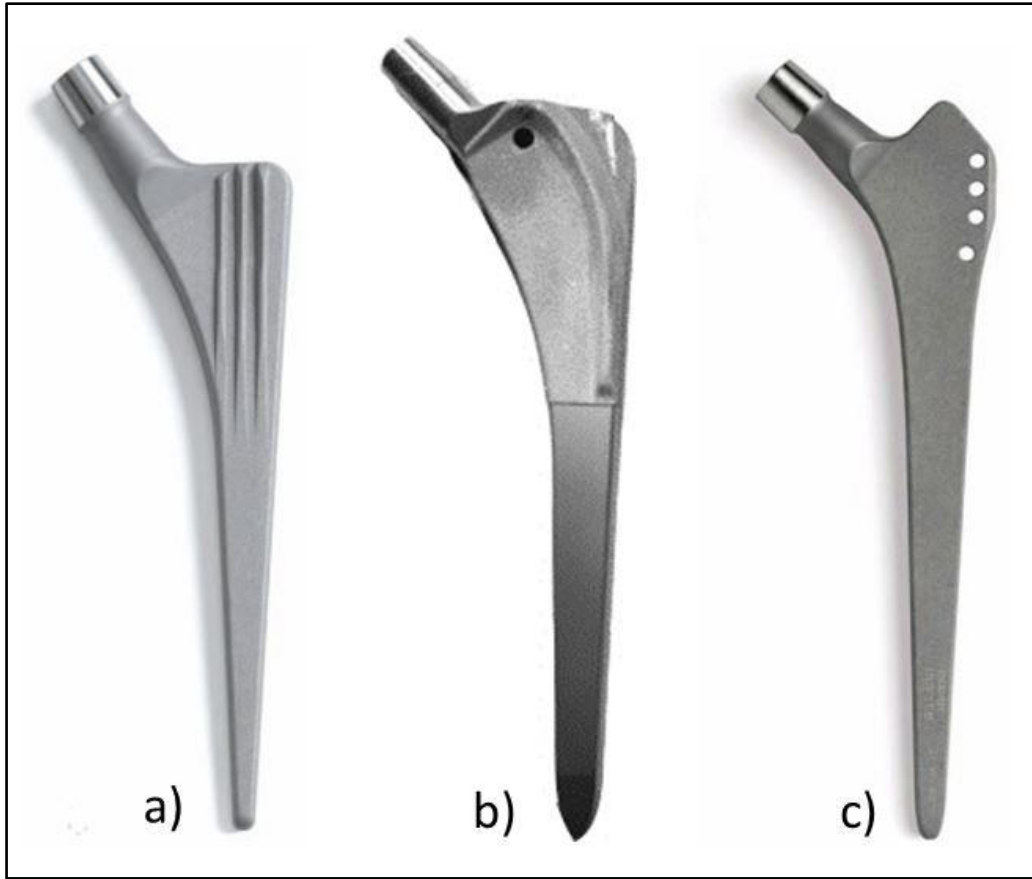


Fig. 8: Examples of the conventional cementless THA stems (Kim and Yoo 2016, Gronewold 2014):

- a) CLS Spotorno stem (Zimmer, USA)
- b) Bicontact stem (Aesculap, Germany)
- c) Zweymüller Alloclassic stem (Zimmer, USA)

The first short stems were already introduced from the 1940s, while the long-term results were not satisfactory due to the high failure rate (Judet and Judet 1950). Since the 1980s the Mayo and CFP prostheses have been introduced in the clinic with the concepts of short-stemmed femoral components. They revealed reliable stem survival in the long-term follow-up (Morrey 1989, Morrey 2000, Pipino 2000, Pipino 2004). A variety of new short stem designs have been introduced, with encouraging clinical results (Khanuja 2014a, Van Oldenrijk 2014) (Fig. 9). These short stems intend to offer a stable metaphyseal or meta-diaphyseal fixation, which is supposed as one of the requirements for physiological load transfer (Chen 2009, Mazoochian 2007, Ghera and Pavan 2009). The concept might offer advantage such as minimizing perioperative soft tissue and bone loss in the greater trochanteric and subtrochanteric region and moreover facilitating the implantation for future revision due to conserved bone stock (Tahim 2012, Falez 2008, Schmidutz 2012b, Khanuja 2011, Morrey 1989).

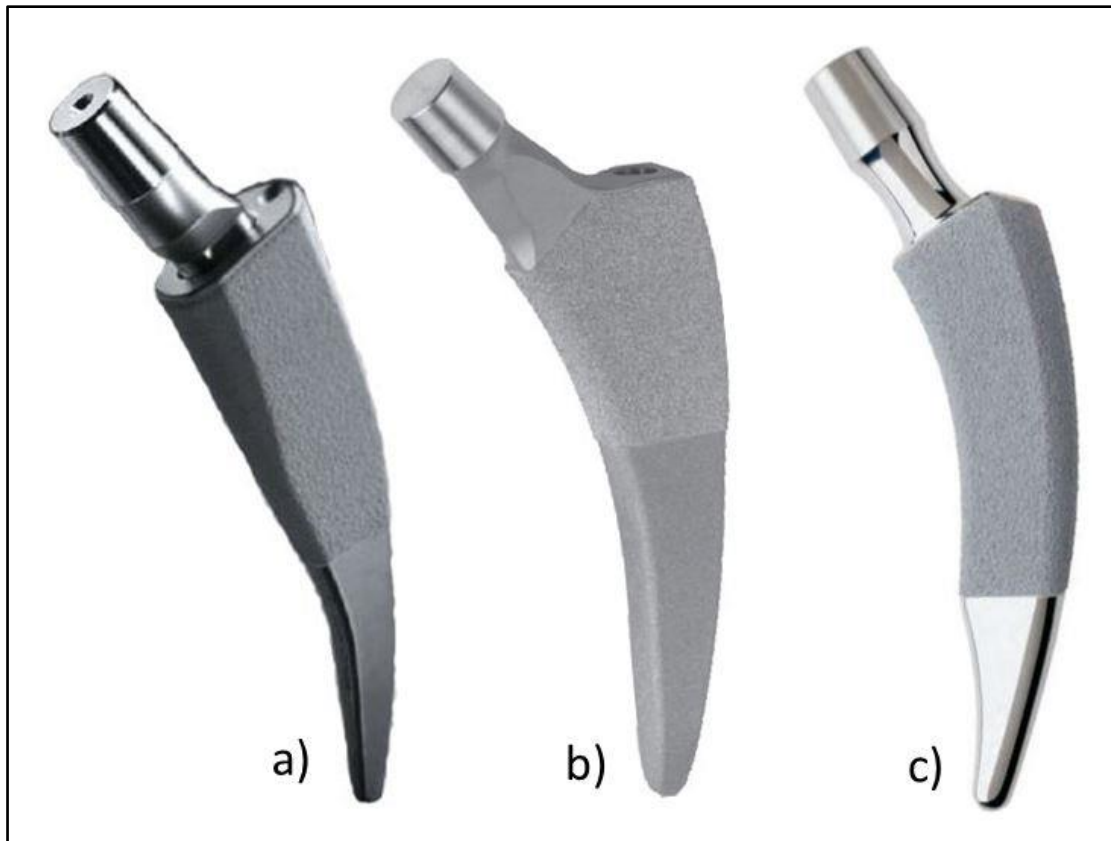


Fig. 9: Examples of short cementless THA stems (Falez 2015):

- a) Metha stem (Aesculap, Germany)
- b) Fitmore stem (Zimmer, USA)
- c) Nanos stem (Smith & Nephew, UK)

However, numerous different designs of short stem total hip arthroplasty (SHA) currently exist. Although they have clear differences in their biomechanical behavior, a clear and uniformly established definition for their classification does not exist. Several classifications have been proposed according to the length of stem (Feyen and Shimmin 2014), the amount of preserved proximal femur (Falez 2015), or the fixation principles and location of proximal loading (Khanuja 2014a). For example, Feyen and Shimmin (Feyen and Shimmin 2014) defined the short stem as the stem with a length less than the twofold distance between the greater trochanter tip and the lesser trochanter base, however, there is no available specific definition on the length of a short stem. Besides, Falez et al. proposed the classification and categorized the SHA into four types (collum, partial collum, trochanter sparing, trochanter harming) according to the amount of preserved proximal femur (Falez 2015) (Fig. 10).



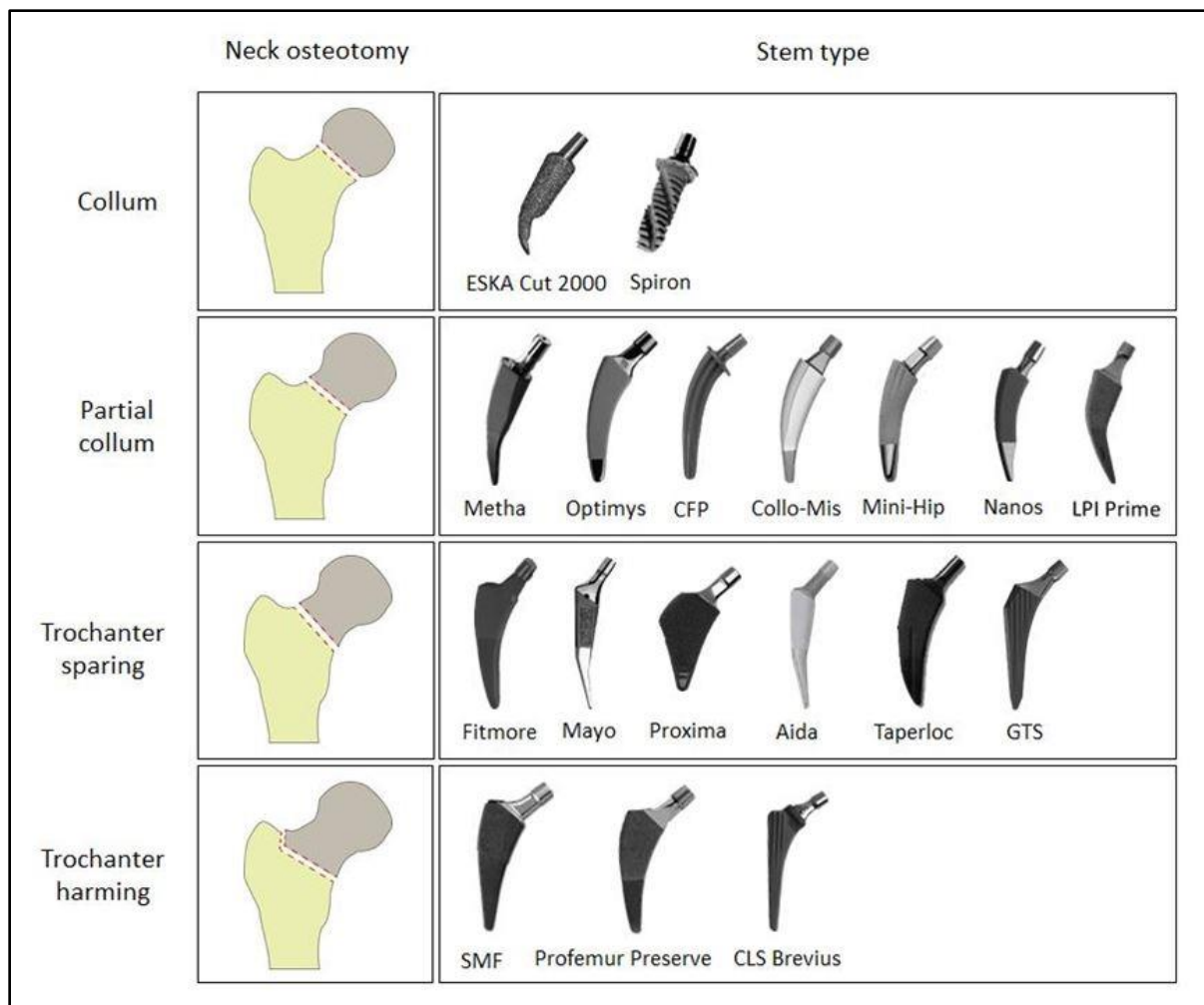


Fig. 10: Classification of the commercially available short stems for THA (Falez 2015)

### 1.3.4. Revision total hip arthroplasty

Although THA is a successful procedure with well-documented survivorship, patients experiencing failures due to various reasons require the revision operations. Revision of a hip prosthesis is performed by either exchanging or removing the partial or entire prosthesis. Aseptic implant loosening has been recognized as the major reason for implant failure, accounting for 71% of the revisions (Herberts and Malchau 2000). Kevin et al. (Bozic 2009) also reported that aseptic loosening and instability were the main reasons for the revision surgery. The cause of aseptic loosening may be biological or mechanical. The main biological cause is osteolysis produced by wear of the mobile components between the acetabular shell and head (Schmalzried and Callaghan 1999). Mechanical causes include loosening due to the stress shielding of bone or the excessive relative movement between bone and implant (Behrens 2008). Further reasons for revisions include infection, wear, dislocation, breakage of



implants or the periprosthetic femoral fracture (Wittenberg 2013).

A systematic review of worldwide registry experiences (Labek 2011) revealed that the revision rate within one year after primary hip arthroplasty was a mean of 1.29%, 6.5% after five years, and 12.9% after ten years. Especially, the Swedish joint arthroplasty register clearly revealed that the revision rate in young patients increased compared to elderly patients (Garellick 2013) (Fig. 11). The most possible reason is the fact that young patients have a greater activity level than old ones, leading to a higher wear and mechanical usage. Besides, the longer length of life makes at least one revision more likely compared to elderly patients. Failure of hip implants is always connected to the bone loss requiring larger implants. The larger components and inevitable soft tissue damage in the revision THA are connected to inferior functions compared to the primary THA.

Stable and long-term fixation in the revision THA for patients with severe bone deficiency is a great challenge for surgeons. Cemented implants were introduced in the revision THA due to the immediate firm fixation, however, the long-term result after revision surgery with cemented stem revealed a high re-revision rate, ranging from 9% to 19% (Kershaw 1991, Amstutz 1982, Gramkow 2001).

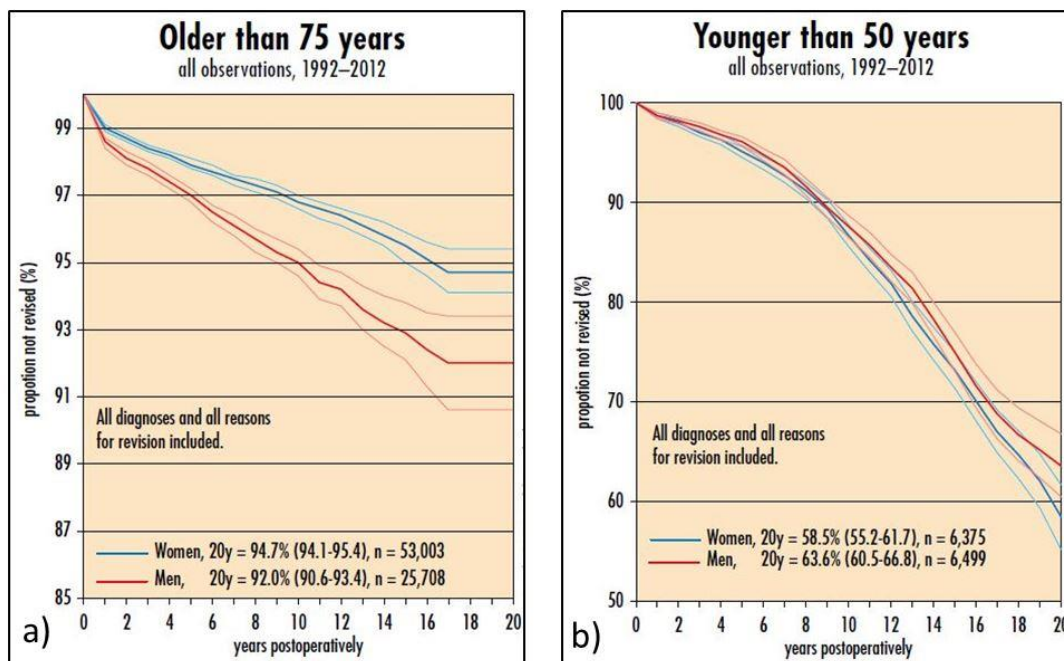


Fig. 11: Difference in the revision rate for patients with different ages (Swedish Hip Arthroplasty Register, Annual Report 2012) (Garellick 2013):

- a) Older than 75 years
- b) Younger than 50 years

Cementless implants have been increasingly used in the revision hip arthroplasty as a promising alternative (Raman 2005, Reikeras and Gundersen 2006, Bohm and Bischof 2001, Tauber and Kidron 2000). Especially the use of cementless implants may be favorable for young patients, who require at least one or several revisions in their lifetime. In contrast, Weiss et al. demonstrated higher survival rates for cemented implant than those for cementless implant in elder patients without severe bone loss. Thus, they recommended the usage of long cemented implants for those patients (Weiss 2011).

#### **1.4. Osseous integration of cementless THA**

The area between bone and an artificial stem is called the bone-implant interface. The bone needs to grow into the stem to archive a firm bondage. This process of osseous integration is the crucial site of a cementless implant, and two main steps can be distinguished.

Initially, primary stability is achieved by the press-fit during operation to guarantee the implant stability in the direct post-operative period. Then, secondary stability or biological fixation is achieved when new bone gradually grows into the bone-metal interface. For a good long-term implant survival, the primary stability needs to be gradually followed with the secondary stabilization process.

##### **1.4.1. Primary stability of hip prostheses**

The primary stability of a prosthetic implant is associated with the early postoperative stage before the starting of the osseous integration. It is crucial for the long-term fixation of a cementless hip arthroplasty. Insufficient primary stability may lead to a fibrous tissue at the bone-implant interface, and consequently causes implant failure or loosening (Mckellop 1991, Pilliar 1986, Jasty 1997). Primary stability can be evaluated by testing the relative movement at the bone-implant interface. The movement is defined as the motion between pairs of points on the surface of implant and the adjacent points on the endosteal bone (Burke 1991) (Fig.12).

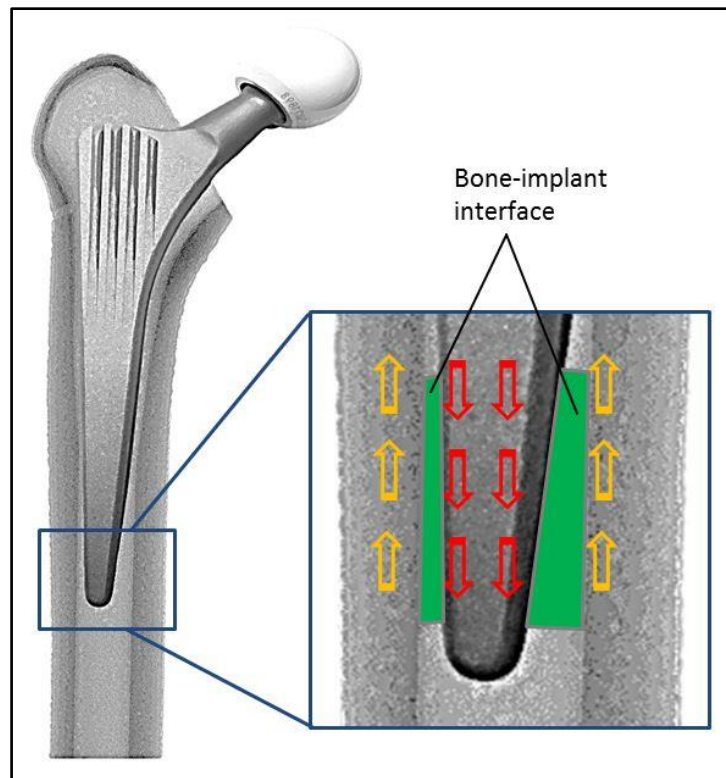


Fig. 12: Illustration of the relative movement of prosthesis at the bone-implant interface

Two different types of motions can be characterized: the reversible movement of the implant under a cycle of loading (termed micromotion) and the irreversible movement of the implant within the femoral canal over time (termed migration) (Buhler 1997).

In order to investigate the primary stability of femoral stem, several measurement methods have been developed, such as micrometers (Whiteside and Easley 1989), extensometers (Engh 1992), LVDT's (Whiteside 1993, Sugiyama 1989), strain-gauge displacement transducers (Mckellop 1991), and optoelectronic tracking device (Nogler 2004). The LVDT called linear variable differential transducer, is an electromechanical transducer converting linear displacement into an electrical signal and is the most widely applied method to determine micromotions. With the development of techniques, three-dimensional (3D) interfacial micromotions can be registered to describe the primary stability (Buhler 1997, Fottner 2009, Chareancholvanich 2002).

#### 1.4.2. Secondary stability of hip prostheses

Secondary stability is referred to the osseous integration of the implant by the living bone and cannot be obtained without sufficient primary stability. A good primary stability is a

prerequisite for the successful osseous integration (Westphal 2006). Both the primary stability and secondary stability are essential for complete osseous integration after implantation.

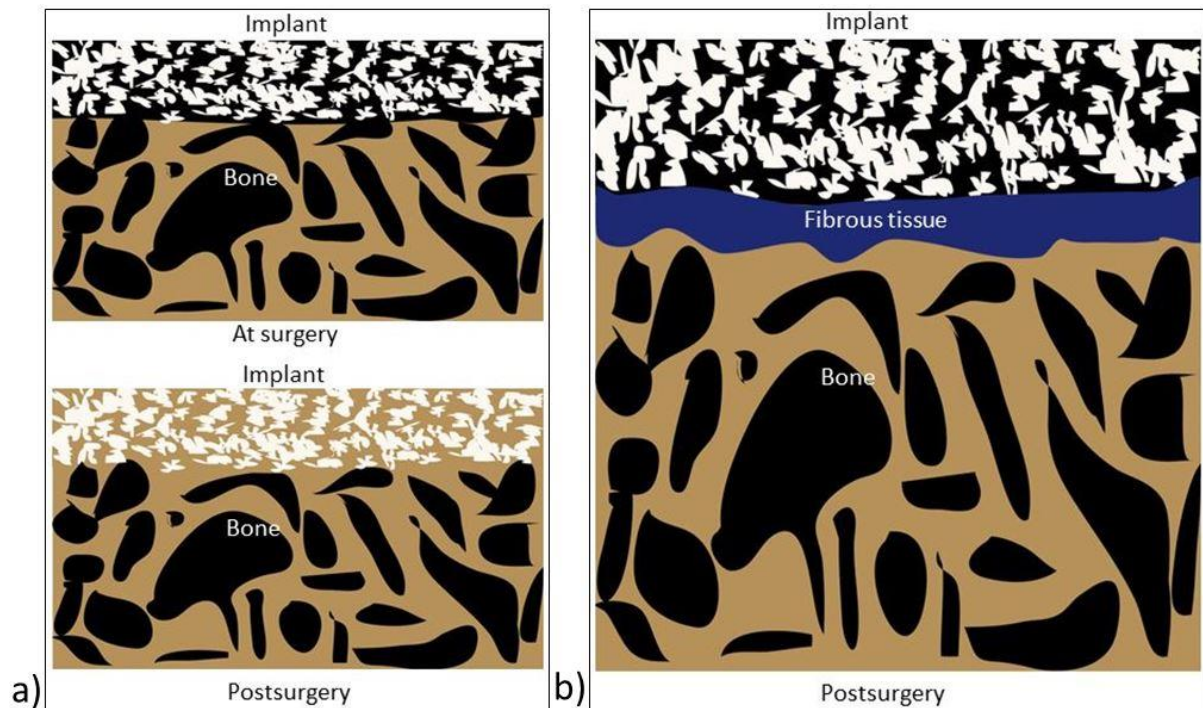


Fig. 13: Schematic drawing of osseous integration:

- a) New bone tissue grows into the porous, coated region of an implant after surgery
- b) Fibrous tissue forms between the bone and implant instead of osseous integration

Small amounts of implant micromotions are required to activate the bone formation on the implant surface. However, excessive implant micromotions will lead to the failure of osseous integration (Isaacson and Jeyapalina 2014) (Fig. 13). The failure of osseous integration will compromise the durable fixation and may lead to failure of the implant in the short- or long-term course. Studies have described that reversible micromotions exceeding 150  $\mu\text{m}$  lead to connective tissue ingrowth (Pilliar 1986, Jasty 1997).

### 1.5. Load transfer and stress shielding of cementless THA

The load applied to the top of the femoral head mainly consists of partial body weight, muscular strength of abductors, and hip contact force (Claes 2011) (Fig. 14).

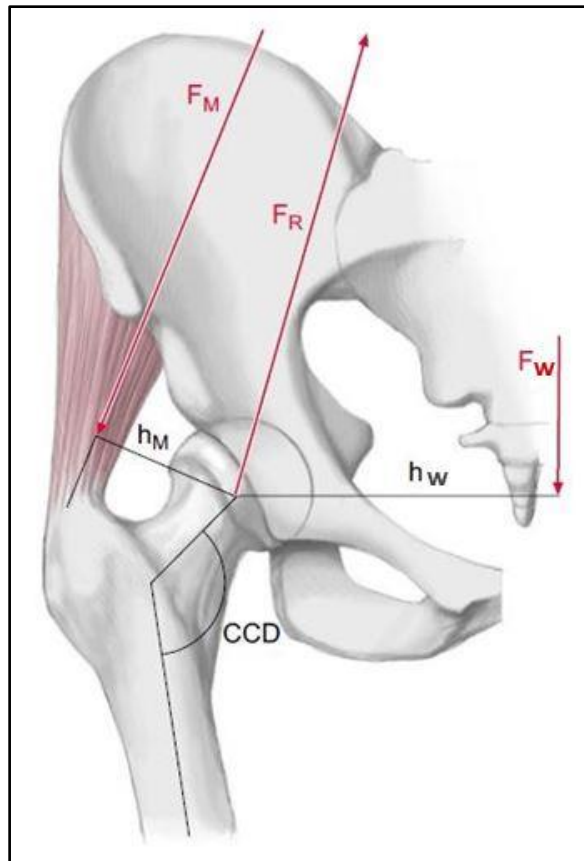


Fig. 14: Schematic drawing of the most important forces on the hip joint (Claes 2011):

- $F_W$ : partial body weight
- $F_M$ : muscular strength of abductors
- $F_R$ : hip contact force
- $h_W$ : level arm of  $F_W$
- $h_M$ : level arm of  $F_M$

In the normal healthy femur, the external load applied on the head is transmitted through the femoral neck and intertrochanteric region to the cortex of proximal femur. This native load transfer pattern will be changed when the femur is implanted with a prosthesis, which is much stiffer than the bone and takes over the majority of the load (Doitpoms 2011). Then the load transferred through the bone is reduced due to a phenomenon known as stress shielding (Fig. 15). Stress shielding refers to a reduced bone mineral density (BMD) resulting from a decreased typical stress in the bone around a prosthesis (Ridzwan 2007) (Fig. 16). According to the Wolff's law, bone develops a structure and remodels in response to the loads that are placed on it. Areas of bone with higher stress will adapt by the increasing bone mass and become thicker and stronger. In contrast, areas of bone with lower stress will adapt by the decreasing bone mass and become weaker and more susceptible to aseptic loosening.

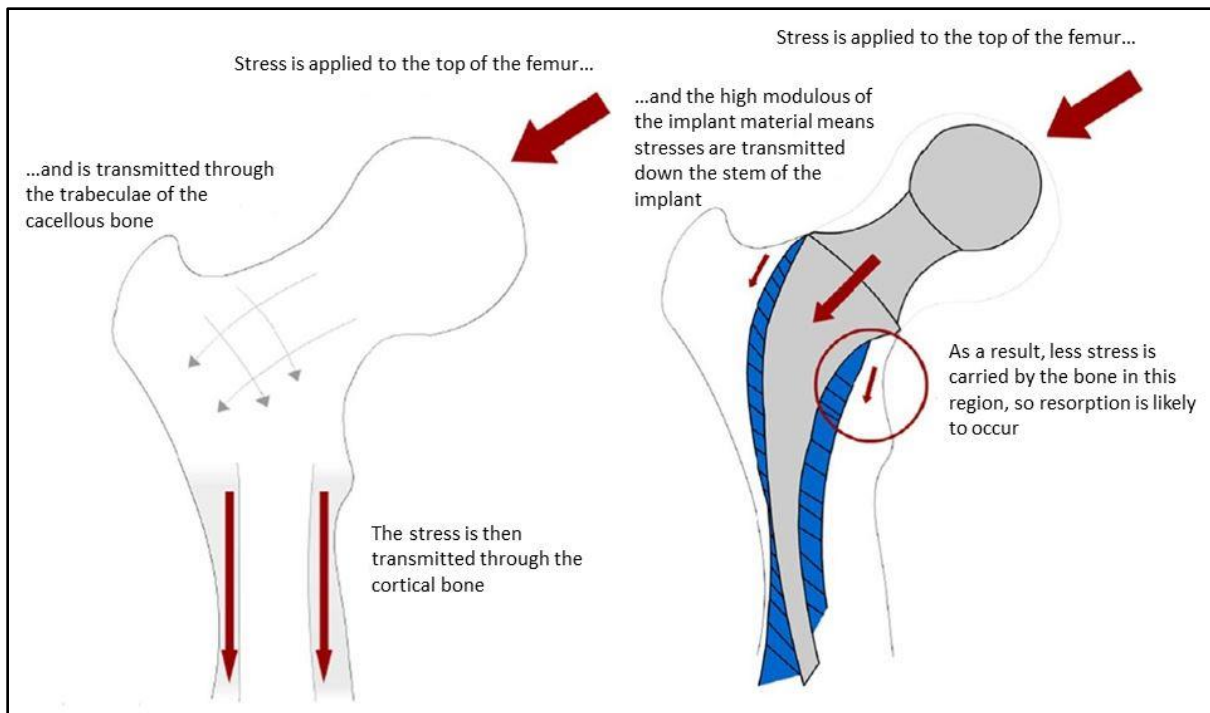


Fig. 15: Simple scheme of the stress shielding (Arifin 2014)

The implant-specific stress shielding depends on the design of the implants, such as material, surface, and geometry (Ruben 2012, Wilkinson 2003, Aamodt 2001). Arno et al. (Arno 2012) demonstrated that as the stem length increased the femurs displayed a typical pattern of reducing proximal strain and increasing distal strain. Chen et al. (Chen 2009) reported that the average bone loss after the insertion of a Mayo (Zimmer, USA) short stem was 3.3% compared to the contralateral native side. Whereas as for the conventional femoral component, the typical bone loss was found 20% (Weinans 1992). In an autopsy retrieval study (Sychterz 2002), an overall decrease in the BMD was 23%, with the most loss adjacent to the proximal third of the standard implant (42.1%) and the least distally (5.5%). Other studies also showed that bone loss in the short stem was less than the conventional stem in the proximal femoral zones (Skoldenberg 2006, Boden 2006).



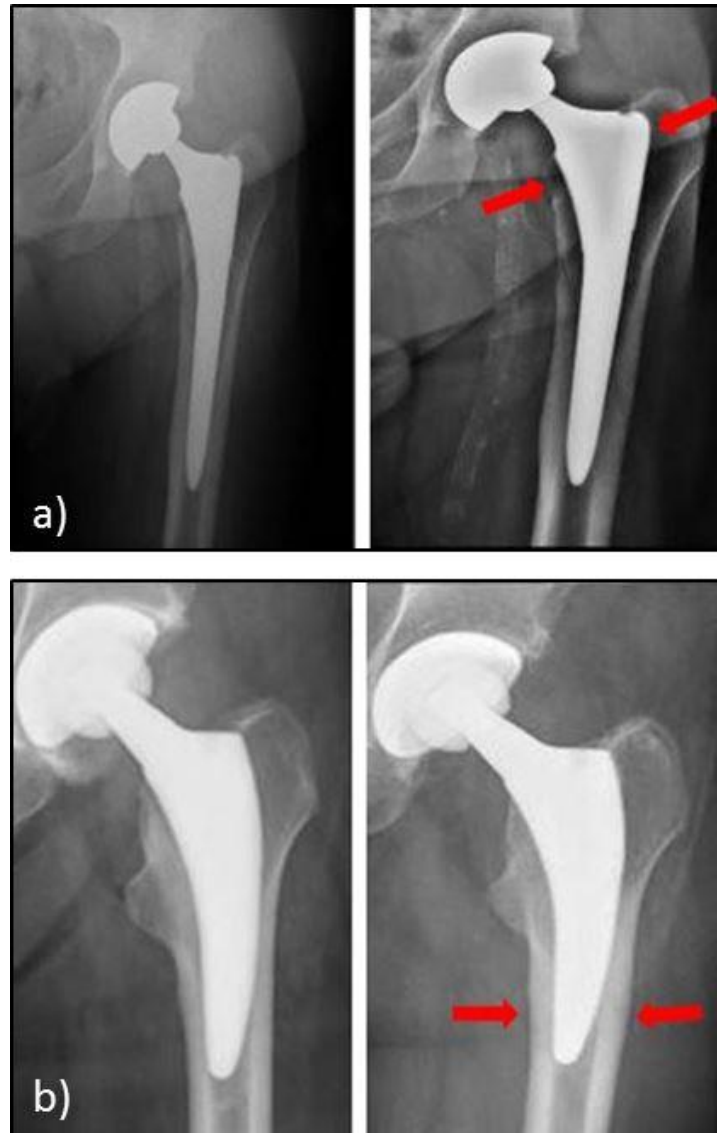


Fig. 16: The X-ray images of THA with cementless stems show stress shielding and bone hypertrophy:

- a) The progression of stress shielding in the proximal femoral region between five years (left) and 15 years after surgery (right) (De Martino 2017)
- b) The progression of cortical hypertrophy between postoperatively (left) and 4 years after surgery (right) (Maier 2015)

Stress shielding can be evaluated experimentally by measuring the cortical strain (Bieger 2012, Gronewold 2014). Schmidutz et al. (Schmidutz 2017) reported an obvious proximal stress shielding of the cementless CLS stem in composite bones. Ralf et al. (Decking 2008) found that the changes in the cortical strain before and after implantation allowed predicting the changes of periprosthetic BMD.

## **1.6. Finite element analysis of total hip arthroplasty**

Apart from traditional methods to measure the stability and stress shielding, computer-based methods have been developed. Finite element analysis (FEA), also termed as finite element method (FEM), is a numerical method for predicting how a product reacts under loading. It is a tool that divides a complex structure into many elements with the advantages of precise representation of targeted geometry, allowing a definition of different material characteristics, easy representation of the total solution and achieving local effects (Reddy 2006).

A finite element (FE) model includes nodes and finite elements that form the finite element mesh and include the material and structural properties. It can be created as one-dimensional, two-dimensional (for example: triangular) or three-dimensional (for example: tetrahedral or hexahedral) models. Types of FEA can vary and contain for example linear statics, linear dynamic and non-linear static. Linear analysis is associated with applied static loads and constraints. Different steps are included in the finite element modeling: modeling of the geometry, mesh, defining of material properties and boundary conditions. The mesh step affects the solution accuracy and convergence. There is a compromise between mesh size and the accuracy due to the time taken to compute the solution.

FEA has been utilized extensively in engineering and physics and recently also in biomechanical and orthopedic studies. With the ongoing improvements in computing resources and numerical modeling methods, it is possible to generate models in three dimensions and analyze them in a semi-automatic fashion (Keyak 1990, Skinner 1994). Finite element modeling of human bone can be generated from medical scanning images using magnetic resonance imaging (MRI) or from computed tomography (CT). Bone material properties can be assigned based on these images (Abdul-Kadir 2008, Reggiani 2008). The accuracy of FEA depends on the appropriate parameters defined, such as contact conditions, contact elements, frictional coefficient, and interface fit (Viceconti 2000, Viceconti 2001, Abdul-Kadir 2008).

### **1.6.1. Primary stability measuring in FEA**

Primary stability has been frequently measured in the biomechanical setting. However, it is limited to some points which can be determined. In contrast, FEA can evaluate the primary stability of cementless stems with the advantages of capturing the full-field map of the interface micromotions and be validated by the results from the biomechanical setting (Dammak 1997, Tarala 2011, Reggiani 2007). However, Hefzy and Singh (Hefzy and Singh



1997) noticed that the credibility of FEA can be established only by comparing its results with experimental data obtained under similar conditions. Reggiani et al. (Reggiani 2007) used FE models to measure the micromotions of cementless femoral stem comparing with experimental results. They showed that the average error on the predicted subject-specific micromotions was only 7% of peak micromotions measured experimentally.

Tarala et al. (Tarala 2011) compared the micromotions at the bone-implant interface between an experiment and FEA. They reported a reduction of the FEA micromotions as the bony reference point moved closer to the implant surface. Whiteside et al. (Whiteside 1993) found that the deflection between the outer bone surface and the implant during loading must contain the elastic bony deformation, apart from the relative motion at the interface.

To the author's knowledge, none of the experimental methods enable to measure three-dimensional (3D)-micromotions directly at the bone-implant interface. In recent studies from our institute (Fottner 2009, Schmidutz 2017), LVDTs were fixed on the outer bone surface, with a remaining distance to the implant caused by the femoral bone. Nevertheless, there were no available studies estimating the contribution of the elastic bony deformation to the deflection between the outer bone surface and the implant.

### **1.6.2. Secondary stability measuring in FEA**

Measuring long-term secondary stability of cementless implants using FEA appears to be useful in the design of hip prostheses. However, unlike the primary stability of implants in THA, the secondary stability has been poorly documented in FEA studies. Orlik et al. (Orlik 2003) conducted an FEA study to investigate secondary stability. They found that frictional coefficient and normal contact stiffness increased several times as the bone grew into the rough surface of the implant, thus providing a more robust interface and fewer micromotions. Viceconti et al. (Viceconti 2004) evaluated the secondary stability using a biomechanical FEA model formulated as rule-based adaptation scheme, assuming that the results from the model were clinically meaningful.

### **1.6.3. Stress distribution studies of FEA**

Besides the evaluation of initial stability, FEA is used to assess local stress distribution in geometrically complex structures. The stress distribution pattern in cemented femoral prostheses has been documented using FEA (Brown 1988, Rohlmann 1987). However, FEA of cementless stems has been reported much less frequently (Huiskes 1987, Rohlmann 1988).

Schileo et al. (Schileo 2007) carried out a study to compare the strains predicted by FEA with those obtained experimentally under different loading conditions. They implemented different density-elasticity relationships in the FEA. The authors found an excellent agreement between FEA and experimental results. Additionally, the density-elasticity relationship significantly influenced the FEA results.

Duda et al. (Duda 1998) studied the effect of muscle forces on femoral strain distribution in an FE model. They showed a considerable overestimation of strains when the muscle loads were ignored. Pettersen et al. (Pettersen 2009b) conducted a study with subject-specific FE models to evaluate the stress shielding in THA, comparing with the experimental results. A strong consistency of the stress distribution pattern between FEA and experiment was found. Thus, they concluded that subject-specific FEA could describe the pattern of stress distribution obtained experimentally.

## **2. Aim of the study**

The purpose of the current study was to evaluate the primary stability/initial fixation as well as stress distribution of a metaphyseal anchored SHA stem. Besides, it was evaluated whether this SHA stem can safely be revised with a standard THA stem.

The Metha SHA stem and standard CLS THA stem are widely used implants. To the authors' knowledge, there are currently no FEA studies comparing the stress distribution pattern of the native bone to a model with Metha SHA stem and standard CLS THA stem inserted. Therefore, the present FE analysis addressed the difference of the stress distribution patterns before and after implantation of those implants, as a predictive assessment of the potential stress shielding effects.

For this purpose, two methods were applied: on one hand a biomechanical experimental setup and on the other hand a finite-element analysis. The biomechanical setting was based on an experimental setup for testing 3-dimensional micromotions at the interface between bone and implant in SHA and THA. The finite element study was based on models reconstructed from CT scanning images of the experimental sawbones and prostheses. Nodal displacements and cortical stress of the models were determined from the analysis of FE models.

The following aims were addressed by these methods:

1. To evaluate the primary stability of the Metha short and CLS standard stems.
2. To evaluate whether revising the Metha short stem with a CLS standard stem can provide a sufficient primary stability.
3. To predict the experimental micromotions using the FEA models.
4. To identify the influence of implant design on the stress distribution using the FEA models, as a means to compare potential stress shielding effects between the tested stems.

### 3. Materials and methods

For this study, two different methodologies were basically applied. Firstly, the experimental test was performed to measure the micromotions of implants in the cementless SHA and standard THA. Then, the FEA study was performed to test the relative displacement and the stress shielding.

#### 3.1. Micromotion setup

##### 3.1.1. Specimen

In this study, standardized synthetic composite bones (4<sup>th</sup> generation femur, Model 3306, sawbones Pacific Research Laboratories, USA) were used (Heiner and Brown 2001) (Fig. 17). Synthetic bones were used to provide a high consistency between specimens, thus obtaining a better sensitivity for comparative studies. The cancellous and cortical bone structures are simulated by the use of rigid polyurethane foam and short-glass-fiber-reinforced (SGFR) epoxy, respectively. The tensile, flexural strengths, moduli, and geometry of composite bones are consistent with the human bone under bending, axial, and torsional loading test (Heiner and Brown 2001).



Fig. 17: Synthetic composite bone (4th generation, sawbone, left side size L) (Sawbones 2017)

##### 3.1.2. Metha short stem prosthesis

In this study for SHA, the Metha short stem (B. Braun, Aesculap, Tuttlingen, Germany) was used. It is a cementless partial collum sparing implant which is double tapered, collarless with a metaphyseal anchorage (Van Oldenrijk 2014, Khanuja 2014a) (Fig. 18). The implant

belongs to a relatively new generation of short stem implants for total hip endoprosthesis. The implant preserves the femoral neck and greater trochanter region in order to save bone stock for further revisions and provide a more physiological load transfer.

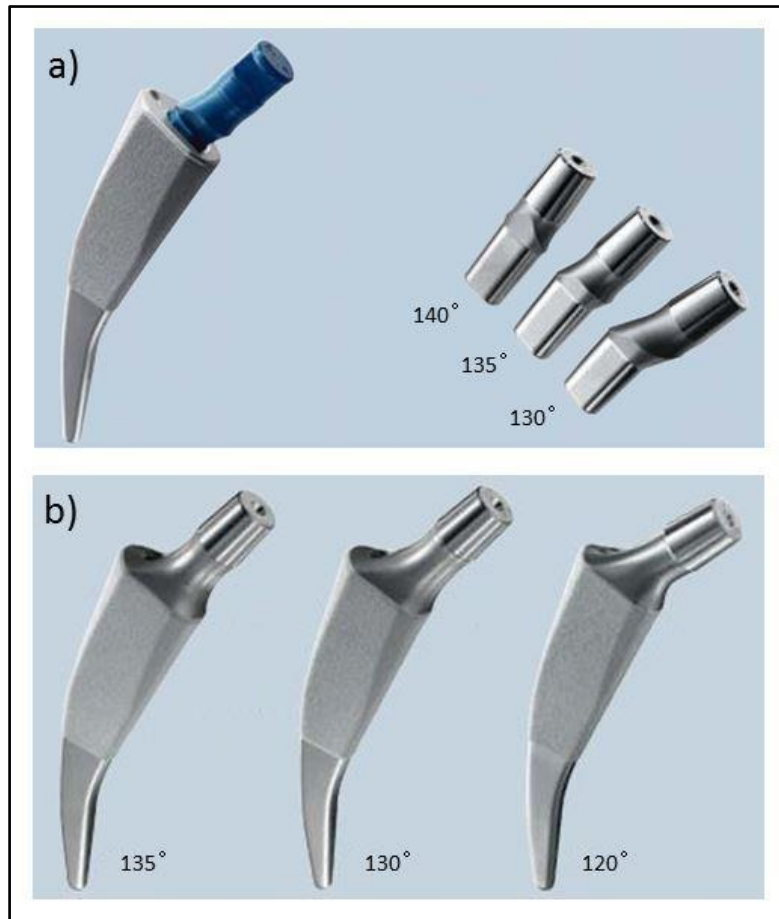


Fig. 18: Metha short stem prosthesis (Aesculap Implant Systems n.d.):

- a) Modular Metha stem
- b) Monoblock Metha stem

The implant is available in a monoblock or a modular design with cone adapters. The modular Metha SHA stem offers nine neck adapters with CCD (caput-collum-diaphyseal) angles ( $130^\circ$ ,  $135^\circ$ ,  $140^\circ$ ) and ante/retro-versions ( $-7.5^\circ$ ,  $0^\circ$ ,  $+7.5^\circ$ ) (Aesculap Implant Systems n.d.). The monoblock Metha stem provides three versions with CCD angles of  $120^\circ$ ,  $130^\circ$  and  $135^\circ$ , without ante/retro-versions. For a better osseous integration, the Metha stem has a rough Plasmapore titanium micro-porous coating at the proximal side. Additionally, a  $20\ \mu\text{m}$  calcium phosphate layer intends to offer an osteoconductive effect and accelerate osseous integration between the bone and implant. In contrast, the distal stem area is polished to avoid

stress shielding (Aesculap Implant Systems n.d.). In this study, a Metha stem size 3 with a 135 ° neck angle and a standard ceramic head size M was used.

### 3.1.3. CLS standard stem prosthesis

For a standard THA stem, the CLS stem (Zimmer, Warsaw, Indiana, USA) was used in this study. It is a cementless, straight and collarless stem with a proven good long-term outcome (Evola 2014) (Fig. 19).



Fig. 19: CLS standard stem prosthesis (Zimmer 2011)

The implant features a rectangular cross-section and a tapered shape in order to offer a good primary and rotational stability. The stem has a proximal anchorage and the implant is a grit-blasted titanium alloy with a microporous surface (Ti6Al7Nb alloy;  $R_a = 4.4 \mu\text{m}$ ). The proximal rib structure with proximally sharpened edges makes it easier for the stem to penetrate into the bone and lower the risk of fissures. The rib intends to increase the contact area between the bone and implant, further promoting osseous integration on the implant surface. The CLS stem offers three different CCD angles (125 °, 135 °, 145 °) (Zimmer 2011).

In this study, a CLS prosthesis size 13.75 with a 135 ° neck angle and a standard ceramic head size M was used.

#### **3.1.4. Specimen preparation**

Insertions of the implants were all performed in a standardized manner by one experienced surgeon, following the manufacturer's instructions. The implantation was implemented under fluoroscopy in 2 plains in order to assure a correct placement of the stem (Fig. 20). The specimens were osteotomized according to the X-ray template with a partial neck preserving osteotomy for the Metha short stem and a standard femoral neck resection for the CLS standard stem. The femoral head was removed and the cavity inside the bone was rasped for subsequent implantation (Fig. 21).

The composite femur was firmly embedded in a pot using methylmethacrylate (Technovit 3040, Merck, Darmstadt, Germany) after cutting them 20 cm below the lesser trochanter. The specimens were positioned and embedded with 9 ° flexion (sagittal plane) and 16 ° adduction (frontal plane).

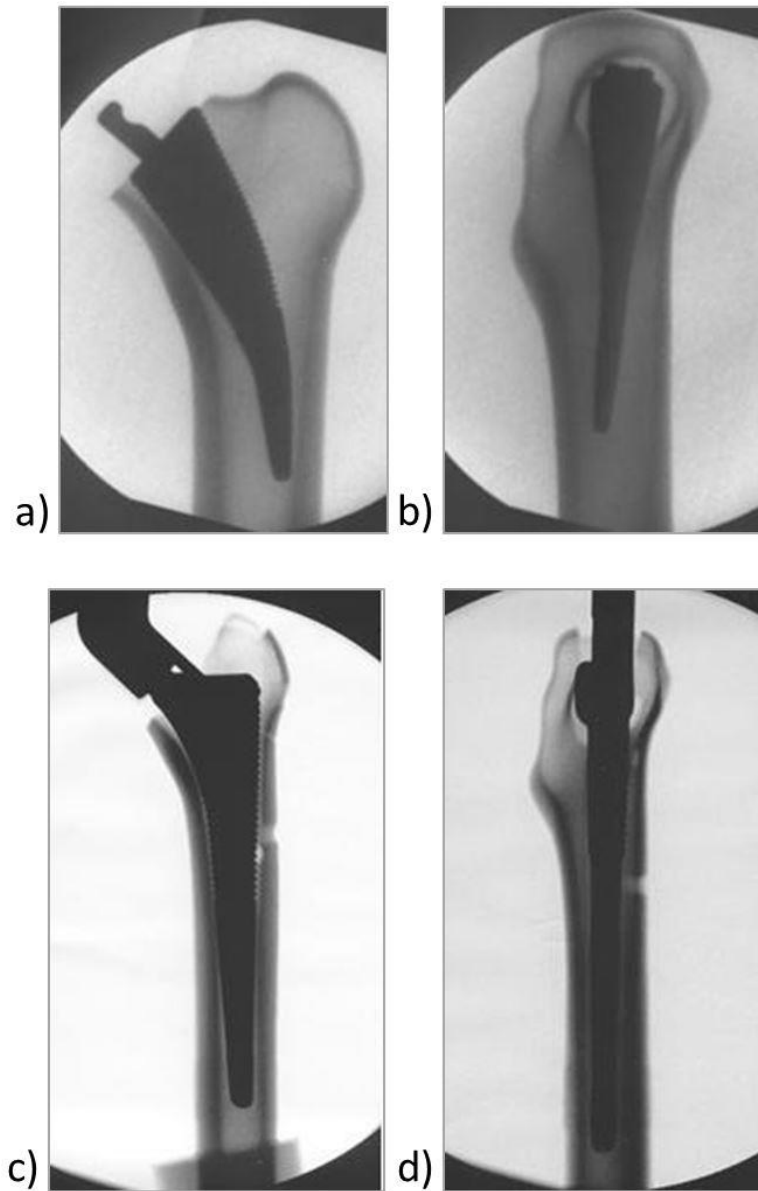


Fig. 20: Implantations operated under fluoroscopy:

- a) Metha short stem for the anterior-posterior view
- b) Metha short stem for the lateral view
- c) CLS standard stem for the anterior-posterior view
- d) CLS standard stem for the lateral view

Positions of implantations are consistent with manufacturer's instructions





Fig. 21: Sawbones with different femoral head osteotomies according to the stem design:

- a) Metha short stem
- b) CLS standard stem

### 3.1.5. Loading procedure

The specimens were loaded in vertical downwards direction with sinusoid dynamic pressure using a hydraulic material testing device (Schenck Process GmbH, Darmstadt, Germany). The load was applied at the top of the standard 32 mm ceramic head and transmitted via a ceramic acetabular liner. The load parameters were adjusted to simulate a physiological load of the post-operative patient with 70 kg body weight while walking on the level ground (Bergmann

1993). The sinusoid dynamic load was applied for 30 s (30 cycles) in each measurement with the amplitude from 300 N to 1700 N and the frequency 1 Hz. The specimens were preconditioned by applying this loading pattern until there was no change in the LVDT readings for at least 10 cycles. Every specimen was loaded for 10 minutes (600 cycles, 300 N to 1700 N, 1 Hz) before the first measurement in order to ensure a firm settlement and obtain an initial press-fit scenario for simulating a THA surgery.

### **3.1.6. Measurement of the primary stability under dynamic loading**

Three-dimensional micromotions in 6 degrees of freedom between the implant and composite femur were obtained by using a highly accurate device similar to the one described before (Fottner 2009, Chareancholvanich 2002), with a resolution of 0.1  $\mu\text{m}$  and the accuracy of angular measurement of 0.0001  $^\circ$ . The measurement unit consists of an outer rack (6 $\times$ 6 $\times$ 6 cm) and an inner cuboid (3 $\times$ 2 $\times$ 3 cm) (Fig. 22). For the registration of the relative movement, a metal rod with a diameter of 3 mm was fixed to the center of the inner cuboid and the other end was fixed to the prosthesis at different desired points. Before this fixation, the corresponding points on the femur were drilled through the bone to make holes with a diameter of 7 mm, allowing for the rod to pass through the femur.

In order to reduce the testing error from the effect of the bone deformation and bending, the outer rack was placed on a fixation system that was firmly fixed to the outer bone surface at the same level of the measuring point. A metal ring with four holes was used in this fixation system. Three holes were used to fix the ring to the femur and the last hole with a diameter of 10 mm was used to allow the rod passing through it. The rack was designed to hold six LVDTs (HBM Weta 1/2mm, Hottinger, Darmstadt, Germany) in a 3-2-1 configuration (Fig. 22). All the LVDT tips were adjusted to contact the inner cuboid with enough flexible space for the movements.

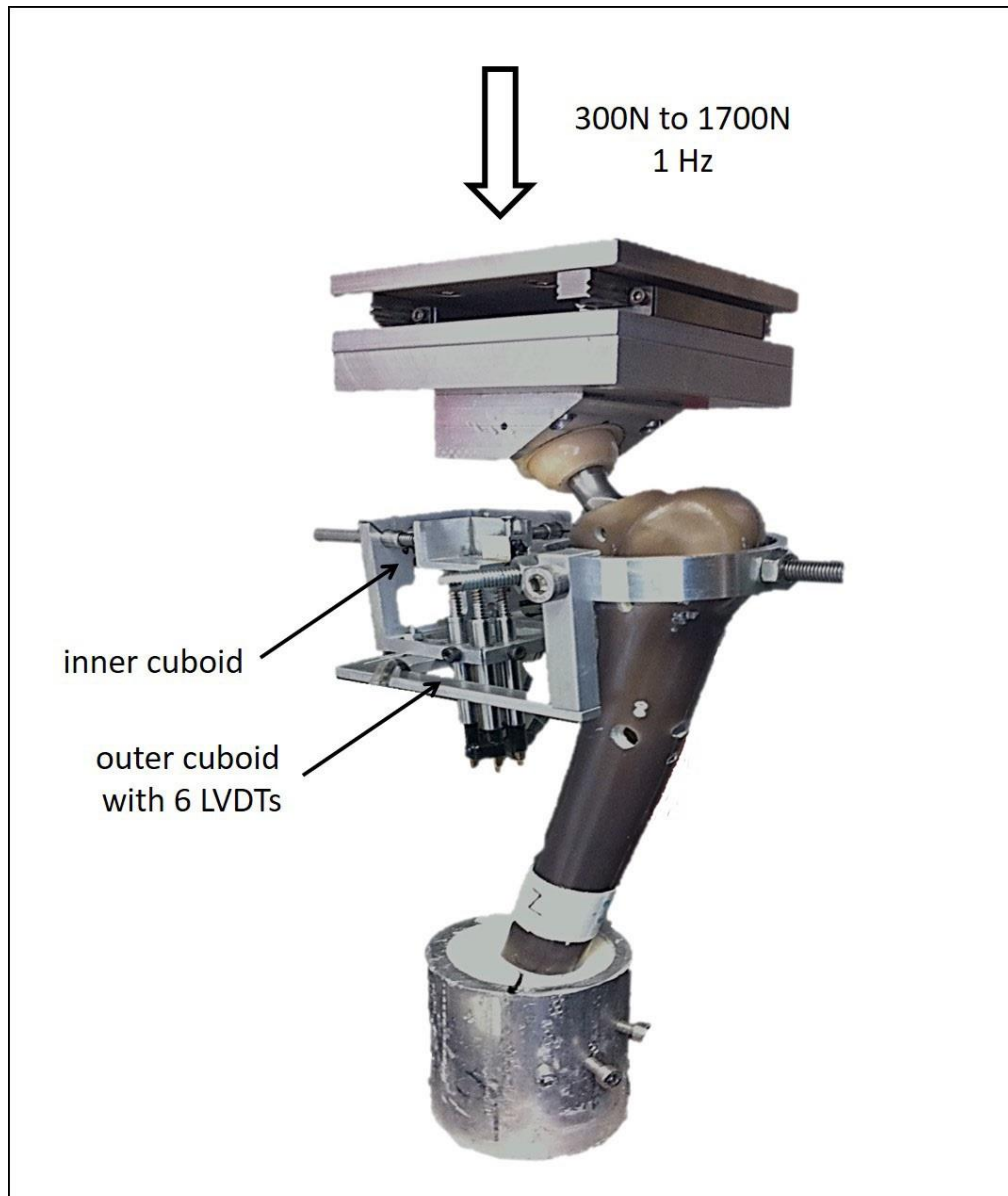


Fig. 22: Experimental setup for determining the 3D micromotions between the bone and implant interface. The outer rack with six LVDTs (3-2-1 configuration) is fixed to the bone at the level of the medial proximal point. The inner cuboid is fixed to the prosthesis through a metal rod at the same measurement point.

### 3.1.7. Study design of revising SHA with standard THA

The design of this study was firstly performed by evaluating the micromotions of Metha stem in primary SHA and CLS stem in primary standard THA (Metha-Primary vs. CLS-Primary) (Fig. 23).

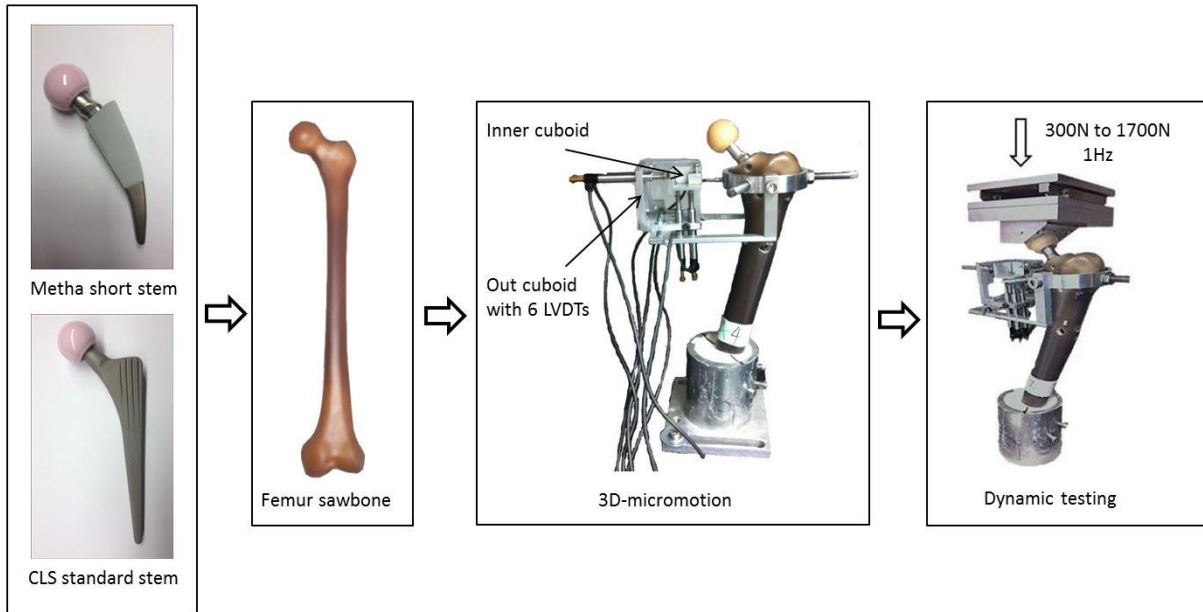


Fig. 23: Flowcharts depicting the preparation and 3D-measurement in the micromotion setup

After then, the revision scenario was simulated by removing the Metha short stem and revising it with CLS standard stem. The subsequent micromotions of CLS standard stem in revision THA were measured similarly to the micromotion setup in primary THA (CLS-Revision vs. CLS-Primary) (Fig. 24).

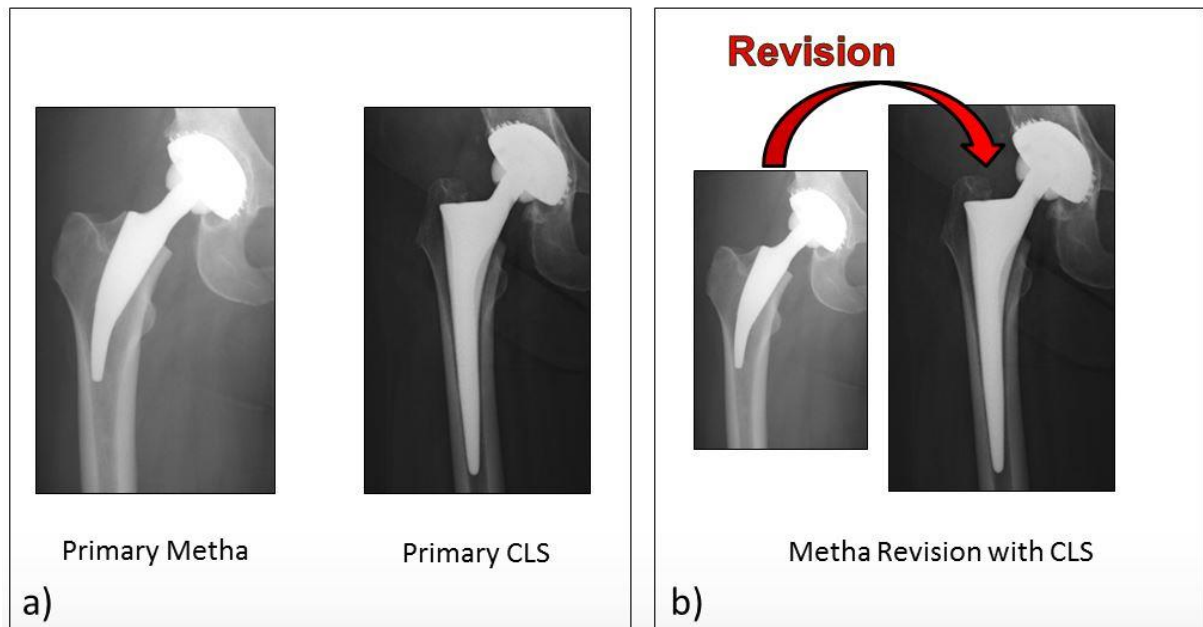


Fig. 24: The procedure of revision scenario:

- a) Primary THA (Metha and CLS stems)
- b) Metha revision with CLS

### **3.1.8. Primary setting (Metha and CLS stem)**

In the primary implantation setting, 3D-micromotions were determined at 5 defined points (P1-5) for both implants: For the Metha short stem (Fig. 25 a), points 1 (medial-proximal) and 2 (ventral-proximal) were at the resection level 3 cm above the lesser trochanter. Point 3 (ventral-median) was located at the height of the lesser trochanter. Points 4 (ventral-distal) and 5 (lateral-distal) were located 5cm below the lesser trochanter level.

Due to the difference in the implant design in terms of size and shape, the points of the SHA and standard THA did not correspond to the identical locations. For the CLS standard stem (Fig. 25 b), points 1 (medial-proximal) and 2 (ventral-proximal) were located at the height of the lesser trochanter. Point 3 (ventral-median) was located 5cm below the lesser trochanter level. Points 4 (ventral-distal) and 5 (lateral-distal) were added at the level 12 cm below the lesser trochanter.

### **3.1.9. Revision setting (Metha revised by a CLS stem)**

In order to simulate a revision case, the short stem was removed after measuring the 3D-micromotions to simulate an aseptic failure of the implant. Then the femur was prepared for the CLS standard stem as given in the manufacturer's instructions. Firstly, the osteotomy was performed for a standard stem and the femoral canal was broached manually. Finally, the standard CLS stem was inserted into the femur and prepared equally as described before in the primary situation. 3D-micromotions of revision CLS stem were determined at 5 defined points as in the CLS primary scenario.

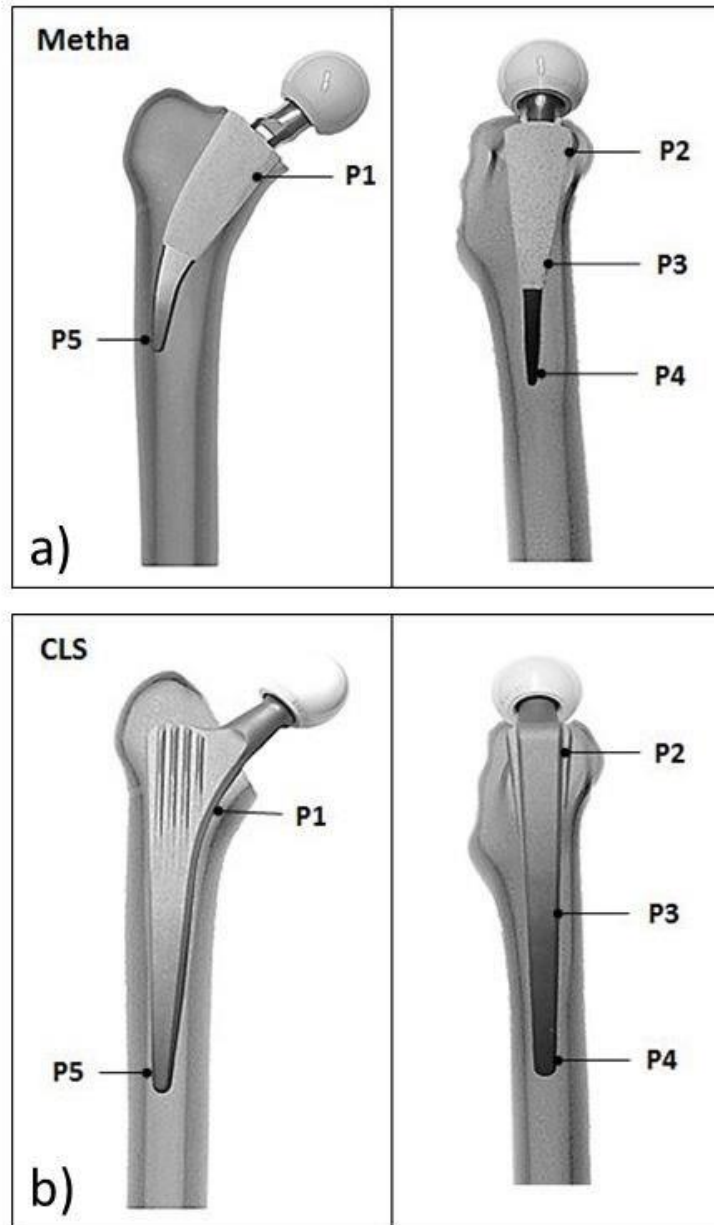


Fig. 25: Measurement points of micromotions:

- a) Metha short stem
- b) CLS standard stem

### 3.2. Finite Element Analysis

FEA was performed after biomechanical testing to allow a prediction of stress distributions for the tested implant designs, after matching the predicted micromotions to the experimentally measured ones. Because the FEA can account for bone deformations that are overlooked by the experimental approach, the FEA predictions of micromotions can also be used to complement the experimental observations.

To create the FE models, implants and femurs from the biomechanical experiment were chosen. One intact composite femoral bone and two composite femoral bones implanted with Metha and primary CLS stems were scanned with CT. The scans of the implanted femurs were used to align the position of implantation and simulate the experimental situation precisely.

The FE models based on the homogenization method were created as shown in Fig. 26. The main processes of the model creation could be divided into four steps:

- a. 3D-model generation from the clinical quantitative CT images of the femurs and implants
- b. alignment of the implants
- c. assignment of material properties
- d. assignment of boundary condition

The post-process was applied to solve the models. The steps were performed using custom-made programs in Python, C++ and Fortran (Dr.techn. Yan Chevalier, Munich, Germany) (Chevalier 2015).

### **3.2.1. CT scanning and 3D model generation**

CT scans of the implanted and native specimens, as well as the two selected femoral stems, were conducted using Siemens Sensation scanner (64-slice) (Siemens Somatom Emotion 6, Siemens AG, Germany). The phantom was regularly scanned for quality control. The specimens were all put in a standardized, neutral position and were scanned with an image resolution of  $512 \times 512$  pixels and a slice thickness of  $600 \mu\text{m}$ . Due to the metal-induced artifacts, the femoral stems were removed after scanning the sawbones with implanted prostheses. Then only the implants and subsequently only the sawbones with the removed prostheses were scanned independently.

In the next step, the cortical and trabecular bones were segmented separately based on grayscale values from the CT scans by means of an in-house written code (Chevalier 2015). Similarly, 3D models of the two selected implants were created.

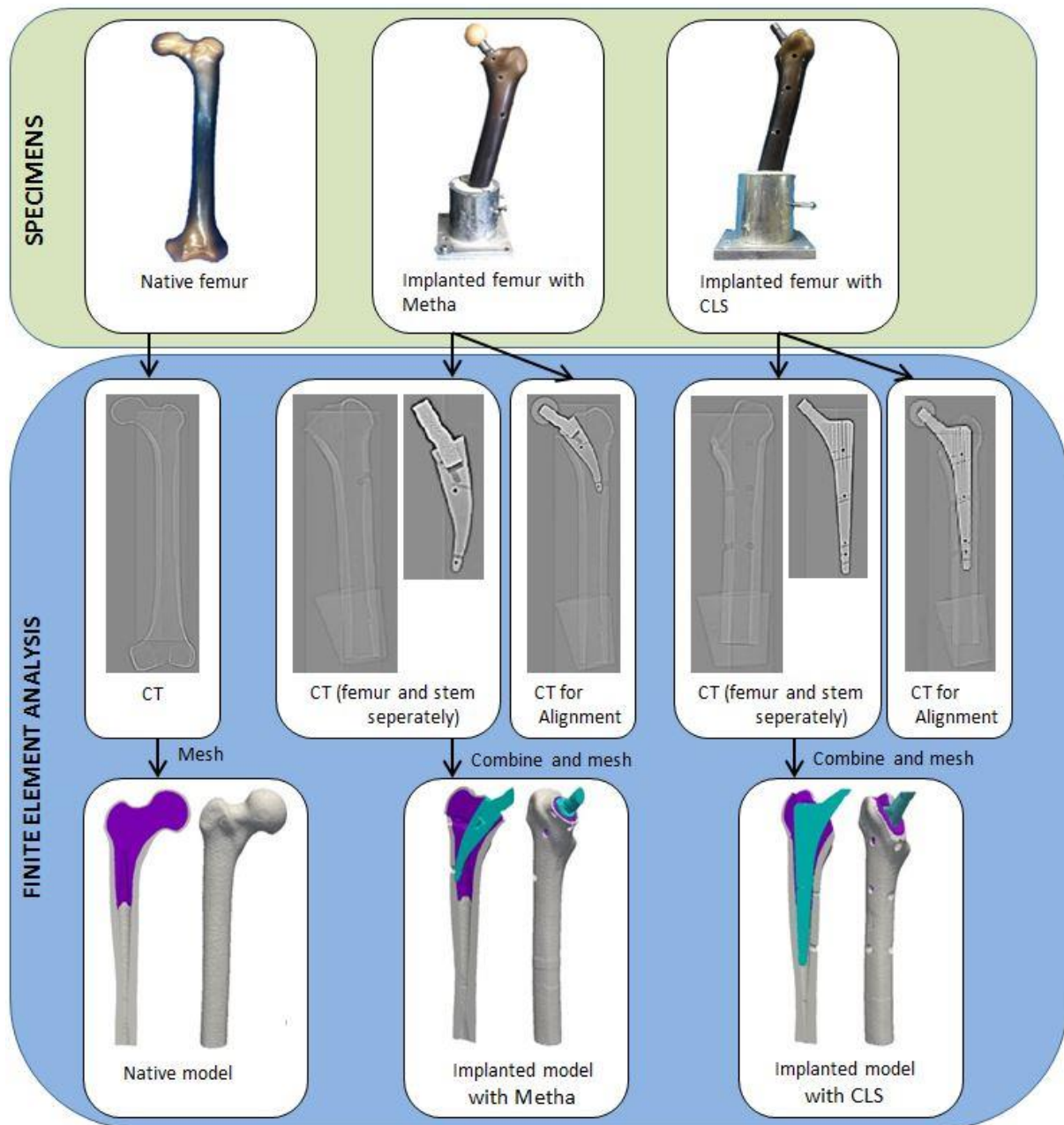


Fig. 26: Flowcharts depicting the process of creating the homogenized FE models

### 3.2.2. Alignment of the Hip Stems

After constructing the 3D triangular mesh models of the bones and hip stems, the implants were positioned into the bone to mimic hip arthroplasties. To acquire an accurate position of the implantation being comparable to the in vitro test, the alignment of placing stems into the bone was achieved by matching the position of the isolated implant geometry coming from the implant-only CT scan with the image of the implanted femurs. This was done visually in Paraview v3.14 (Ayachit 2015). The implant models were then reconverted to digitized



images of the implants with custom codes in Python and ITK (Chevalier 2015). Afterwards, the bone and implant images were combined into a binarized image with three distinct regions (compact bone, trabecular bone, and stem), and then meshed with 2-mm 4-noded tetrahedral with CGAL (Pierre Alliez 2014) to create 3D models of the implanted femurs based on the methodology described by Chevalier et al. (Chevalier 2015). The merged model of the native femur contained approximately  $66 \times 10^3$  nodes and  $29 \times 10^4$  elements. The merged models of implanted femurs for Metha short stem and CLS standard stem contained between 52 and  $58 \times 10^3$  nodes, and 21 and  $24 \times 10^4$  elements, respectively.

In the mesh step, the bone-implant interface in the FEM models was constructed simultaneously. In previous FEA studies, the bone-implant interface is often simulated by two ways, called direct contact and gap elements (Zachariah and Sanders 2000, Viceconti 2000). Direct contact allows interface discontinuity, separation and sliding. It was found to be sensitive to the frictional coefficient and better reflect the local nodal displacement (Zachariah and Sanders 2000). However, gap elements are specialized interface elements linking the interface discontinuity and allowing load transfer at the interface.

In the current FE analysis, all structural interfaces were modeled bonded at their shared nodes. Therefore the analyses only included one surface to describe the bone-implant interface, which didn't allow separation and sliding. Furthermore, it was irrespective of gap, penetration, and loading and thus resulting in a linear type of FEA, ignoring the friction between the bone and implant.

### **3.2.3. Material Properties Assignment**

After the final merged triangular 3D mesh models of the implanted composite femurs were completed, the material properties of the implant and bone were assigned. The two prostheses were assigned homogeneous and isotropic materials. Although the proximal surface of the Metha short stem was coated with different materials compared to the distal and inner parts, it was still assumed to be homogeneous and isotropic for simplicity in the present FEA. In contrast, the bone was not homogeneous because of the different properties of cortical and trabecular bones. Previous FEA studies separated the cortex from trabeculae and defined homogeneous properties for cortical and trabecular bones (Pettersen 2009b, Viceconti 2000, Baca 2008). Other studies used a more sophisticated approach to define the material properties by estimating gray-level values based on the element-by-element unit from photographs or radiographs (Keaveny and Bartel 1993).

In the present study, isotropic linear elasticity was used for all materials. The cortical and trabecular bones were assigned a Poisson's ratio and Young's modulus in line with the sawbone materials modeled the experimental test conditions:  $E_{\text{cortical bone}} = 16.7 \text{ GPa}$  and  $\nu_{\text{cortical bone}} = 0.3$ ,  $E_{\text{trabecular bone}} = 155 \text{ MPa}$  and  $\nu_{\text{trabecular bone}} = 0.3$  (Grover 2011). For the selected two implants,  $E_{\text{implant}} = 25 \text{ GPa}$  and  $\nu_{\text{implant}} = 0.3$  (Oldani and Dominguez 2012).

#### **3.2.4. Boundary Conditions**

Physiological loading configurations were assigned after completing the model and assignment of material properties. It has to be noted that in the current literature, the loading configurations vary significantly among the studies due to several factors, such as the weight of the patient, the physical status of the patient and the activities analyzed. Therefore different loading conditions on the hip joint prosthesis have been applied in FEA studies which are derived from experimentally measured forces during gaits and stairs climbing in different musculoskeletal studies (Bergmann 2001, Stansfield and Nicol 2002).

In the present FEA, the analyzed models were loaded corresponding to the experimental conditions of the specimens tested in the biomechanical in vitro study. A resultant load with 1400N was applied on the tip nodes of the prosthesis neck, while bottom nodes of the bone were fully constrained. The models were then solved using commercial software (ABAQUS 6.13, Simulia, Dassault Systèmes, Vélizy-Villacoublay, France) for acquiring nodal displacements and bone stresses.

#### **3.2.5. Calculation of relative interface displacements and stress distribution**

To calculate and display the relative displacement between the implant surface and outer bone surface as well as the cortical stress distribution pattern, a special custom subroutine was written for the linear analyses.

A first custom post-processing subroutine provided in Python, ABAQUS Python and Fortran allowed storing the nodes chosen from the implant surface and the corresponding nodes from the outer surface of cortical bone. Due to the small holes in the biomechanical experiment from which the FE models were created, it was impossible to choose the identical reference points from the experiment. Therefore, the nodes were taken right next to the implant hole on the implant surface, and around the cortical hole on the outer surface. The code therefore calculated the relative displacement by subtracting the nodal displacement of the implant (Fig. 27 a) from that of cortical bone (Fig. 27 b).

Of note, the fixation frame in the experimental setting was fixed to the bone with three screws at different locations. Therefore, the reference point was a virtual, averaged point of these attachment points. In the present FEA, the reference point was chosen around the edge of the cortical hole. In order to evaluate if the rigid frame of the experimental setting was amplifying the predicted bone deformations, one additional point was defined and calculated as control ( $P_A$ ). This was done by subtracting the medial proximal nodal displacement of the stem (Fig. 27 a) from that of the lateral proximal outer surface of femoral cortex at the same height (Fig. 27 c).

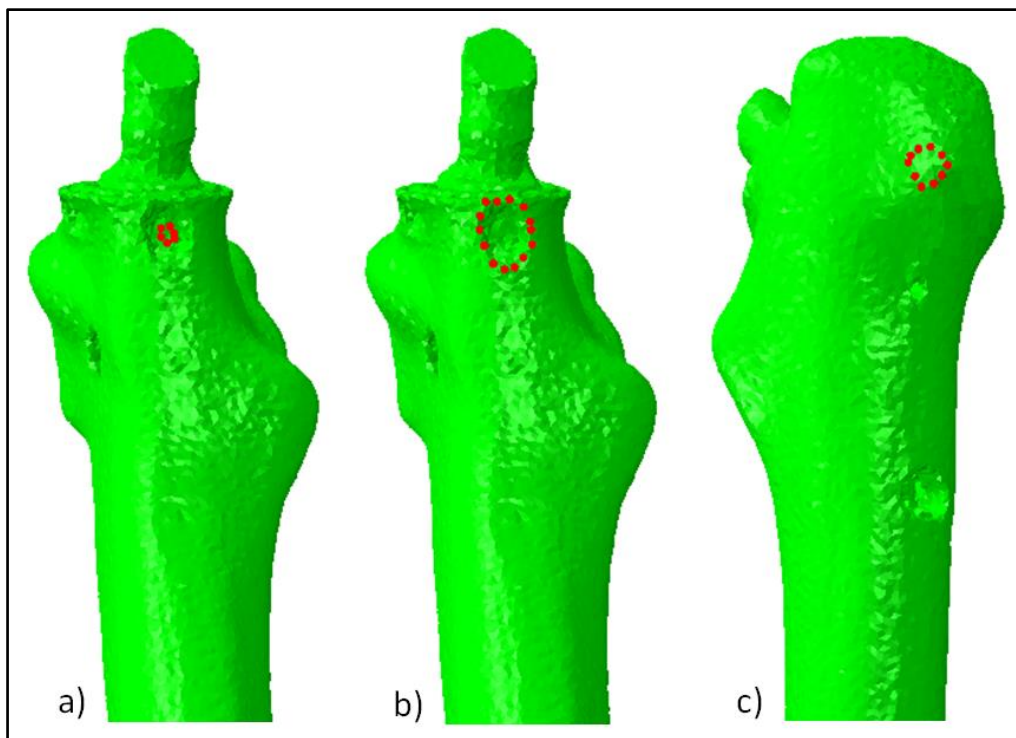


Fig. 27: Nodes chosen in the FE model:

- a) Nodes on the implant surface around the implant hole
- b) Nodes on the outer surface of the cortex around the edge of the cortical hole
- c) Nodes on the outer surface at the lateral proximal cortex at the level of (a)

To analyze the cortical stress distribution patterns of the FE native and implanted models, another custom subroutine provided in ABAQUS Python allowed dividing the FE models into equal vertical regions with a thickness of 10 mm starting from the femoral top to the femoral shaft in the z-axis direction (Fig. 28). The mean and peak values of von Mises stress were analyzed for each region and compared among the modeled implant scenarios.

### **3.3. Data analysis**

For the biomechanical study, a reference coordinate system was virtually defined around the three planes of the small, inner cuboid for calculating the micromotions in 6 degrees. The 3D-micromotions were calculated using a custom software program written in MATLAB (MathWorks, USA, Version R2013a.), according to the formulas described by Görtz et al. (Gortz 2002).

For the FEA study, visualization of results and part of the post-processing was performed using ABAQUS/Viewer 6.13 (Simulia, Dassault Systèmes, Vélizy-Villacoublay, France). Final visualization of mean stresses in the models after regional postprocessing was done in Paraview v3.14 (Ayachit 2015).

### **3.4. Statistics**

Statistical analysis and graphs were performed with GraphPad Prism 5 (GraphPad Software, Inc. La Jolla California, USA) and SPSS 18.0 (SPSS Inc., Chicago, IL, USA). Data are displayed as mean  $\pm$  standard deviation (SD). An unpaired Student's t-test was performed after testing the normality with the Kolmogorov Smirnov test, for comparing the CLS-Primary vs. Metha-Primary stems in the primary scenario and the CLS-Primary vs. CLS-Revision stems in the revision scenario. A  $p$ -value  $< 0.05$  was defined to be significant.

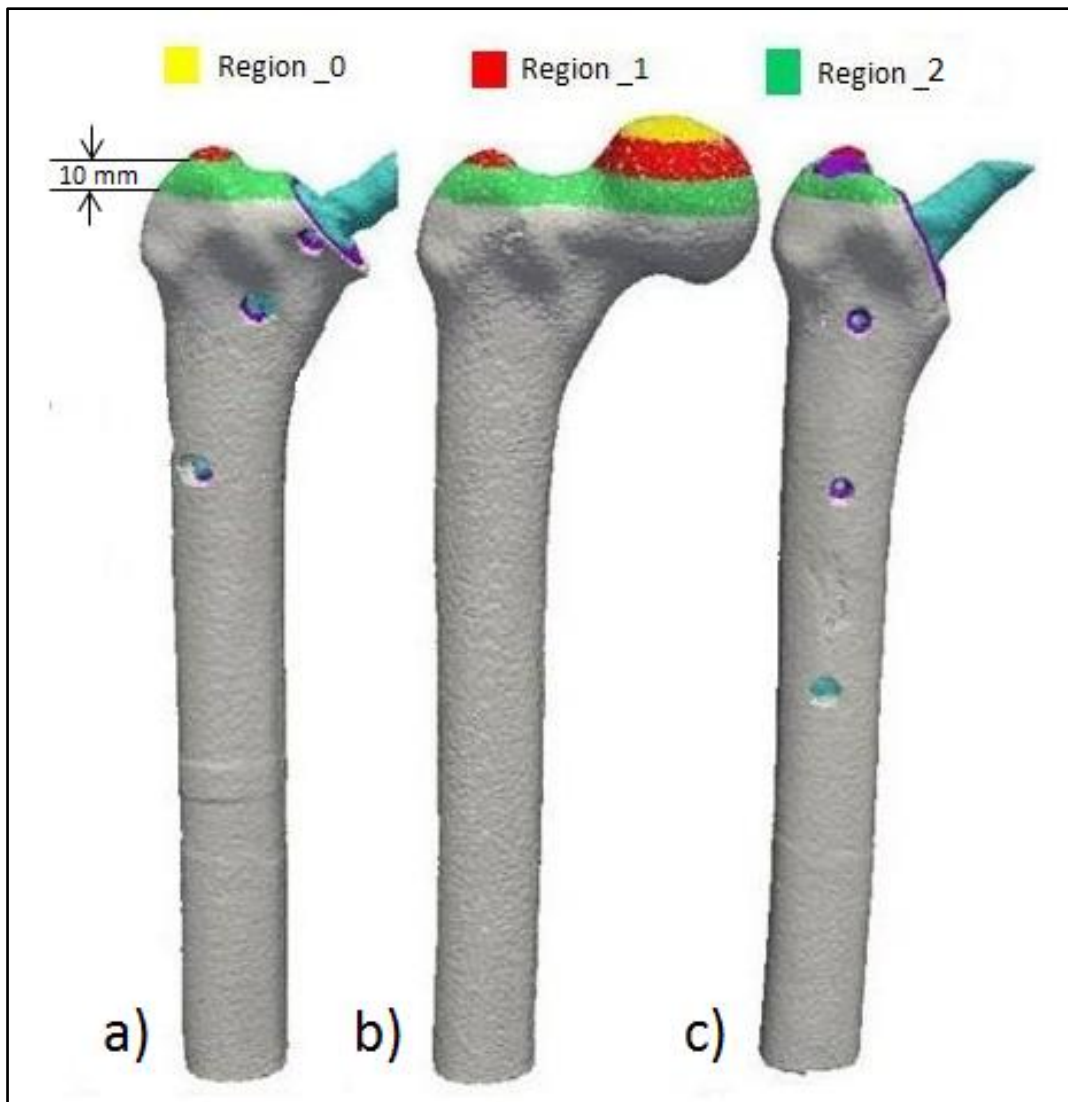


Fig. 28: Illustration showing the method of stress analysis in the three FE models:

- a) Implanted bone with Metha short stem
- b) Native bone
- c) Implanted bone with CLS standard stem

Vertical regions with a thickness of 10 mm for comparing the von Mises stress were at the same level in z-axis direction, e.g. regions 0-2

## 4. Results

### 4.1. Results of biomechanical 3D-Micromotion study

All the dynamic loading procedures were performed successfully without damaging composite femurs. Mean micromotions were below 150  $\mu\text{m}$  at all tested points for both the Metha short and CLS standard stems, except for the lateral distal point (155.4  $\mu\text{m}$ ) of CLS stem in the revision scenario.

#### 4.1.1. Primary setting (Metha short and CLS standard stems)

In the Primary scenario, Metha short stem showed the highest 3D-micromotions at the medial proximal point (P1), which was significantly higher than the other 4 tested points ( $p < 0.05$ ). No significant difference was recorded between the points at less trochanter level (P3) and stem tip level (P5) (Fig. 29).

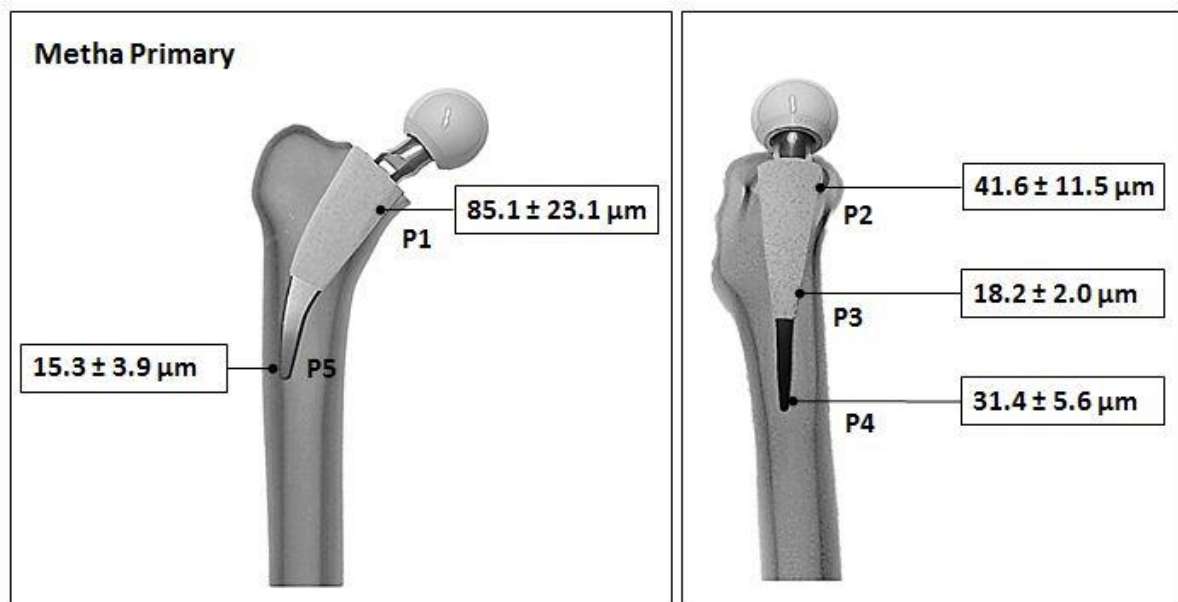


Fig. 29: 3D-micromotions determined for Metha-Primary stem (Yan 2017)

For the CLS standard stem, the highest 3D-micromotions were recorded for two points (P4 and P5) at the distal tip of the implant, which were significantly higher than the other 3 tested points ( $p < 0.05$ ). No significant difference between the points at less trochanter level (P1) and middle stem level (P3) was observed (Fig. 30).

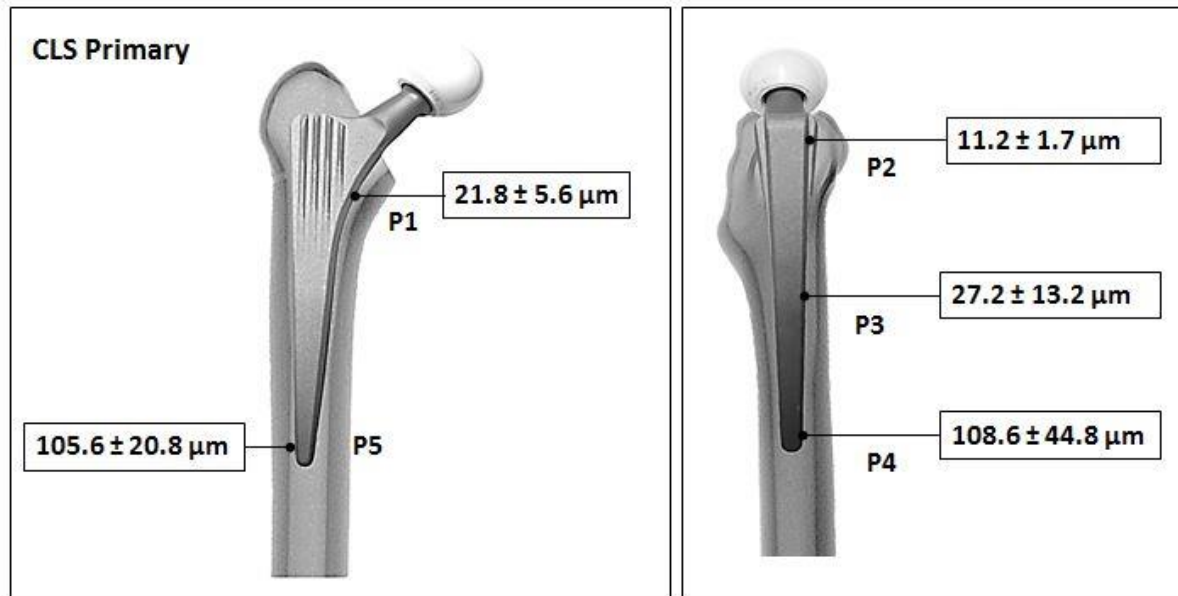


Fig. 30: 3D-micromotions determined for CLS-Primary stem (Yan 2017)

Comparing the 3D-micromotions of Metha-primary to CLS-primary stem revealed a clear difference in the micromotions. Significant differences were found for the proximal points P1 and P2 (both  $p < 0.0001$ ) as well as for the distal points P4 ( $p = 0.002$ ) and P5 ( $p < 0.0001$ ). No significant difference was observed for the middle point P3 ( $p = 0.127$ ).

The highest 3D-micromotions at the medial proximal point of Metha short stem (P1) were significantly higher than the corresponding point of the CLS stem (P1: Metha  $85.1 \pm 23.1 \mu\text{m}$  vs. CLS  $21.8 \pm 5.6 \mu\text{m}$ ;  $p < 0.05$ ). The highest 3D-micromotions at the distal tip of the CLS standard stem (P5) were significantly higher than the corresponding point of the Metha stem (P5: Metha  $15.3 \pm 3.9 \mu\text{m}$  vs. CLS  $105.6 \pm 20.8 \mu\text{m}$ ;  $p < 0.0001$ ) (Fig. 31).

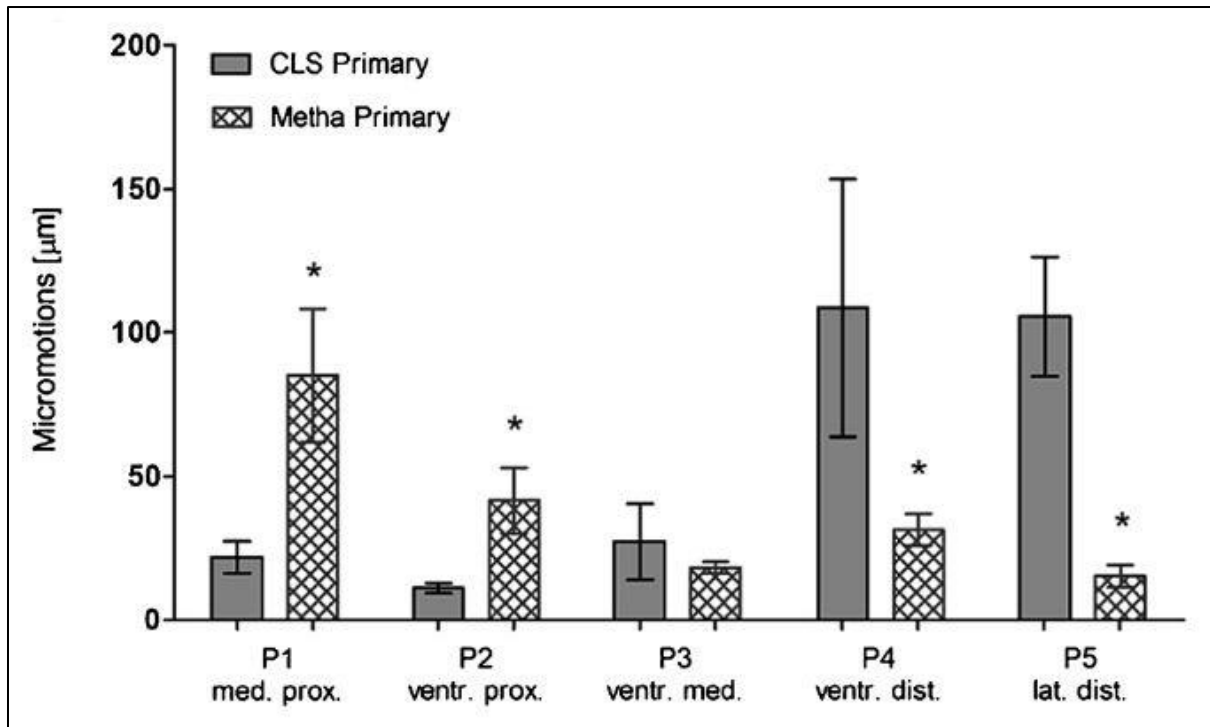


Fig. 31: Comparison of 3D-micromotions for the 5 interface points between CLS-Primary and Metha-Primary stems. Significant differences of micromotions were found at the P1, 2, 4 and 5. Asterisk (\*) indicates significance to the CLS-Primary ( $p < 0.05$ ) (Yan 2017)

#### 4.1.2. 3D-Micromotions in the Revision setting (Metha revised by a CLS stem)

In the revision scenario, the two distal points at the distal stem tip of CLS stem were significantly higher than the other 3 tested points ( $p < 0.05$ ) (Fig. 32). No significant difference was found between the points at less trochanter level (P2) and middle stem level (P3).

For comparing the primary stability of CLS-Primary and CLS-Revision stems, no significant differences in the 3D-micromotions were recorded between them at the proximal points P1 ( $p = 0.746$ ) and P2 ( $p = 0.669$ ) and distal points P4 ( $p = 0.459$ ) and P5 ( $p = 0.063$ ) (Fig. 33). Only in the middle part at P3 the CLS-Revision group revealed significantly different 3D-micromotions, which however were lower compared to the CLS-Primary scenario (P3: CLS-Primary  $27.2 \pm 13.2 \mu\text{m}$  vs. CLS-Revision  $10.2 \pm 8.2 \mu\text{m}$ ;  $p = 0.022$ ).



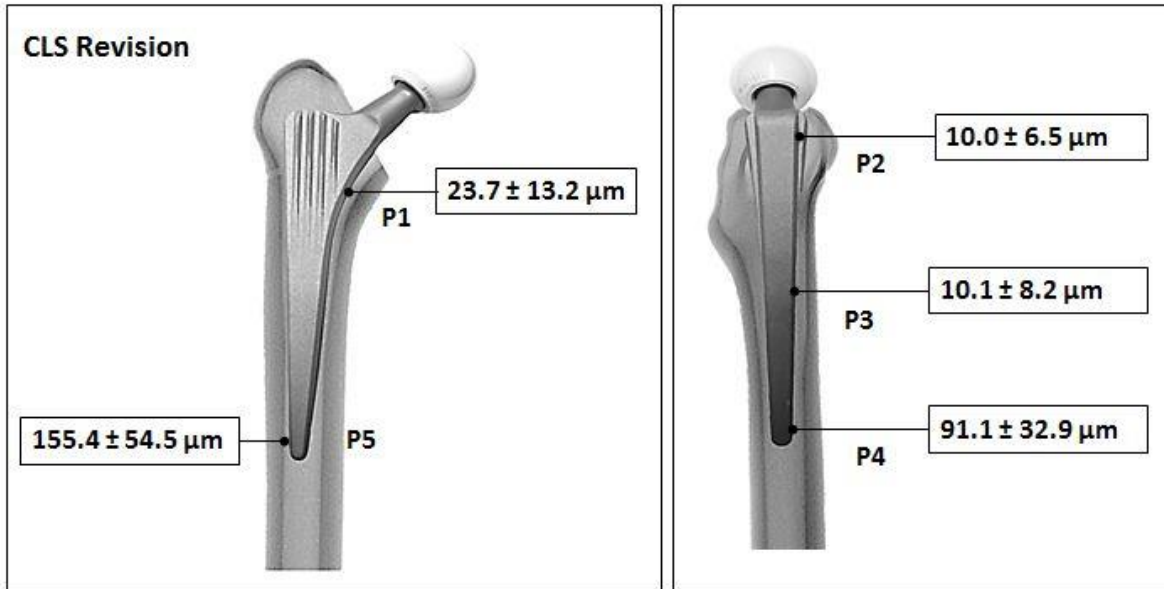


Fig. 32: 3D-micromotions determined for CLS-Revision stem (Yan 2017)

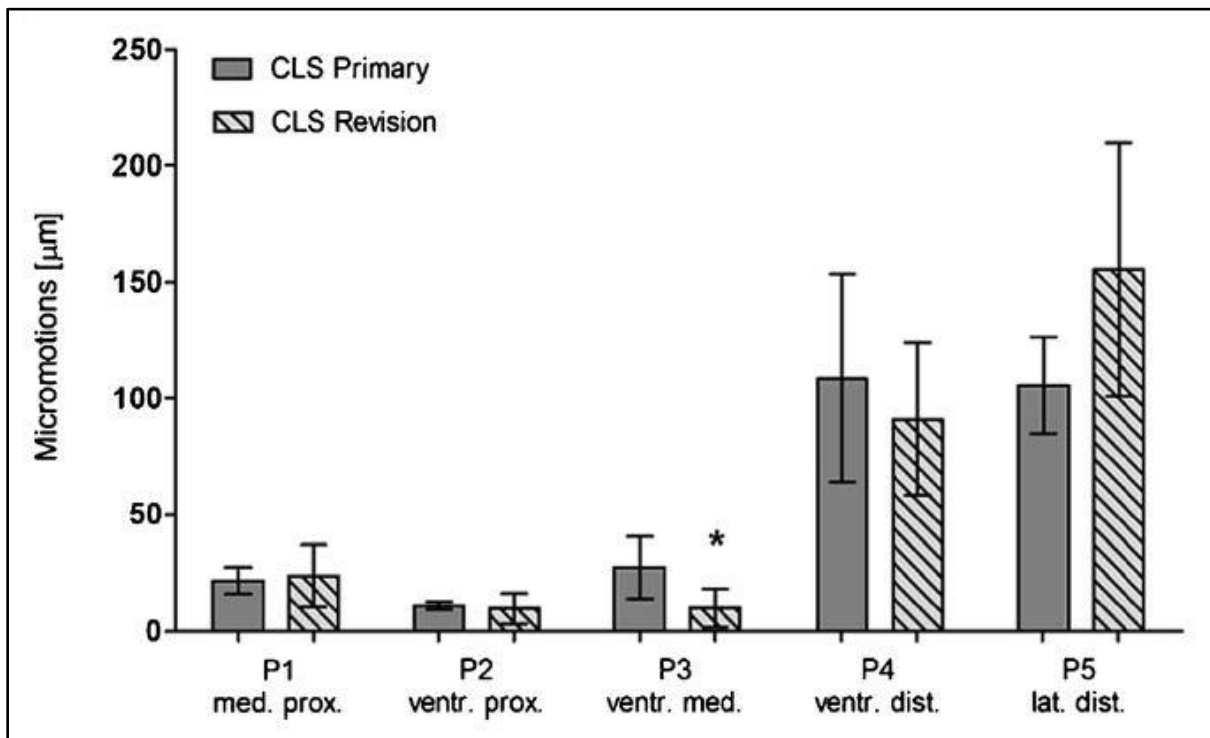


Fig. 33: Comparison of 3D-micromotions for the 5 interface points between CLS-Primary and CLS-Revision stems. No significantly higher 3D-micromotions were registered for the CLS-Revision stem after revising the Metha short stem. Asterisk (\*) indicates significance to the CLS-Primary ( $p < 0.05$ ) (Yan 2017)

Notably, in the revision scenario a bony defect at the calcar was observed in all specimens, which was not fully filled by the medial proximal part of the CLS-Revision stem (Fig. 34). In the primary setting, the CLS-Primary stem did not reveal a bony defect at this region. However, the lateral, anterior and posterior surface of the proximal part of CLS-Revision stem contacted sufficiently with the inner bone surface.

Despite this defect at the calcar, the 3D-micromotions of the CLS-Revision stem at the points adjacent to the defect showed no significant difference compared to the CLS-Primary stem (P1: CLS-Primary  $21.8 \pm 5.6 \mu\text{m}$  vs. CLS-Revision  $23.7 \pm 13.2 \mu\text{m}$ ;  $p = 0.746$  and P2: CLS-Primary  $11.2 \pm 1.7 \mu\text{m}$  vs. CLS-Revision  $10.0 \pm 6.5 \mu\text{m}$ ;  $p = 0.669$ ) (Fig. 33).

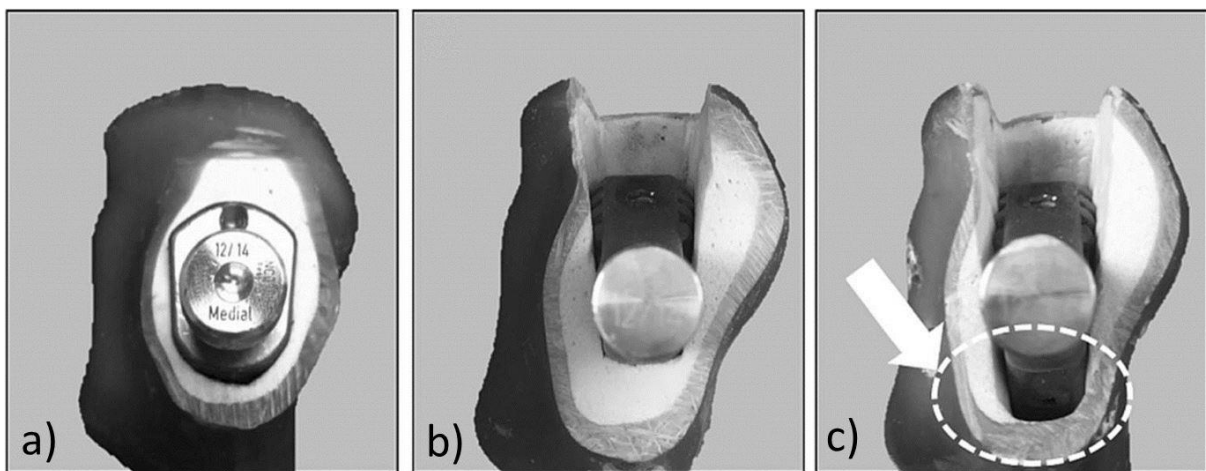


Fig. 34: Implanted sawbones showing a bone defect in revision:

- a) Metha short stem as a primary implant (Metha-Primary)
- b) CLS standard stem as a primary implant (CLS-Primary)
- c) The revision of a Metha short stem (a) with a CLS standard stem (b) (CLS-Revision)

A remaining defect in the revision scenario at the calcar is observed (white arrow and circle) (Yan 2017)

## 4.2. Results of FEA study

All the FEA under loading procedures were performed successfully without damaging the FE models. All the relative displacements were below  $150 \mu\text{m}$  at all tested points for both the Metha short and CLS standard stems, except for the lateral distal point ( $165.9 \mu\text{m}$ ) of CLS stem.

#### 4.2.1. 3D relative displacement in the FEA models of primary SHA and THA

In the FE models of SHA, Metha short stem showed the highest 3D-relative displacement at the ventral proximal point (P2), and a lowest 3D-relative displacement at the lateral distal point (P5) (Fig. 35). The additional test point P<sub>A</sub> (relative displacement of the medial proximal surface of the implant to the lateral cortical surface at the same level), showed an obviously higher value than P1.

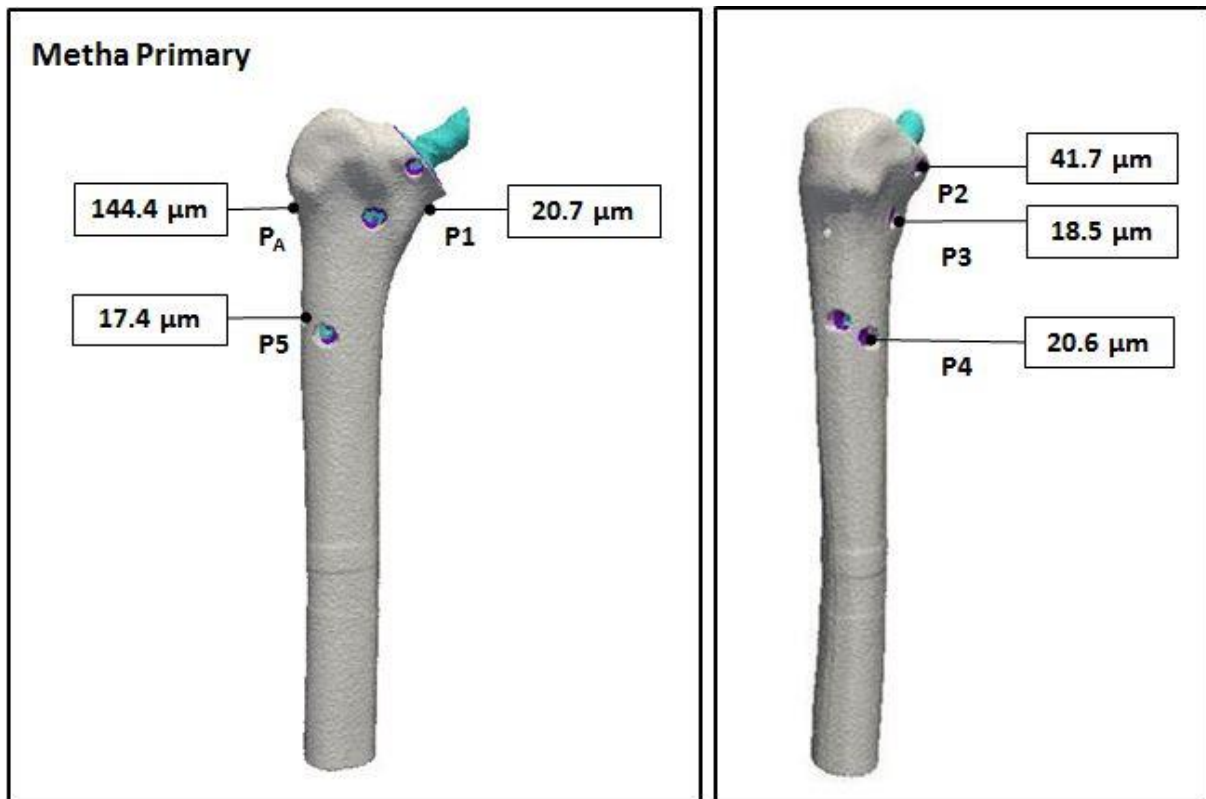


Fig. 35: 3D relative displacement determined for Metha-Primary stem in the FE model.

In the FE models of THA, CLS standard stem showed the highest 3D-relative displacement at the lateral distal point (P5), and a lowest 3D-relative displacement at the ventral proximal point (P2) (Fig. 36). The additional test point P<sub>A</sub> showed an obviously higher value than P1.

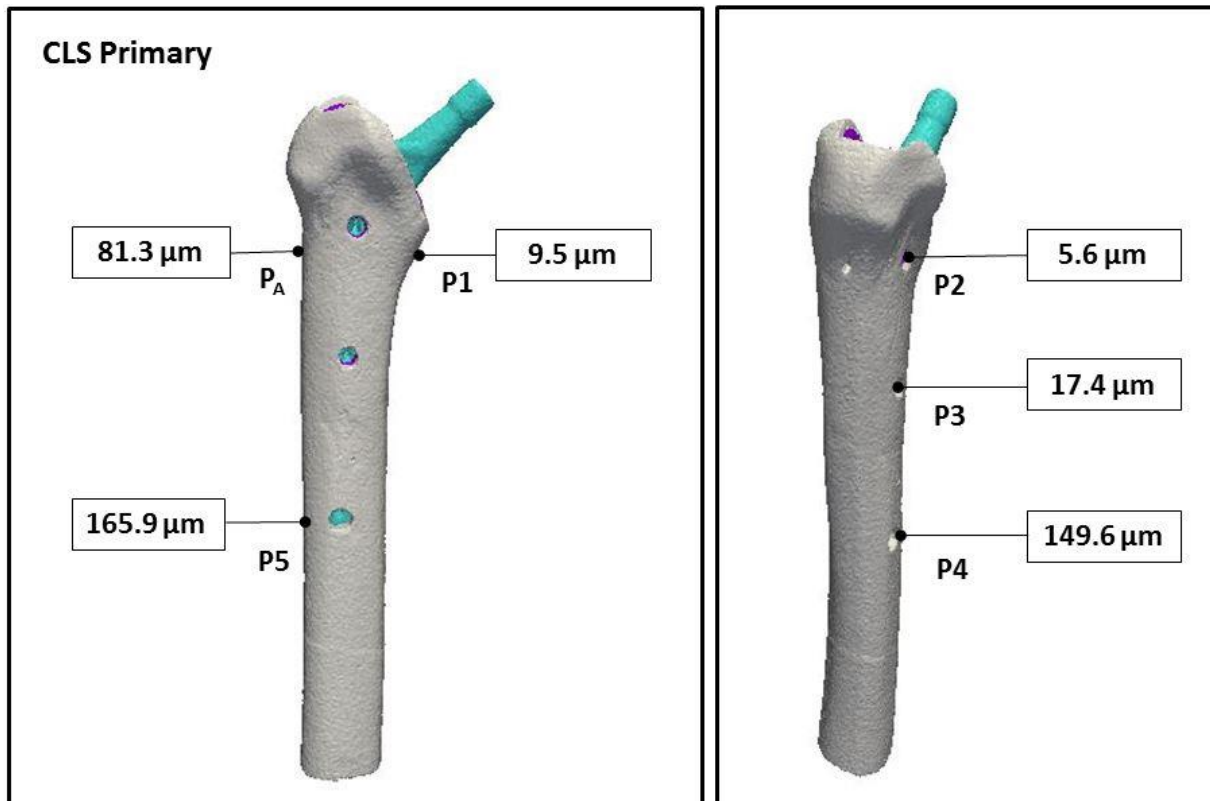


Fig. 36: 3D relative displacement determined for CLS-Primary stem in the FE model

#### 4.2.2. Comparison of primary stability between FEA and biomechanical setting

Comparing the relative displacement of Metha stem in FEA to the mean experimental micromotions revealed a consistency between the FEA and biomechanical setting. However, a clear difference was found at the medial proximal point (P1: Metha-FEA 20.7 μm vs. Metha-experiment 85.1 μm) (Fig. 37). In the FE model with CLS stem, comparing the relative displacement in FEA to the mean experimental micromotions demonstrated a consistency between the FEA and biomechanical setting (Fig. 38).

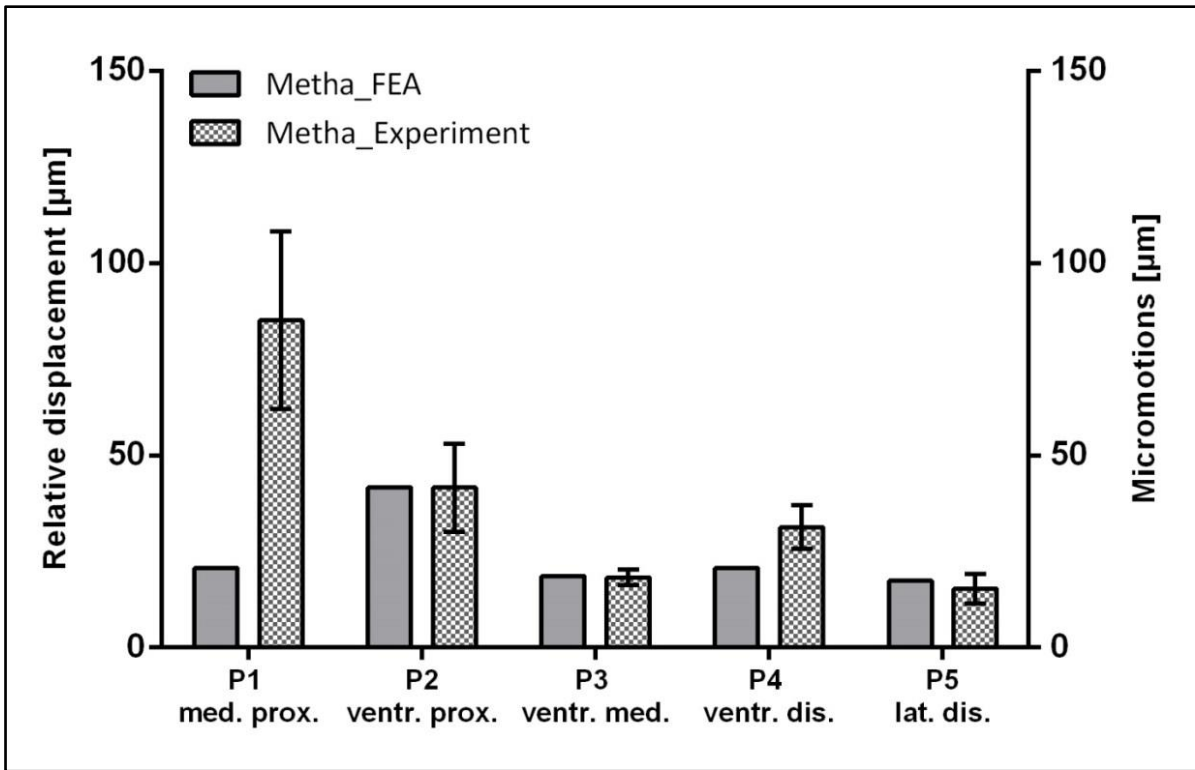


Fig. 37: Comparison between the 3D relative displacement in FEA and 3D-micromotions in experimental primary SHA. A rough consistency between them was found from P2 to P5

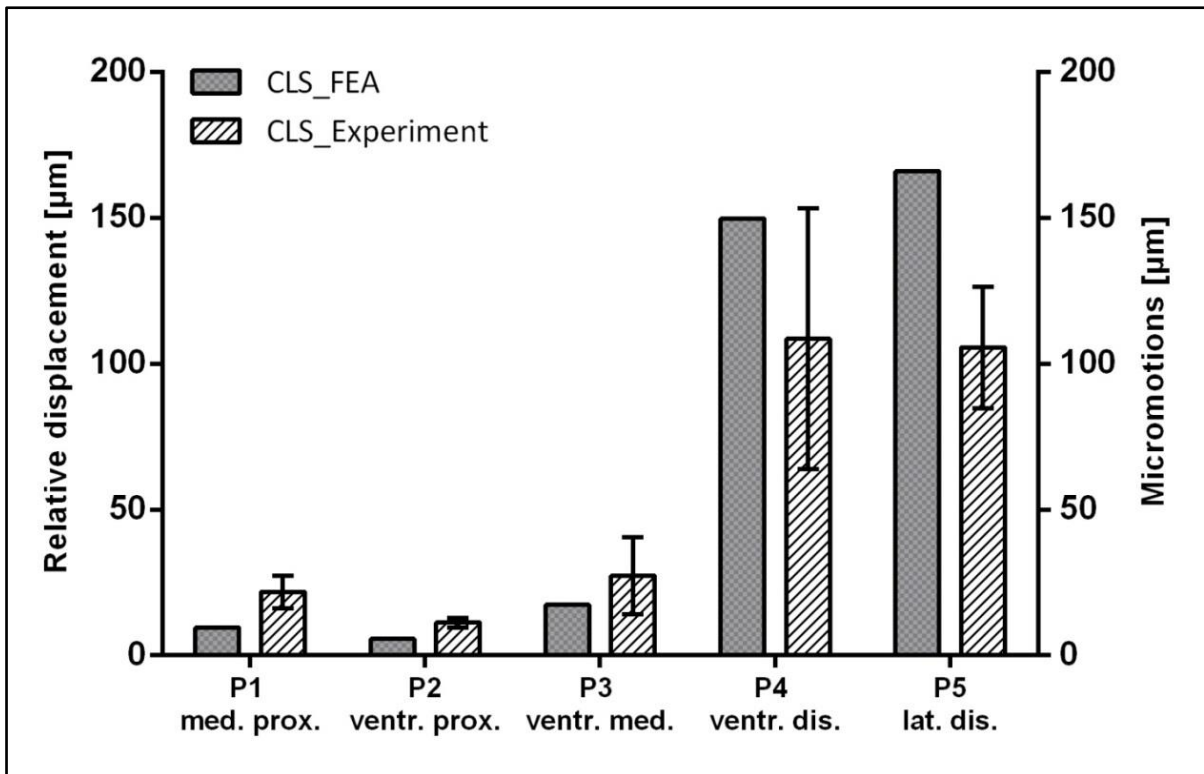


Fig. 38: Comparison between the 3D relative displacement in FEA and 3D-micromotions in experimental primary THA. A consistency between them was found from P1 to P5

### **4.2.3. Cortical stress distribution patterns of native and implanted femurs**

The analysis of mean and peak values of cortical von Mises stress for SHA and THA revealed a considerable reduction for both the Metha SHA and CLS THA stems, compared to the native femur (Fig. 39 and 40). However, clear differences could be observed between the SHA and THA designs.

The Metha SHA showed a tendency towards lower cortical stress reduction in the proximal femoral regions compared to the CLS THA, especially at the regions from less trochanter to the tip of short stem (region 11). In contrast, the cortical stress around CLS stem was more evenly distributed than that of Metha stem, but clearly showed higher stresses in distal femoral regions (regions 17 to 19).

The clear differences in the patterns of cortical von Mises stress distribution can also be obtained from the frontal, coronal and cross-sectional views of the FE models for the native bone, the SHA and the THA (Fig. 41 and 42). In native bone the stress transferred mainly along the medial-anterior and lateral-posterior cortex. In contrast, in the femurs with the THA and SHA the stress transferred mainly along the prostheses and the cortical bone was clearly unloaded.

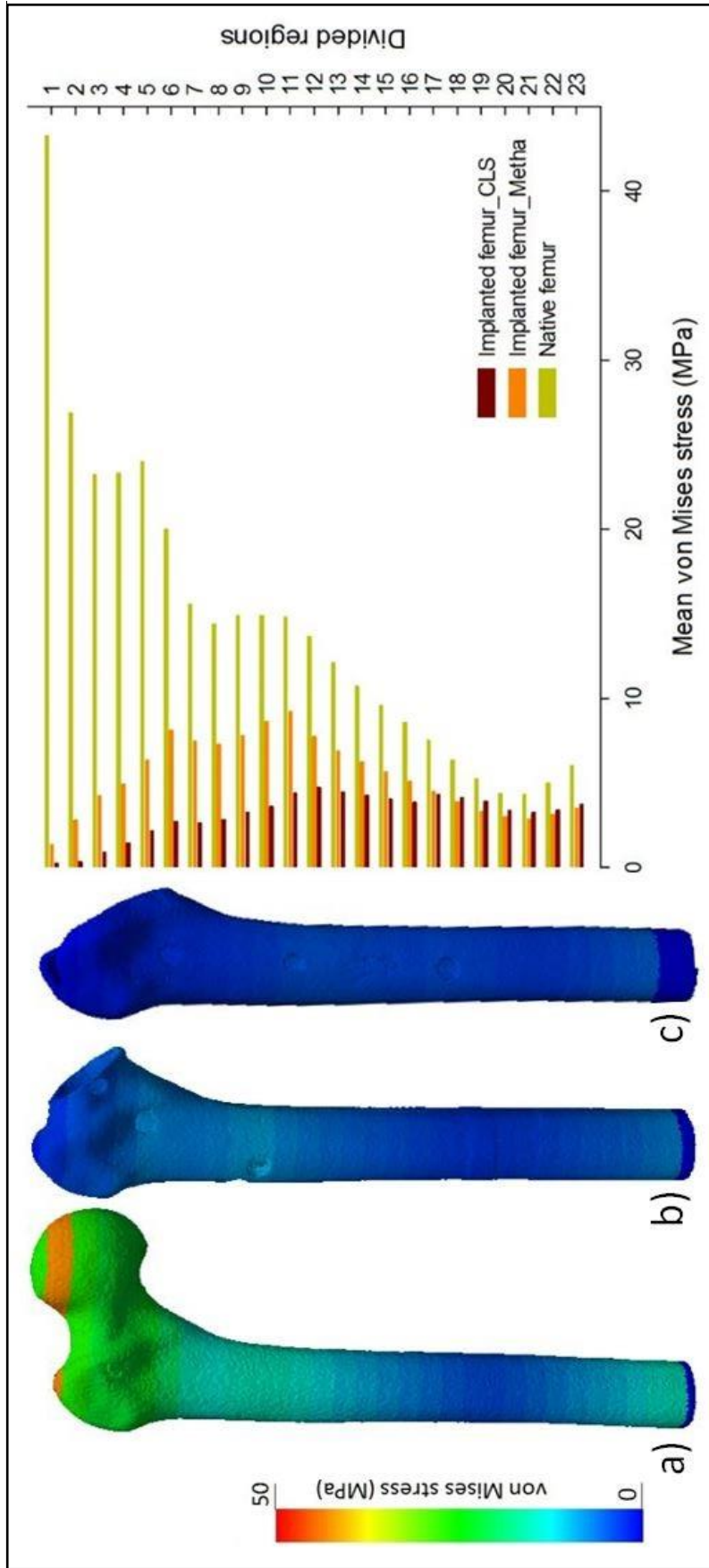


Fig. 39: Mean cortical stress distributions in the three FE models:

- a) Native bone
- b) Implanted bone with Metha short stem
- c) Implanted bone with CLS standard stem

A reduction of mean cortical stress is observed for both stems, and Metha stem shows lower reduction in the proximal femoral regions than CLS stem

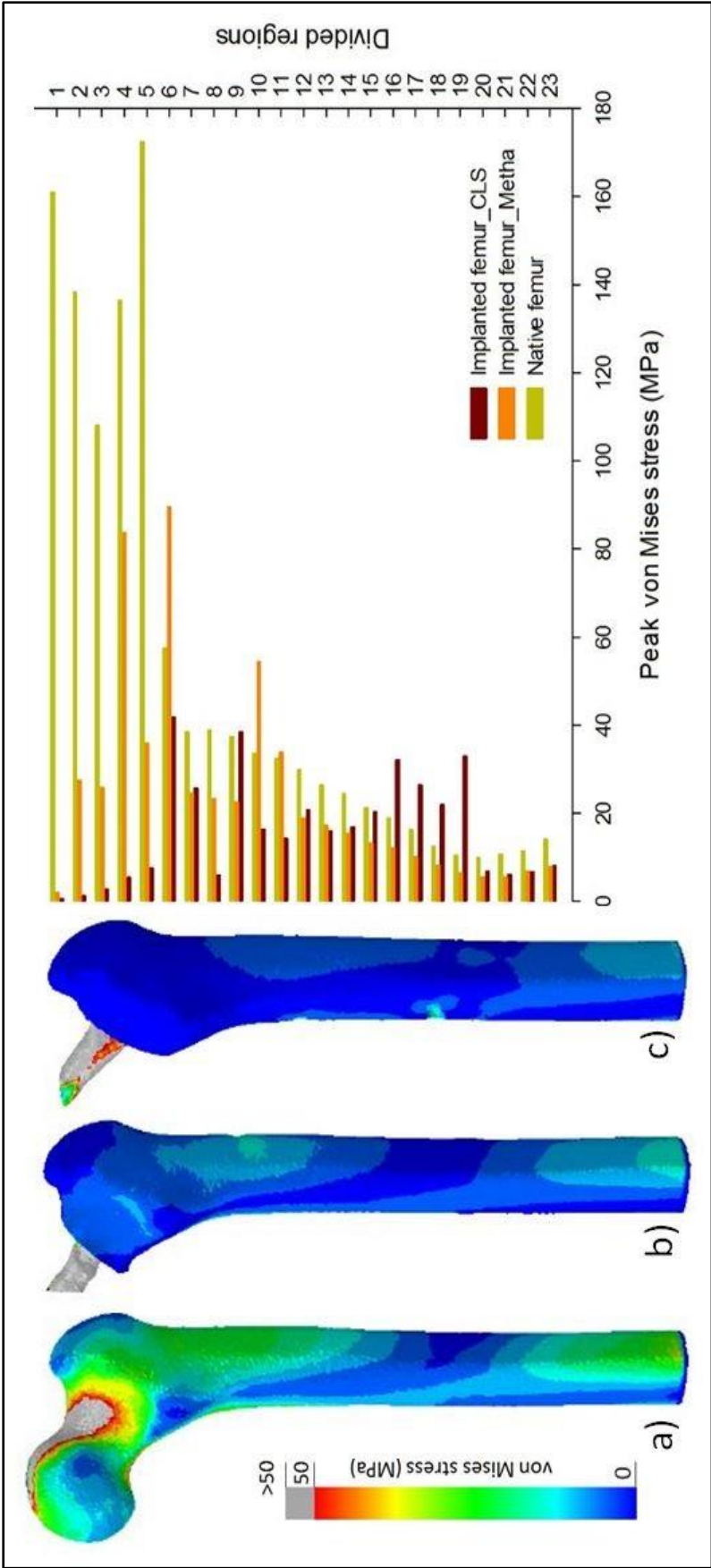


Fig. 40: Peak cortical stress distributions in the three FE models:

- a) Native bone
- b) Implanted bone with Metha short stem
- c) Implanted bone with CLS standard stem

A reduction of peak cortical stress is observed for both stems, and Metha stem shows lower reduction in the proximal femoral regions than CLS stem



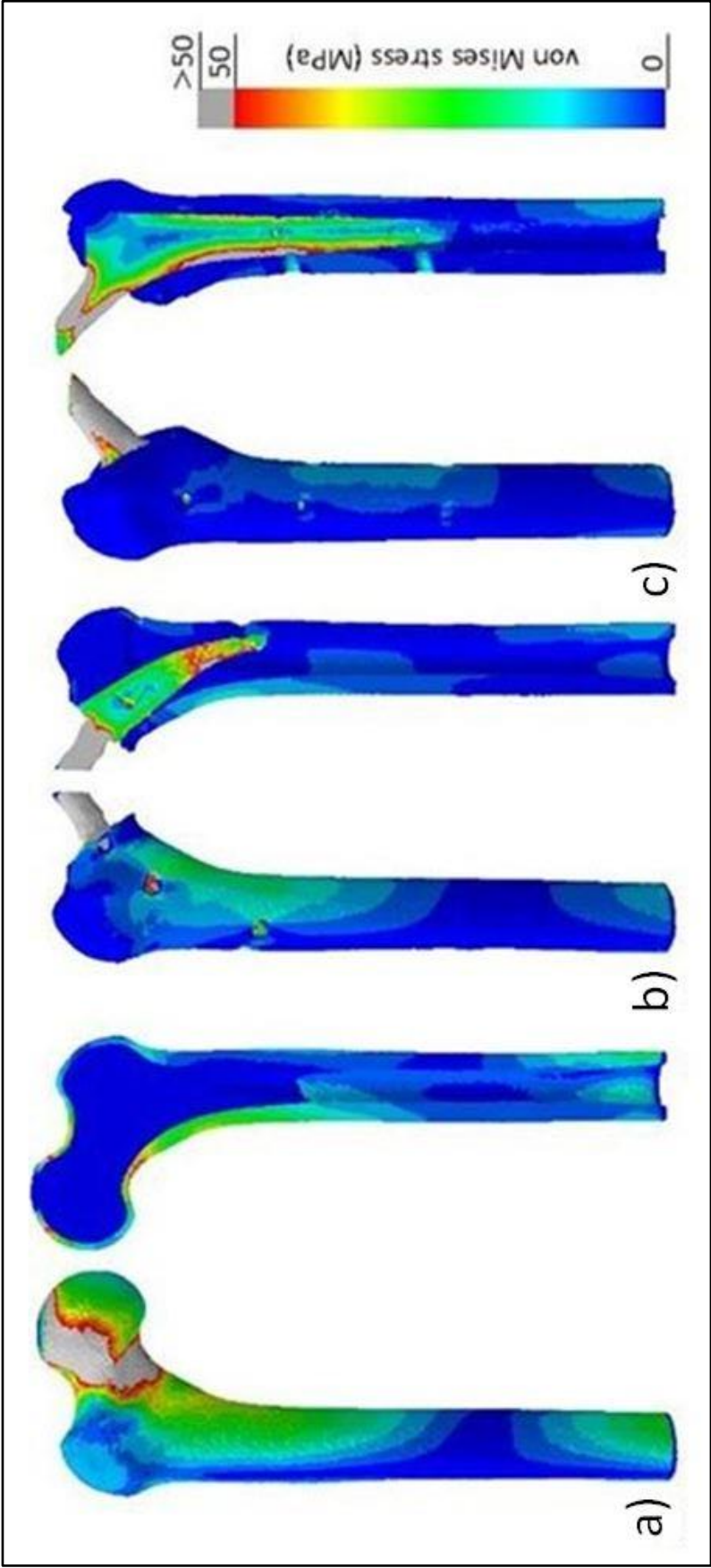


Fig. 41: Frontal and coronal views of von Mises stress distribution patterns in the three FE models:

- a) Native bone
- b) Implanted bone with Metha short stem
- c) Implanted bone with CLS standard stem

In the native bone the stress transfers mainly along the cortex. In the implanted bones the stress transfers mainly along the prostheses and the cortical bone is clearly unloaded

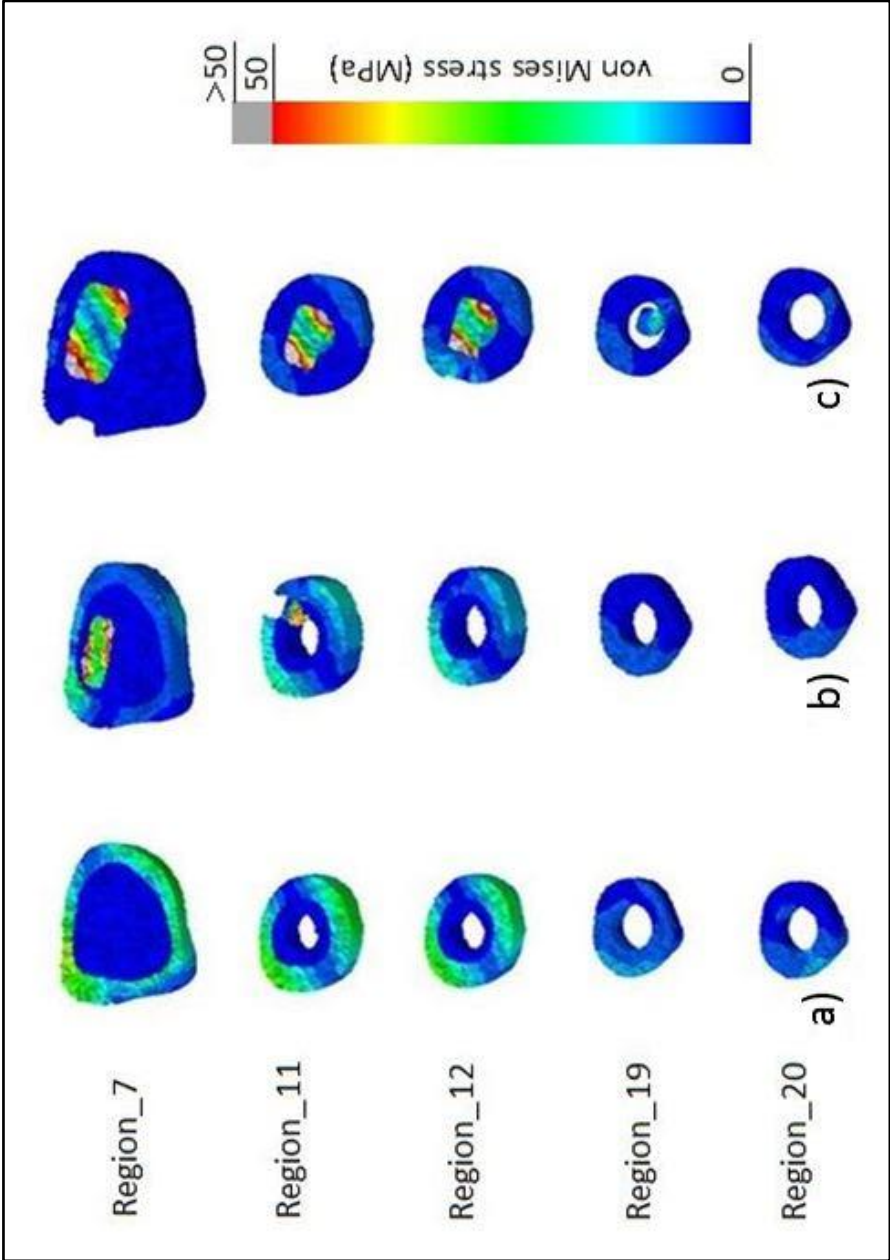


Fig. 42: Cross-sectional view of von Mises stress distribution patterns in the three FE models:

- a) Native bone
- b) Implanted bone with Metha short stem
- c) Implanted bone with CLS standard stem

In the native bone the stress transfers mainly along the cortex. In the implanted bones the stress transfers mainly along the prostheses and the cortical bone is clearly unloaded

## **5. Discussion**

The first purpose of this study was to measure and compare the micromotions of the SHA (Metha short stem) to THA (CLS standard stem) in a primary implantation scenario and further evaluate if this SHA stem (Metha) can safely be revised with a standard THA (CLS) stem in a revision scenario. For both primary implantation scenarios, the Metha and CLS stems, we found sufficient primary stability, which was predictive for a good osseous integration. However, in the primary scenario, we could observe a clear effect of the stem design on the primary stability, with the Metha SHA and CLS THA stems showing significant differences in the pattern of micromotions due to their different anchorage philosophies. In the revision scenario of the Metha SHA, we demonstrated that the micromotions for the CLS stem in the revision scenario were not higher than those of the primary CLS stem. Therefore we assume that the Metha SHA stem can safely be revised with standard CLS THA stem.

The second purpose was to develop FEA models to predict the experimentally determined micromotions and also allow comparing the stress distribution between the SHA and THA stems. Our results revealed that FEA can approximately predict the micromotions of implants in the biomechanical setting, however with the bone deformation influencing the results. Furthermore, we revealed a lower stress shielding of Metha short stem in the proximal femoral region compared to the CLS standard stem.

### **5.1. 3D-Micromotion**

Comparison between the micromotions in the primary implantation scenario of the Metha SHA and CLS THA indicated sufficient primary stability for both implants. For the Metha stem, micromotions at all tested points were less than the critical threshold of 150  $\mu\text{m}$ . According to Pillar et al. and Jasty et al., the threshold of 150  $\mu\text{m}$  was assumed to be the prerequisite for achieving osseous integration and secondary stability (Pilliar 1986, Jasty 1997). In their studies, they placed implants, which were porous-coated, into the femur of dogs and exerted various micrometers of oscillatory motion on the implants. They described the necessity of small implant micromotions (up to 28  $\mu\text{m}$ ) to allow a stable osseous integration. However, if excessive displacement (150  $\mu\text{m}$  or more) occurred, the described failure of bone integration would result in fibrous connective tissues between the bone and implant (interface).

The good primary stability of Metha short stem in the present study was in line with previous biomechanical studies. Fottner et al. compared 3D-micromotions of two types of short stems

(Metha stem and Mayo stem) to the trust plate prosthesis (TPP) (Fottner 2009). They found that all the measured micromotions of short stems were below 150  $\mu\text{m}$ . They also demonstrated high micromotions of Metha stem concentrated at the proximal femur, which was similar to the present study. Bieger et al. compared the primary stability of two short stems (Fitmore stem and Mayo stem) to a standard stem (CLS stem) using human bones. They found that micromotions did not exceed 150  $\mu\text{m}$  at almost all test points, and concluded that shortening the femoral stem did not impair the initial stability (Bieger 2012). In another study they also compared the micromotions between a short stem (Optimys) and standard stem (CBC stem), and found that both stems proved to have sufficient stability with micromotions below 150  $\mu\text{m}$  (Bieger 2013). However, in contrast to the present studies they used a different biomechanical setup calculating the global micromotions by one-dimensional micromotions measurements.

Other studies evaluated the effect of implant length on the initial stability by shortening the stem. Small et al. (Small 2017) reduced stem length as a variable in the investigation of primary stability in composite femurs. Stems with three different lengths were implanted in the femurs: short (96 mm from the stem shoulder to distal stem tip), medium (118 mm), and long (151 mm). They found no difference in micromotions between those implants with the same design but a reduced length. In another study, the length of an anatomical stem was shortened from 120 mm to 80 mm, but no significant difference of axial migration and rotation was observed between the short and the original stems (Yamako 2015).

For the Metha SHA implant, only clinical studies at a mid-term follow-up are currently available. However, up to now, these studies supported the favorable biomechanical primary stability of Metha short stem. A five-year follow-up study of 250 Metha SHAs revealed a revision rate of 3.6% (9 cases), of which only 1.2% (3 cases) was due to aseptic loosening. The other reasons for revision accounted for 2.4% (6 cases) due to infection, joint noises from ceramic-on-ceramic bearings or malpositioning during surgery (Wittenberg 2013). Schnurr et al. analyzed retrospectively the survival of 1888 Metha SHAs (mean follow-up of 6 years). The revision rate due to any reason was 4.1%. However, only 0.6% occurred due to the aseptic loosening (Schnurr 2017). Similarly, Von Lewinski et al. performed an analysis of revisions in a total number of 1953 Metha SHAs and reported an aseptic revision rate of 1.3% (26 cases) after 3 to 10 years (Von Lewinski and Floerkemeier 2015). Thorey et al. evaluated the outcome of 151 Metha SHAs (mean follow-up of 5.8 years) and found that 3 cases (2%) were revised, of which 2 cases were due to the undersized femoral component with mechanical problems and 1 case due to infection (Thorey 2013). In another retrospective

study with a series of 73 Metha SHAs, a revision rate of 4% (3 cases) was found due to any reason (mean follow-up of 2.8 years), however without any femoral stem loosening (Floerkemeier 2012). A systematic review including 7 Metha SHA studies reported a combined revision rate of 1.2% for any reason (mean follow-up of 3.7 years) (Van Oldenrijk 2014). Therefore, the biomechanical data as well as the clinical medium term data support the assumption that the Metha short stem implant offers a good primary stability, which allows a secondary osseous integration.

The primary stability of the CLS THA in the present study showed low micromotions in the proximal part of the implant. In contrast, high micromotions which reached or even exceeded the threshold of 150  $\mu\text{m}$  were observed at the distal stem tip. Similar results were obtained in two former studies from our institute measuring 3D-micromotions (Schmidutz 2017, Fottner 2011). In one study, different sizes of CLS implants were investigated, of which the same and appropriate stem size of 13.75 was used. The results similarly showed the highest micromotions at the distal stem tip and also exceeding 150  $\mu\text{m}$  (Schmidutz 2017). The other study evaluated various offset versions of the CLS stem (all stems with size 13.75) and similarly revealed the highest micromotions at the distal stem tip even exceeding 200  $\mu\text{m}$  (Fottner 2011). Furthermore, Nadorf et al. measured the rotational stability of CLS stem using the setup for capturing 3D-micromotions. In accordance with our results, they reported the lowest micromotions within the proximal part of the stem and the highest micromotions near the distal stem tip.

Although comparison with other studies is difficult due to the differing biomechanical setups, the pattern of the CLS stem revealed similar results. Bieger et al. reported the highest micromotions for the distal part of the implant without exceeding 150  $\mu\text{m}$  (Bieger 2012). Heller et al. and Kassi et al. found less micromotions of CLS stem compared to our study, without exceeding the limit of 150  $\mu\text{m}$  (Heller 2005, Kassi 2005). These different results are very likely related to the different methods used for evaluating the micromotions. These studies only employed one LVDT to register one-dimensional micromotions at all tested points, resulting in substantially lower results than using 3D-measurement methods.

Nevertheless, all biomechanical results reflect the anchorage philosophy of the CLS stem which intends to achieve a proximal fixation and proximal load transfer (Evola 2014). The thin distal part doesn't "fit and fill" the medullary canal in order to prevent exceeding load transmission at this area, where the osseous integration for secondary stability is not aimed to be achieved (Pepke 2014). Therefore the micromotions measured in the distal part are higher than the proximal part.

The evidences of good primary stability in CLS THA, based on the available clinical data with medium- to long-term follow-up, have been well documented in multiple studies that reported excellent survival rates (Yamasaki 2014, Merle 2011, Streit 2012). Aldinger et al. evaluated the clinical results of 154 CLS THA in 141 young patients with the age less than 55 years. They showed that the overall revision rate of the stem was 3% due to any reason after 12 years, of which 1% resulting from femoral revision for aseptic loosening (Aldinger 2003). The authors also retrospectively evaluated the survival of 354 THAs in 326 patients (mean age 57 years) in another study. They found that the overall revision rate of the stem was 12% due to any reason after 17 years, of which 6% resulting from the aseptic loosening of femoral component as the endpoint (Aldinger 2009). Similarly, Streit et al. retrospectively reviewed the clinical results of a series of 89 CLS THAs in 88 patients younger than 60 years old, and revealed that a revision rate of the stem was 4% for any reason after 12 years, of which 1% due to aseptic loosening (Streit 2012). De Witte et al. studied a series of 102 CLS THAs with the minimal follow-up of 10 years. The authors reported a total revision rate of 21.6% due to any reason after 15 years, but only a revision rate of 1 % due to aseptic loosening of the femoral component (De Witte 2011). Another study with a series of 92 CLS THAs demonstrated a survival rate of 91.5% after 23 years, however including all component loosening (Evola 2014). Biemond et al. performed a cohort study of CLS THA in young patients, and reported a survival rate of 95.7% after 19 years with revision for aseptic loosening (Biemond 2015). These clinical studies support the assumption that the CLS standard stem implant offers a good primary stability and provides a desirable osseous integration.

After showing the good primary stability of both implants, Metha and CLS, we simulated a revision scenario of the Metha stem and revised this stem with a standard THA CLS stem. In this revision scenario, the CLS stem showed a comparable primary stability as the CLS stem in the primary scenario. No significant higher 3D-micromotions were found in the revision CLS scenario for all the tested points compared to the primary CLS scenario. Furthermore, also in this revision setting, the micromotions of the CLS revision stem revealed the highest micromotions at the distal stem tip and lowest micromotions at the proximal region. In conclusion, this indicated that the CLS design with its proximal fixation can still achieve a firm fixation when revising the Metha SHA stem.

It further indicated that enough bone substance in the proximal femur was conserved during the implantation of the Metha SHA stem, thus allowing a firm fixation for the subsequent CLS stem in a revision setting. This encourages the assumed advantage of the Metha SHA

stem that is supposed to conserve bone stock in the proximal femoral region. In fact, this may facilitate revision procedures in the daily clinic and also allow using a standard cementless stem in such a revision (Falez 2008, Tahim 2012).

Currently, our biomechanical data from the revision scenario are difficult to validate and compare to the clinical data, as only few clinical studies about the revisions after SHA are available. Von Lewinski et al. reported 38 SHA revisions in a total number of 1953 Metha SHAs. Of those revisions, 50% (19 cases) were due to aseptic implant loosening and 32% (12 cases) were due to the modular neck adapter fractures. In 18% (7 cases) periprosthetic fractures or a *via falsa* occurred during implantation. However, in the further revision procedures, 34 of the 38 cases (90%) could be revised by cementless standard THA implants, two (5%) by short SHA implants and two (5%) by revision implants (Von Lewinski and Floerkemeier 2015). Schnurr et al. reported 38 revision cases with stem removal and 34 revision cases without stem removal in a series of 1888 Metha SHAs. 34 cases (90%) of the 38 Metha stem revisions were revised with primary cementless stems (Schnurr 2017). Wittenberg et al. reported 9 revision cases from 250 Metha SHAs, and all the revisions were performed using primary standard stems (Wittenberg 2013). Thorey et al. revealed 3 cases of revision THAs in a total of 151 Metha SHAs, of which 2 cases required a revision to a standard hip stem (Thorey 2013). In another retrospective study, 3 cases of revision THA were performed in a series of 73 Metha SHAs, of which 2 cases required a revision to a standard hip stem and 1 case required a revision stem (Floerkemeier 2012). However, a more detailed analysis is currently not available in the literature and long-term follow-up studies of these revision THAs are not yet available.

Other studies documented the survival rate of primary cementless stem revising cemented or standard cementless stems. Tauber et al. performed a retrospective study of 24 CLS revisions for the failed cemented THAs (mean follow-up 4.5 years), of which 1 case was due to septic loosening and 23 cases due to aseptic loosening. They found that 20 cases had a good fit, no loosening, and no revision, indicating that CLS stem can be safely used in revision THA for aseptic loosening (Tauber and Kidron 2000). Thorey et al. studied the use of another primary cementless stem (Bicontact stem) in revision THA. In this study, 79 revision THAs were included, of which 69 cases were for the reason of aseptic loosening. They found a survival rate of 96.2% with the revision as endpoint after 10 years (Thorey 2008). Similarly, Gastaud et al. reported an adequate fixation of a primary anatomical cementless femoral stem in revision THA, with the survival rate of 85% after 6.7 years (Gastaud 2016). These studies

provide the assumption that the primary cementless stem can also be used in the revision THA, confirming the biomechanical data in the present study.

Notably, we found a bony defect in the calcar region in the revision scenario. This defect is derived from the curved and wider design of the short stem with the aim of achieving calcar support and restoring a more physiological load (Von Lewinski and Floerkemeier 2015). This bony defect caused an absence of contact at the medial proximal part of the revision CLS stem in the calcar region (Fig. 34). However, when comparing the points (P1 and P2) at the calcar level between the revision and primary CLS, no significant difference in the micromotions was detected. Therefore, it can be assumed that this visible defect at the calcar didn't negatively affect the initial stability of the CLS revision stem. Probably this is a result of the trapezoidal cross-section and longitudinal fins on the posterior and anterior surfaces of the proximal part of the CLS stem. Those ribs allow a slight embedding of the implant into the trabecular bone and increase the area of bone-to-implant contact, hence increasing the axial and rotational stability of the CLS stem (Evola 2014, Pepke 2014). However, this only accounts for the estimated CLS stem and might be different for other standard THA stems.

Furthermore, this in vitro biomechanical setup only evaluated a simple revision. We didn't take into account the presence of large bone loss due to osteolysis, infection or fracture. The bone defect in the revision THA can be classified into four types: type I and type II indicates a minimal to an extensive defect of metaphyseal trabecular bone and a fully intact diaphysis; type III and type IV shows severely damaged metaphysis and slightly to severely damaged cortical bone (Della Valle and Paprosky 2004). Khanuja et al. performed a study on the survival rate of a primary cementless stem in 19 revision THAs, of which 6 hips were type I and 13 hips were type II. They found the aseptic stem survival rate was 95% after a mean of 4.1 years, indicating that the primary cementless stem can be safely used in revision THA with the bone defect of Type I and II (Khanuja 2014b). For the large bone defects, the situations are a completely different entity and are not tested in the present study. Surgeons should be aware of the larger defect situation, especially the bone loss at the anterior and posterior surface, which might reduce the stability of the CLS stem. In such situations, implants with a more distal anchorage or even a long revision stem need to be taken into account (Gortz 2002, Jakubowitz 2008, Valle and Paprosky 2003).

Comparing our biomechanical data to other studies is difficult due to the diversities in the loading conditions, specimens and ways of data capturing (Gheduzzi and Miles 2007). Gortz et al. and Thomsen et al. tested 3D-micromotions using a similar setup compared to ours, while they only applied torsional loads (Gortz 2002, Thomsen 2002). Most other studies



measured micromotions using only one LVDT at each point which resulted in considerably smaller micromotions than the present study (Bieger 2012, Bieger 2013, Heller 2005, Kassi 2005). Three previous studies performed in our institute used a similar biomechanical setup and loading conditions as the present study, demonstrating comparable micromotions results (Schmidutz 2017, Fottner 2009, Fottner 2011).

Besides, it has to be noted that a variety of short stems (SHA), are currently available, however with different geometries and anchorage philosophies. This probably results in different revision scenarios due to different resection levels and more or less femoral filling designs (Van Oldenrijk 2014, Khanuja 2014a). Therefore, the current data can only be suitable for the Metha and CLS stems, and should be critically applied to other implants.

As a limitation of the present study, the use of composite femur instead of fresh frozen human cadaveric femur has to be noted. Human bones can offer more realistic conditions than composite femurs, while the composite bones are characterized by consistent geometries and mechanical properties. The variability of structural and mechanic properties of composite femurs are much smaller than those seen in natural human bones (Heiner and Brown 2001), Therefore in this study, we preferred the composite femurs which provided a higher comparison and more standardized conditions, as being desired for this study.

Further limitations of the present experimental study have to be considered. First, we only simulated a revision scenario with the absence of a large bony defect. Larger bone defects, which might result from osteolysis, infection or fracture, have to be analyzed separately. Second, no muscle forces were simulated in the present study, which might influence the micromotions and thus the global primary stability of the implants. Stolk et al. (Stolk 2001) suggested that a loading profile including the abductor muscle forces and hip joint contact force was adequate to generate physiological stress on the implant in pre-clinical tests. Third, it was impossible to observe the bone growth with respect to the secondary stability of the implant in the composite femur, although the relationship between the primary stability and osseous integration had been demonstrated (Pilliar 1986, Jasty 1997). Last, in vitro biomechanical studies do not necessarily reflect the in vivo situation as the patients' characteristics, such as muscles, activity, and bone quality, which might influence the implant stability, were not considered in the present study (Britton 2003, Pancanti 2003, Maier 2016). Thus the results have to be furtherly reevaluated based on clinical studies and should not be transferred in an uncritical way to the clinical practice.

## 5.2. FEA study

In the second section, we used FE analysis to predict the micromotions obtained from the biomechanical setting, and further evaluated stress distribution in bone and implant structures to assess the potential stress shielding of the tested implants. The FE analyses showed a sufficient primary stability for both the Metha short and CLS standard stems. For the Metha stem, the relative displacements were below the critical threshold of 150  $\mu\text{m}$  at all tested points, which allowed osseous integration. Only few studies performed a similar comparison between a biomechanical and FEA setup in determining micromotions. Dabirrahmani et al. performed an FEM study for the Birmingham Mid Head Resection (BMHR) stem and evaluated the primary stability and long stability. In their study, the FE models were reconstructed from CT scanning images of cadaveric bone and implants. They found micromotions below 150  $\mu\text{m}$  at the whole bone-implant interface (Dabirrahmani 2010). Gabarre et al. performed a comparative study to assess the biomechanical behaviors of two short stems (Linea Anatomic and Minihip). In this study, FE models were established based on the CT scanning images of cadaveric bone and implants. Micromotions at the bone-implant interface were obtained under gait cycles. They found that the average micromotions for both stems were below the critical limit of 150  $\mu\text{m}$  (Gabarre 2016). However, it has to be noted that the stems used in these studies were different with the Metha stem. Besides, rather than testing micromotions at the bone-implant interface, the present study measured the relative displacement between the implant surface and outer cortical surface in order to simulate the biomechanical setup.

In our FE model with CLS stem, low micromotions were observed in the proximal femur, and high micromotions reached or exceeded the threshold of 150  $\mu\text{m}$  at the distal stem tip. This result was in accordance with other FEA studies. Pancanti et al. performed an FEA study to evaluate the initial stability of a cementless anatomical stem (ANCAFit stem) under different activities. In their study, micromotions of the stem were determined as the relative nodal movements between the stem surface and the inner bone surface. They found that low micromotions concentrated in the proximal part of the implant and the high micromotions concentrated at the distal part of the implant, however without exceeding 150  $\mu\text{m}$  (Pancanti 2003). Ong et al. evaluated the primary stability of a cementless straight stem (Omnifit-HA). The load was applied with hip and muscle forces to simulate daily activity. The authors demonstrated higher micromotions of distal stem compared to the proximal stem, and the maximum micromotions exceeded 1000  $\mu\text{m}$  under stair climbing (Ong 2009). Baharuddin et

al. conducted an FEA study to investigate the primary stability of an anatomical cementless stem. They found that the micromotions were 1.5-2.0  $\mu\text{m}$  in the proximal region and 10-12  $\mu\text{m}$  in the distal region (Baharuddin 2014). These data of different studies showed a high variability compared to ours. This is probably related to the different conditions simulated, such as the specimens, loading conditions, and simulation methods. It also shows the need for further research in this field as well as the need for standardization of the simulation conditions.

In the presented FE model, the area where the outer implant surface and the inner bone surface had contact were fully bonded at nodes and therefore the contact model didn't allow the interface to be separated and slide. Thus the micromotions registered at this area were due to the elastic bony deformation, especially for the median tested points where the implant had full contact with the bone. It indicated that the experimental micromotions obtained from the present biomechanical setting also included, at least in part, the elastic bony deformation and movement at the interface. This was also reported by Whiteside et al., who noticed that the relative deflection between the surfaces of outer bone and implant included the elastic bony deformation and the relative movement at bone-implant interface (Whiteside 1993).

The current finding of the elastic bony deformation is also in accordance with Tarala et al. (Tarala 2011), who compared the micromotions of a femoral implant in a case-specific FE model to an experiment. Sensors used in the experimental study were fixed to the implant surface and outer surface of cortical bone. In the case-specific FE model, the authors changed the bony reference point from the outer to the inner bone surface, while the implant point was only selected at the implant surface. They revealed that the FEA micromotions became smaller with decreasing the distance between the implant point and the bony reference point. Monti et al. (Monti 1999) measured the effect of elastic bony deformation by an experimental study. In their study the anchorage of an LVDT was fixed to the outer bone surface, and a pin was fixed to bone cortex at three different depths to measure the movements in response to the bone deformation: 0.5mm above the bone-implant interface, 0.5mm below the outer bone surface, and the midpoint between the two former levels. They showed that the movement caused by the cortical deformation reduced as the distance of the reference points decreased. However, the authors didn't show the contribution of it to the micromotions between the surfaces of outer bone and implant. Furthermore, the movement caused by the deformation of trabecular bone was not included.

In this study, the phenomenon could be demonstrated as the relative displacement at the lateral proximal point  $P_A$  showing a considerable higher value than that at P1 (Metha:  $P_A$

144.4  $\mu\text{m}$  vs P1 20.7  $\mu\text{m}$ ; CLS: P<sub>A</sub> 81.3  $\mu\text{m}$  vs P1 9.5  $\mu\text{m}$ ). P<sub>A</sub> and P1 had the same implant reference points. The bony reference point of P<sub>A</sub> located at the outer surface of the lateral proximal bone, while the bony reference point of P1 located at the outer surface of the medial proximal bone. The difference can be explained by the elastic bony deformation between the two different bony reference points during loading.

Furthermore, the present FE study showed a considerable reduction in cortical stress after implantation of the stems, indicating that stress shielding occurred for both the short and standard stems. This result can be explained by the insertion of a rigid implant into the femoral cavity. By this, the normal stress distribution of proximal femur will change and stress will be transferred through the prosthesis to the distal femur. This stands in clear contrast to the native bone where stress is transferred through the femoral neck to the distal cortical bone (Arifin 2014). The transfer via the implant reduces the stress on the bone and leads to stress shielding effects, especially in the proximal femur (De Martino 2017). This finding is consistent with previous FEA studies. Pozowski et al. conducted an FEA study to analyze the biomechanical parameters of Metha stem hip replacement. They found that in the correct stem setting, the stress distribution on the bone was different between the lateral side and medial side. Lower stresses were found at the calcar region and higher stresses were observed in the region of the distal stem tip. However, their study didn't compare the stress of implanted bone to the native bone (Pozowski 2013). Another FEA study compared the stress-strain state of the intact human femur to the implanted femur with cementless femoral stems. A clear stress shielding on the proximal femur was found in this study (George and Saravana Kumar 2013). Fraldi et al. identified the stress at the interface between bone and cementless stem. Although the FE models were constructed using different parameters, they found consistently that in all the models the stress shielding existed after implantation (Fraldi 2010). In the present study, we did not measure the stress distribution experimentally in a 3D setup, which is not possible experimentally. However, a previous study performed in our institute supported the finding of stress shielding in the present FEA of the CLS implant (Schmidutz 2017). In this study, strain gauges were attached to the femoral cortex from the proximal femur to the distal level of stem tip at three heights. The strain measurements were performed on both the intact and implanted bones, and the same load with the present study was applied. The authors found a typical stress shielding in the CLS THA, and a high reduction of cortical strain especially in the proximal region, which was in line with our data.

The evidence of stress shielding in the FE analysis is furthermore in line with available clinical studies. Jahnke et al. (Jahnke 2014) conducted a study to investigate the bone

remodeling of 40 Metha SHAs with 1-year follow-up. The BMD values were measured by using dual-energy-X-ray absorptiometry (DEXA). Gruen zones 1-7 were used to assess the bone remodeling in different regions (Gruen 1979). The change of BMD was defined between 1 week postoperatively and the final follow-up. The authors found a higher reduction of BMD at Gruen zone 7 (calcar region) by - 11.5% and Gruen zone 1 (greater trochanter region) by - 8.4%. In the other regions, the BMD changed from - 1.4% to + 6.4. Synder et al. studied the periprosthetic bone remodeling in a series of 36 Metha SHAs with 1-year follow-up. They reported a higher reduction of BMD at calcar region by - 23.3% and at the greater trochanter region by - 10.5%. Furthermore, a change of BMD at Gruen 2-6 was observed ranging from - 7.8% to + 1.8% (Synder 2015).

For the CLS stem, Wolf et al. performed a study on 38 CLS THAs to evaluate the bone remodeling. They observed that the highest bone loss occurred in the calcar region and revealed a BMD loss of - 22% at the 5 years follow-up. In contrast, the bone loss at Gruen 1-6 was clearly lower ranging from - 4.8% to - 1.1% (Wolf 2010). Freitag et al. investigated the pattern of periprosthetic bone remodeling in a total of 138 CLS THAs. They revealed a bone loss by - 16.7% at the calcar regions. In other regions, the reduction of BMD was lower ranging from - 10.8% to - 2.2% (Freitag 2016). All these clinical studies showed a considerable bone loss in the proximal femoral region due to the stress shielding after implantations, confirming the FEA data of the present study.

Comparing the SHA and THA in our study, the FEA data revealed a lower stress shielding of the short Metha SHA stem to the standard CLS THA stem in the proximal femur. This is consistent with the design of Metha short stem, which includes the double tapered shape, the high level of the femoral resection, the medial calcar support, and the lateral support of the distal tip of the stem. These factors probably contribute to the reduced stress shielding and more physiological load transfer. Besides, our analysis confirmed the more proximal load transfer of the Metha short stem with a metaphyseal anchorage. This was in contrast to the pattern of the CLS standard stem. The stress at the calcar level was clearly reduced and gradually increased toward the distal part of the stem. This indicated that the load transfer for the conventional CLS standard stem existed in both the metaphyseal and diaphyseal femoral regions.

These FEA findings of lower stress shielding in SHA were in accordance with previous biomechanical studies. Gronewold et al. compared the changes in stress distribution between the Metha SHA and Bicontact THA using a biomechanical setup. Strain gauges were fixed at the same level for these Metha SHA and Bicontact THA stems, and 6 different loading

configurations were applied. The authors reported that for the Metha stem the cortical strains were similar to the intact bone, even at the calcar which accounted for 87% of the intact bone. For the Bicontact stem, higher reduction of strain was observed in the proximal femur. They concluded therefore a more metaphyseal anchorage for the Metha stem and in contrast a more metaphyseal-diaphyseal anchorage of the Bicontact stem (Gronewold 2014).

Similarly, Bieger et al. compared the cortical strain for the Optimys SHA stem to the standard CBC THA stem and tested the strain at three levels along the implant (proximal, middle and distal). Their results revealed a lower stress reduction in the proximal and distal levels for SHA compared to THA. In the middle level, the stress shielding was similar for both stems (Bieger 2013). They also conducted another study to compare the cortical strain changes of a new short stem THA (Fitmore stem) to an established short stem (Mayo stem) and standard stem (CLS stem) THAs, and reported a lower stress shielding of the new Fitmore SHA short stem compared to the Mayo and CLS stems (Bieger 2012).

Besides, multiple clinical studies supported the more physiological load transfer of short stems compared to the standard stems. Salemyr et al. conducted a randomized clinical trial with DEXA to compare the bone remodeling in SHA to standard THA. 26 SHAs with ultra-short stem (Proxima stem) and 25 THAs with standard stem (Bi-metric stem) were included. They found a lower bone loss of SHA than THA in the proximal femur after 2 years. The changes of BMD at Gruen zones 1 and 7 were - 2.5% and - 12.8% in SHA, which were - 20.6% and - 17.3% in THA (Salemyr 2015). Kim et al. established a randomized DEXA study to compare the periprosthetic bone remodeling following SHA and THA with a follow-up of 11.8 years. 200 SHAs with ultra-short stem (Proxima stem) and 200 THAs with standard stem (Profile stem) were included. They found that SHA provided a better bone remodeling than THA in the proximal femur. At the calcar region (Gruen zone 7), the bone loss was - 40.5% for SHA and - 72% for THA. In the greater trochanter region (Gruen zone 1), the changes in BMD were + 3.5% for SHA and - 12% for THA (Kim 2016). Freitag et al. performed a randomized study with 1-year follow-up, including 57 SHAs (Fitmore stem) and 81 standard THAs (CLS stem). The authors reported a comparable bone loss at the calcar region for the two stems. However, at the Gruen zone 6 (proximal medial region) the SHA showed a significantly less BMD loss (- 4.7%) compared to the THA (- 10.8%) (Freitag 2016). These clinical studies demonstrate that short femoral stems seem to produce less stress shielding compared to the standard stem in the proximal femoral region.

However, also for the FE analysis, several limitations have to be considered. First, the bone-implant surface was simulated to be bonded without sliding, separation, and penetration. Thus

the relative movement could not be obtained at the area where the bone and implant fully contacted. Second, there were only two specific FE models subjected to simple loading configurations without muscle forces. Third, the holes in the models would alter the mechanical behavior of bone and produce an effect on the stress distribution. Last, the load transfer pattern was estimated by the mean and peak cortical von Mises stress in divided regions, regardless of the direction of the stress, such as compressive or tensile stress.

### **5.3. Comparison of the FE analysis and biomechanical study**

In the present study, the relative displacements obtained from the FEA were able to predict the pattern and amount of micromotions measured experimentally, but did not perfectly match with the experimental data. Therefore, it can be assumed that the FE analysis can to some extent be used to predict the primary stability of a cementless femoral stem, but it remains unclear if without refinement this method can allow an accurate determination of the amount of micromotions. For the Metha SHA, the relative displacements in the FE model were lower than the mean experimental micromotions at the medial proximal (P1) point. Similar results were observed between them at the other four testing points. For the conventional THA CLS stem, the relative displacements in the FE model were similar to the mean experimental micromotions at all testing points. Therefore, the results from FE models with both stems were in line with the patterns of experimental micromotions. Notably, the relative displacements at the medial proximal point in the SHA was obviously lower than the experimental micromotions. This can be in part explained by the different bony reference point chosen, the bonded interfaces and the elastic bony deformation which was not accounted experimentally. In the FEA, the bony reference point on the outer cortical bone was chosen next to the implant reference point. Nevertheless, in the biomechanical setting, the fixation system was fixed through three screws fixed to the femur. Thus, a virtual average point combining the three attachment points should be considered as the actual bony reference point.

The predictability of the primary stability using FEA was also supported by other FEA studies. Pettersen et al. used subject-specific FE model to test the micromotions of a cementless femoral stem, and validated it with the experimental method. The FE models were built using the same experimental cadaver femurs and the boundary conditions of the experimental set-up were replicated into the model. They found a high correlation of axial rotation between

experiment and FEA ( $R^2 = 0.74$ ). However, they also stated a poor correlation of axial translation between the experimental study and the FE analysis ( $R^2 = 0.05$ ) (Pettersen 2009a). Viceconti et al. (Viceconti 2000) studied the primary stability of an implanted composite femur using FEA. The FEA results were also compared to the experimental results. They demonstrated that FEA could predict the experimentally determined micromotions with a peak error of 14  $\mu\text{m}$ . In another study, Vicenti et al. used an FE model to assess the bone-implant micromotions under stair-climbing joint loads. They simulated various thicknesses of soft tissue layers around a cementless femur stem and found that the torsional stability of implant was reduced with increasing the thickness of the soft tissue layer. However, more importantly in this context, they reported that the results of the FE model were well validated by the experimental study and only revealed a peak error of 15  $\mu\text{m}$  (Viceconti 2001). Besides, Pettersen et al. demonstrated that subject-specific FE models allowed prediction of the stress shielding processes which had been obtained experimentally. They generated the FE models based on the same experimental femurs and boundary conditions. The authors found a high correlation of cortical strain between the experiment and FEA: stress shielding ( $R^2 = 0.70$ ), cortical strain on the intact femur ( $R^2 = 0.94$ ) and implanted femur ( $R^2 = 0.86$ ) (Pettersen 2009b).



## 6. Conclusion

Summarizing the results from both the biomechanical study and the FE analysis, we conclude that both the Metha short stem and CLS standard stem provided sufficient stability after primary implantation. It also became obvious that due to the different designs and anchorage philosophies the micromotions were significantly different between the short and standard stems.

We could further demonstrate that after revising the Metha SHA with a conventional CLS THA, the 3D-micromotions were not significantly higher compared to the primary CLS THA scenario. Therefore, it can be assumed that the metaphyseal anchored Metha SHA can safely be revised with a CLS standard stem in the absence of large bone defects or fractures.

Furthermore, our FE analysis revealed that the relative displacement obtained from the FE analysis was related to the experimentally determined micromotions. However, we also found that the absolute values were not equal for all reference points. This finding can at least partly be referred to the elastic bony deformation which was not accounted during the biomechanical testing, the bonded interfaces of the FEA, and the differing interface points to determine the relative displacement applied by both methods. Nevertheless, we can show that despite the respective limitations, both the FE analysis and the biomechanical test provide a means to quantify the pattern of displacement and micromotions. As it is currently unclear how well each of the methods is able to reflect the true absolute value, further research is required.

## 7. Summary

Short stem total hip arthroplasty (SHA) has recently become popular as it conserves bone stock and thus is supposed to allow revision with a standard primary stem. Besides, it is assumed to provide a more physiological load transfer to the femoral bone compared to standard total hip arthroplasty (THA). Currently, only few data are available which provide evidence that a standard stem can provide sufficient stability in such a revision procedure and also apply a better load transmission to the femoral bone. Therefore, this study was designed to evaluate the load transfer of THA as well as SHA and analyze whether an aseptic failure of SHA can safely be revised with a standard THA.

To address these questions, two different methods, an experimentally based biomechanical study and a computationally based FE analysis, were applied. The biomechanical setting was performed to determine the primary stability at the bone-implant interface. For this purpose, 3-dimensional micromotions were measured for a metaphyseal anchored SHA (Metha short stem) and compared to the results of a conventional THA (CLS standard stem) after implantation in the composite femora.

The FE analysis was applied to predict the experimentally determined micromotions and also allow comparing the stress distribution as well as the potential stress shielding between the SHA and THA stems. The FE models were reconstructed from CT images of the experimental composite femora and prostheses. The nodal displacements and cortical stress of the models were determined using ABAQUS/Viewer 6.13.

Our results of the biomechanical study revealed a good primary stability for the Metha SHA as well as for the CLS THA. However, the data also showed a significant difference in the pattern of micromotions between both implant designs. Revising the Metha SHA with a standard CLS THA stem did not show significantly higher micromotions compared to the primary CLS THA situation.

The results of the FEA revealed a moderate consistency between the relative displacement and the experimentally determined micromotions. Furthermore, a lower tendency for stress shielding was predicted for the Metha SHA in the proximal femoral region compared to the standard CLS THA.

In summary, we could demonstrate that both the Metha SHA stem and CLS standard THA stem provide sufficient stability during primary implantation. However, the different pattern of micromotions clearly demonstrated the differing load transfer to the femur according to their varying design philosophies. Our experimental data further demonstrated that in the

absence of large bony defects, the metaphyseal anchored Metha SHA stem can safely be revised with a standard CLS THA stem. The FE analysis was able to predict the displacement of implants but did not exactly match the absolute values of the biomechanical setting. Finally, the FE analysis clearly confirmed that the Metha SHA can provide a more physiological load transfer compared to CLS standard stem, which was in accordance with the biomechanical setup.

## 8. Zusammenfassung

Kurzschafthprothesen der Hüfte (SHA) werden zunehmend in der primären Hüftgelenksendoprothetik verwendet, da diese femorale Knochensubstanz erhalten und somit eine Revisionen mit einer konventionellen Hüftprothese (THA) ermöglichen sollen. Zudem wird angenommen, dass Kurzschafthprothesen, verglichen mit Standard Hüftgelenksendoprothesen (THA), eine physiologischere Lastübertragung auf das Femur ermöglichen.

Bislang gibt es jedoch wenig Evidenz die diese beiden Annahmen klar belegen. Ziel dieser Studie war es daher, die Lastübertragung von je einem etablierten SHA- und THA-Schaft zu analysieren und zudem zu überprüfen, ob der SHA-Schaft sicher mit einem konventionellen THA-Schaft revidiert werden kann.

Die Fragestellungen wurden durch zwei unterschiedliche Methoden, einen experimentellen, biomechanischen Testaufbau und eine computergestützte Finite Element (FE) Analyse adressiert. Die biomechanische Studie wurde durchgeführt um die primäre Stabilität am Knochen-Implantat Interface zu messen. Hierfür wurden die 3-dimensionalen Mikrobewegungen am Knochen-Implantat Interface von einem metaphysär verankernden SHA-Schaft (Metha Kurzschafth) und einem konventionellen THA-Schaft (CLS Standardschaft) nach Implantation in biomechanische Femora bestimmt. Danach wurde eine Revisionssituation simuliert und der Metha SHA-Schaft mit dem konventionellen CLS THA-Schaft revidiert und die Mikrobewegungen in dieser Revisionssituation erneut bestimmt und mit der Primärsituation verglichen.

Die FE Analyse wurde verwendet um die Spannungsverteilung nach der Implantation von SHA und THA Implantaten zu evaluieren und um die experimentellen Ergebnisse zu validieren. Hierzu wurden FE Modelle aus den CT-Scans der experimentell verwendeten Kunstknochen und Prothesen erstellt. Die Knoten-Verschiebungen und kortikalen Spannungen der FE-Modelle wurden mit ABAQUS / Viewer 6.13 ermittelt.

Die Resultate der biomechanischen Versuche zeigten eine gute Primärstabilität für den Metha SHA-Schaft als auch für den konventionellen CLS THA-Schaft. Allerdings zeigte sich auch klare Unterschied hinsichtlich der 3D-Mikrobewegungen. In der Revision des Metha SHA-Schaftes mit dem konventionellen CLS THA-Schaft zeigten sich keine signifikant höheren Mikrobewegungen verglichen mit dem primären CLS THA-Schaft.

Die Ergebnisse der FE-Analyse zeigten eine moderate Übereinstimmung zwischen der relativen Verschiebungen und den experimentell bestimmten Mikrobewegungen. Daneben

zeigte sich ein geringeres „stress shielding“ für den Metha SHA-Schaft im Bereich des proximalen Femurs verglichen mit dem konventionellen CLS THA-Schaft.

Zusammenfassend konnte gezeigt werden, dass sowohl der Metha SHA-Schaft als auch der konventionellen CLS THA-Schaft eine ausreichende Primärstabilität bei der Erstimplantation erreichen. Allerdings besteht ein klarer Unterschied in dem Muster der Mikrobewegungen, welche auf die unterschiedlichen Verankerungsphilosophien der Implantatdesigns zurückzuführen sind. Die experimentellen Ergebnisse legen zudem nahe, dass der metaphysär verankerte Metha SHA-Schaft, bei Ausbleiben von größeren knöchernen Defekten, sicher mit einem konventionellen CLS THA-Schaft revidiert werden kann. Die FE-Analyse erlaubte dabei näherungsweise die Verschiebung am Implantat-Interface vorherzusagen, korrespondierte jedoch nicht exakt mit den Mikrobewegungen der biomechanischen Analyse. Allerdings konnte die FE-Analyse bestätigen, dass der Metha SHA-Schaft zu einer physiologischeren Lastübertragung verglichen mit dem konventionellen CLS THA-Schaft führt und somit mit der biomechanischen Analyse übereinstimmt.

## 9. References

- Aamodt, A., Lund-Larsen, J., Eine, J., Andersen, E., Benum, P. & Husby, O. S. 2001. Changes in proximal femoral strain after insertion of uncemented standard and customised femoral stems. An experimental study in human femora. *J Bone Joint Surg Br*, 83, 921-9.
- Abdul-Kadir, M. R., Hansen, U., Klabunde, R., Lucas, D. & Amis, A. 2008. Finite element modelling of primary hip stem stability: the effect of interference fit. *J Biomech*, 41, 587-94.
- Abdulkarim, A., Ellanti, P., Motterlini, N., Fahey, T. & O'byrne, J. M. 2013. Cemented versus uncemented fixation in total hip replacement: a systematic review and meta-analysis of randomized controlled trials. *Orthop Rev (Pavia)*, 5, e8.
- Aesculap Implant Systems. n.d. Metha® Short Hip Stem System [Online]. Available: <http://implantesclp.com/uploads/pdf/Metha.pdf> [Accessed June 14 2017].
- Aldinger, P. R., Jung, A. W., Breusch, S. J., Ewerbeck, V. & Parsch, D. 2009. Survival of the cementless Spotorno stem in the second decade. *Clin Orthop Relat Res*, 467, 2297-304.
- Aldinger, P. R., Thomsen, M., Mau, H., Ewerbeck, V. & Breusch, S. J. 2003. Cementless Spotorno tapered titanium stems: excellent 10-15-year survival in 141 young patients. *Acta Orthop Scand*, 74, 253-8.
- Amstutz, H. C., Ma, S. M., Jinnah, R. H. & Mai, L. 1982. Revision of aseptic loose total hip arthroplasties. *Clin Orthop Relat Res*, 21-33.
- Arifin, A., Sulong, A. B., Muhamad, N., Syarif, J. & Ramli, M. I. 2014. Material processing of hydroxyapatite and titanium alloy (HA/Ti) composite as implant materials using powder metallurgy: a review. *Materials & Design*, 55, 165-175.
- Arno, S., Fetto, J., Nguyen, N. Q., Kinariwala, N., Takemoto, R., Oh, C. & Walker, P. S. 2012. Evaluation of femoral strains with cementless proximal-fill femoral implants of varied stem length. *Clin Biomech (Bristol, Avon)*, 27, 680-5.
- Ayachit, U. 2015. *The ParaView Guide: A Parallel Visualization Application*, Kitware, Inc.
- Baca, V., Horak, Z., Mikulenska, P. & Dzupa, V. 2008. Comparison of an inhomogeneous orthotropic and isotropic material models used for FE analyses. *Med Eng Phys*, 30, 924-30.

- Baharuddin, M. Y., Salleh Sh, H., Hamed, M., Zulkifly, A. H., Lee, M. H., Mohd Noor, A., Harris, A. R. & Abdul Majid, N. 2014. Primary stability recognition of the newly designed cementless femoral stem using digital signal processing. *Biomed Res Int*, 2014, 478248.
- Behrens, B. A., Wirth, C. J., Windhagen, H., Nolte, I., Meyer-Lindenberg, A. & Bouguecha, A. 2008. Numerical investigations of stress shielding in total hip prostheses. *Proc Inst Mech Eng H*, 222, 593-600.
- Bergmann, G., Deuretzbacher, G., Heller, M., Graichen, F., Rohlmann, A., Strauss, J. & Duda, G. N. 2001. Hip contact forces and gait patterns from routine activities. *J Biomech*, 34, 859-71.
- Bergmann, G., Graichen, F. & Rohlmann, A. 1993. Hip joint loading during walking and running, measured in two patients. *J Biomech*, 26, 969-90.
- Bieger, R., Ignatius, A., Decking, R., Claes, L., Reichel, H. & Dürselen, L. 2012. Primary stability and strain distribution of cementless hip stems as a function of implant design. *Clinical Biomechanics*, 27, 158-164.
- Bieger, R., Ignatius, A., Reichel, H. & Durselen, L. 2013. Biomechanics of a short stem: In vitro primary stability and stress shielding of a conservative cementless hip stem. *J Orthop Res*, 31, 1180-6.
- Biamond, J. E., Venkatesan, S. & Van Hellemond, G. G. 2015. Survivorship of the cementless Spotorno femoral component in patients under 50 years of age at a mean follow-up of 18.4 years. *Bone Joint J*, 97-b, 160-3.
- Boden, H. S., Skoldenberg, O. G., Salemyr, M. O., Lundberg, H. J. & Adolphson, P. Y. 2006. Continuous bone loss around a tapered uncemented femoral stem: a long-term evaluation with DEXA. *Acta Orthop*, 77, 877-85.
- Bohm, P. & Bischel, O. 2001. Femoral revision with the Wagner SL revision stem : evaluation of one hundred and twenty-nine revisions followed for a mean of 4.8 years. *J Bone Joint Surg Am*, 83-A, 1023-31.
- Bordini, B., Stea, S., De Clerico, M., Strazzari, S., Sasdelli, A. & Toni, A. 2007. Factors affecting aseptic loosening of 4750 total hip arthroplasties: multivariate survival analysis. *BMC Musculoskelet Disord*, 8, 69.

- Bozic, K. J., Kurtz, S. M., Lau, E., Ong, K., Vail, T. P. & Berry, D. J. 2009. The epidemiology of revision total hip arthroplasty in the United States. *J Bone Joint Surg Am*, 91, 128-33.
- Britton, J. R., Walsh, L. A. & Prendergast, P. J. 2003. Mechanical simulation of muscle loading on the proximal femur: analysis of cemented femoral component migration with and without muscle loading. *Clin Biomech (Bristol, Avon)*, 18, 637-46.
- Brown, T. D., Pedersen, D. R., Radin, E. L. & Rose, R. M. 1988. Global mechanical consequences of reduced cement/bone coupling rigidity in proximal femoral arthroplasty: a three-dimensional finite element analysis. *J Biomech*, 21, 115-29.
- Brown, T. E., Larson, B., Shen, F. & Moskal, J. T. 2002. Thigh pain after cementless total hip arthroplasty: evaluation and management. *J Am Acad Orthop Surg*, 10, 385-92.
- Bugbee, W. D., Culpepper, W. J., 2nd, Engh, C. A., Jr. & Engh, C. A., Sr. 1997. Long-term clinical consequences of stress-shielding after total hip arthroplasty without cement. *J Bone Joint Surg Am*, 79, 1007-12.
- Buhler, D. W., Berlemann, U., Lippuner, K., Jaeger, P. & Nolte, L. P. 1997. Three-dimensional primary stability of cementless femoral stems. *Clin Biomech (Bristol, Avon)*, 12, 75-86.
- Burke, D. W., O'connor, D. O., Zalenski, E. B., Jasty, M. & Harris, W. H. 1991. Micromotion of cemented and uncemented femoral components. *J Bone Joint Surg Br*, 73, 33-7.
- Carstens, E. B. & Lu, A. 1990. Nucleotide sequence and transcriptional analysis of the HindIII P region of a temperature-sensitive mutant of *Autographa californica* nuclear polyhedrosis virus. *J Gen Virol*, 71 ( Pt 12), 3035-40.
- Chareancholvanich, K., Bourgeault, C. A., Schmidt, A. H., Gustilo, R. B. & Lew, W. D. 2002. In vitro stability of cemented and cementless femoral stems with compaction. *Clin Orthop Relat Res*, 290-302.
- Charnley, J. 1961. Arthroplasty of the hip. A new operation. *Lancet*, 1, 1129-32.
- Chen, H. H., Morrey, B. F., An, K. N. & Luo, Z. P. 2009. Bone remodeling characteristics of a short-stemmed total hip replacement. *J Arthroplasty*, 24, 945-50.



- Chevalier, Y. 2015. Numerical Methodology to Evaluate the Effects of Bone Density and Cement Augmentation on Fixation Stiffness of Bone-Anchoring Devices. *J Biomech Eng*, 137.
- Claes, L., Kirschner, P., Perka, C. & Rudert, M. 2011. *AE-Manual der Endoprothetik: Hüfte und Hüftrevision*, Springer-Verlag.
- Dabirrahmani, D., Hogg, M., Kohan, L. & Gillies, M. 2010. Primary and long-term stability of a short-stem hip implant. *Proc Inst Mech Eng H*, 224, 1109-19.
- Dammak, M., Shirazi-Adl, A. & Zukor, D. J. 1997. Analysis of cementless implants using interface nonlinear friction--experimental and finite element studies. *J Biomech*, 30, 121-9.
- De Martino, I., De Santis, V., D'apolito, R., Sculco, P. K., Cross, M. B. & Gasparini, G. 2017. The Synergy cementless femoral stem in primary total hip arthroplasty at a minimum follow-up of 15 years. *Bone Joint J*, 99-b, 29-36.
- De Witte, P. B., Brand, R., Vermeer, H. G., Van Der Heide, H. J. & Barnaart, A. F. 2011. Mid-term results of total hip arthroplasty with the CementLess Spotorno (CLS) system. *J Bone Joint Surg Am*, 93, 1249-55.
- Decking, R., Rokahr, C., Zurstege, M., Simon, U. & Decking, J. 2008. Maintenance of bone mineral density after implantation of a femoral neck hip prosthesis. *BMC Musculoskelet Disord*, 9, 17.
- Della Valle, C. J. & Paprosky, W. G. 2004. The femur in revision total hip arthroplasty evaluation and classification. *Clin Orthop Relat Res*, 55-62.
- Doitpoms. 2011. Materials selection of femoral stem component [Online]. Available: <https://www.doitpoms.ac.uk/tlplib/bones/stem.php> [Accessed June 12 2017].
- Duda, G. N., Heller, M., Albinger, J., Schulz, O., Schneider, E. & Claes, L. 1998. Influence of muscle forces on femoral strain distribution. *J Biomech*, 31, 841-6.
- Engh, C. A., Jr., Young, A. M., Engh, C. A., Sr. & Hopper, R. H., Jr. 2003. Clinical consequences of stress shielding after porous-coated total hip arthroplasty. *Clin Orthop Relat Res*, 157-63.

- Engh, C. A., O'Connor, D., Jasty, M., McGovern, T. F., Bobyn, J. D. & Harris, W. H. 1992. Quantification of implant micromotion, strain shielding, and bone resorption with porous-coated anatomic medullary locking femoral prostheses. *Clin Orthop Relat Res*, 13-29.
- Eorthopod. n.d. A Patient's Guide to Artificial Joint Replacement of the Hip [Online]. Available: <http://eorthopod.com/hip-replacement> [Accessed June 12 2017].
- Evola, F. R., Evola, G., Graceffa, A., Sessa, A., Pavone, V., Costarella, L., Sessa, G. & Avondo, S. 2014. Performance of the CLS Spotorno uncemented stem in the third decade after implantation. *Bone Joint J*, 96-B, 455-61.
- Falez, F., Casella, F., Panegrossi, G., Favetti, F. & Barresi, C. 2008. Perspectives on metaphyseal conservative stems. *J Orthop Traumatol*, 9, 49-54.
- Falez, F., Casella, F. & Papalia, M. 2015. Current concepts, classification, and results in short stem hip arthroplasty. *Orthopedics*, 38, S6-13.
- Feyen, H. & Shimmin, A. J. 2014. Is the length of the femoral component important in primary total hip replacement? *Bone Joint J*, 96-B, 442-8.
- Floerkemeier, T., Tscheuschner, N., Calliess, T., Ezechieli, M., Floerkemeier, S., Budde, S., Windhagen, H. & Von Lewinski, G. 2012. Cementless short stem hip arthroplasty METHA(R) as an encouraging option in adults with osteonecrosis of the femoral head. *Arch Orthop Trauma Surg*, 132, 1125-31.
- Fottner, A., Peter, C. V., Schmidutz, F., Wanke-Jellinek, L., Schroder, C., Mazoochian, F. & Jansson, V. 2011. Biomechanical evaluation of different offset versions of a cementless hip prosthesis by 3-dimensional measurement of micromotions. *Clin Biomech (Bristol, Avon)*, 26, 830-5.
- Fottner, A., Schmid, M., Birkenmaier, C., Mazoochian, F., Plitz, W. & Volkmar, J. 2009. Biomechanical evaluation of two types of short-stemmed hip prostheses compared to the trust plate prosthesis by three-dimensional measurement of micromotions. *Clin Biomech (Bristol, Avon)*, 24, 429-34.
- Fraldi, M., Esposito, L., Perrella, G., Cutolo, A. & Cowin, S. C. 2010. Topological optimization in hip prosthesis design. *Biomech Model Mechanobiol*, 9, 389-402.

- Freitag, T., Hein, M. A., Wernerus, D., Reichel, H. & Bieger, R. 2016. Bone remodelling after femoral short stem implantation in total hip arthroplasty: 1-year results from a randomized DEXA study. *Arch Orthop Trauma Surg*, 136, 125-30.
- Gabarre, S., Herrera, A., Ibarz, E., Mateo, J., Gil-Albarova, J. & Gracia, L. 2016. Comparative Analysis of the Biomechanical Behaviour of Two Cementless Short Stems for Hip Replacement: Linea Anatomic and Minihip. *PLoS One*, 11, e0158411.
- Garellick, G., Rogmark, C., Kärholm, J. & Rolfson, O. 2013. Swedish Hip Arthroplasty Register - Annual Report 2012.
- Gastaud, O., Cambas, P. M. & Tabutin, J. 2016. Femoral revision with a primary cementless stem. *Orthop Traumatol Surg Res*, 102, 149-53.
- George, S. P. & Saravana Kumar, G. 2013. Patient specific parametric geometric modelling and finite element analysis of cementless hip prosthesis. *Virtual and Physical Prototyping*, 8, 65-83.
- Gheduzzi, S. & Miles, A. W. 2007. A review of pre-clinical testing of femoral stem subsidence and comparison with clinical data. *Proc Inst Mech Eng H*, 221, 39-46.
- Ghera, S. & Pavan, L. 2009. The DePuy Proxima hip: a short stem for total hip arthroplasty. Early experience and technical considerations. *Hip Int*, 19, 215-20.
- Gortz, W., Nagerl, U. V., Nagerl, H. & Thomsen, M. 2002. Spatial micromovements of uncemented femoral components after torsional loads. *J Biomech Eng*, 124, 706-13.
- Gramkow, J., Jensen, T. H., Varmarken, J. E. & Retpen, J. B. 2001. Long-term results after cemented revision of the femoral component in total hip arthroplasty. *J Arthroplasty*, 16, 777-83.
- Gronewold, J., Berner, S., Olender, G., Hurschler, C., Windhagen, H., Von Lewinski, G. & Floerkemeier, T. 2014. Changes in strain patterns after implantation of a short stem with metaphyseal anchorage compared to a standard stem: an experimental study in synthetic bone. *Orthop Rev (Pavia)*, 6, 5211.
- Grover, P., Albert, C., Wang, M. & Harris, G. F. 2011. Mechanical characterization of fourth generation composite humerus. *Proc Inst Mech Eng H*, 225, 1169-76.

- Gruen, T. A., Mcneice, G. M. & Amstutz, H. C. 1979. "Modes of failure" of cemented stem-type femoral components: a radiographic analysis of loosening. *Clin Orthop Relat Res*, 17-27.
- Hefzy, M. S. & Singh, S. P. 1997. Comparison between two techniques for modeling interface conditions in a porous coated hip endoprosthesis. *Med Eng Phys*, 19, 50-62.
- Heiner, A. D. & Brown, T. D. 2001. Structural properties of a new design of composite replicate femurs and tibias. *J Biomech*, 34, 773-81.
- Heller, M. O., Kassi, J. P., Perka, C. & Duda, G. N. 2005. Cementless stem fixation and primary stability under physiological-like loads in vitro. *Biomed Tech (Berl)*, 50, 394-9.
- Herberts, P. & Malchau, H. 2000. Long-term registration has improved the quality of hip replacement: a review of the Swedish THR Register comparing 160,000 cases. *Acta Orthop Scand*, 71, 111-21.
- Homma, Y., Baba, T., Sumiyoshi, N., Ochi, H., Kobayashi, H., Matsumoto, M., Yuasa, T. & Kaneko, K. 2014. Rapid hip osteoarthritis development in a patient with anterior acetabular cyst with sagittal alignment change. *Case Rep Orthop*, 2014, 523426.
- Hooper, G. J., Rothwell, A. G., Stringer, M. & Frampton, C. 2009. Revision following cemented and uncemented primary total hip replacement: a seven-year analysis from the New Zealand Joint Registry. *J Bone Joint Surg Br*, 91, 451-8.
- Huiskes, R., Weinans, H., Grootenboer, H. J., Dalstra, M., Fudala, B. & Slooff, T. J. 1987. Adaptive bone-remodeling theory applied to prosthetic-design analysis. *J Biomech*, 20, 1135-50.
- Isaacson, B. & Jeyapalina, S. 2014. Osseointegration: a review of the fundamentals for assuring cementless skeletal fixation. *Orthop Res Rev*, 6, 55-65.
- Jahnke, A., Engl, S., Altmeyer, C., Jakubowitz, E., Seeger, J. B., Rickert, M. & Ishaque, B. A. 2014. Changes of periprosthetic bone density after a cementless short hip stem: a clinical and radiological analysis. *Int Orthop*, 38, 2045-50.

- Jakubowitz, E., Bitsch, R. G., Heisel, C., Lee, C., Kretzer, J. P. & Thomsen, M. N. 2008. Primary rotational stability of cylindrical and conical revision hip stems as a function of femoral bone defects: an in vitro comparison. *J Biomech*, 41, 3078-84.
- Jasty, M., Bragdon, C., Burke, D., O'connor, D., Lowenstein, J. & Harris, W. H. 1997. In vivo skeletal responses to porous-surfaced implants subjected to small induced motions. *J Bone Joint Surg Am*, 79, 707-14.
- Jonsson, B. & Larsson, S. E. 1991. Functional improvement and costs of hip and knee arthroplasty in destructive rheumatoid arthritis. *Scand J Rheumatol*, 20, 351-7.
- Judet, J. & Judet, R. 1950. The use of an artificial femoral head for arthroplasty of the hip joint. *J Bone Joint Surg Br*, 32-B, 166-73.
- Kassi, J. P., Heller, M. O., Stoeckle, U., Perka, C. & Duda, G. N. 2005. Stair climbing is more critical than walking in pre-clinical assessment of primary stability in cementless THA in vitro. *J Biomech*, 38, 1143-54.
- Keaveny, T. M. & Bartel, D. L. 1993. Effects of porous coating, with and without collar support, on early relative motion for a cementless hip prosthesis. *J Biomech*, 26, 1355-68.
- Kershaw, C. J., Atkins, R. M., Dodd, C. A. & Bulstrode, C. J. 1991. Revision total hip arthroplasty for aseptic failure. A review of 276 cases. *J Bone Joint Surg Br*, 73, 564-8.
- Keyak, J. H., Meagher, J. M., Skinner, H. B. & Mote, C. D., Jr. 1990. Automated three-dimensional finite element modelling of bone: a new method. *J Biomed Eng*, 12, 389-97.
- Khanuja, H. S., Banerjee, S., Jain, D., Pivec, R. & Mont, M. A. 2014a. Short bone-conserving stems in cementless hip arthroplasty. *J Bone Joint Surg Am*, 96, 1742-52.
- Khanuja, H. S., Issa, K., Naziri, Q., Banerjee, S., Delanois, R. E. & Mont, M. A. 2014b. Results of a tapered proximally-coated primary cementless stem for revision hip surgery. *J Arthroplasty*, 29, 225-8.
- Khanuja, H. S., Vakil, J. J., Goddard, M. S. & Mont, M. A. 2011. Cementless femoral fixation in total hip arthroplasty. *J Bone Joint Surg Am*, 93, 500-9.
- Kim, J. T. & Yoo, J. J. 2016. Implant Design in Cementless Hip Arthroplasty. *Hip Pelvis*, 28, 65-75.

- Kim, Y. H., Kim, J. S., Park, J. W. & Joo, J. H. 2011. Comparison of total hip replacement with and without cement in patients younger than 50 years of age: the results at 18 years. *J Bone Joint Surg Br*, 93, 449-55.
- Kim, Y. H., Park, J. W. & Kim, J. S. 2016. Ultrashort versus Conventional Anatomic Cementless Femoral Stems in the Same Patients Younger Than 55 Years. *Clin Orthop Relat Res*, 474, 2008-17.
- Labek, G., Thaler, M., Janda, W., Agreiter, M. & Stockl, B. 2011. Revision rates after total joint replacement: cumulative results from worldwide joint register datasets. *J Bone Joint Surg Br*, 93, 293-7.
- Liang, M. H., Cullen, K. E., Larson, M. G., Thompson, M. S., Schwartz, J. A., Fossel, A. H., Roberts, W. N. & Sledge, C. B. 1986. Cost-effectiveness of total joint arthroplasty in osteoarthritis. *Arthritis Rheum*, 29, 937-43.
- Maier, G. S., Kolbow, K., Lazovic, D. & Maus, U. 2016. The Importance of Bone Mineral Density in Hip Arthroplasty: Results of a Survey Asking Orthopaedic Surgeons about Their Opinions and Attitudes Concerning Osteoporosis and Hip Arthroplasty. *Adv Orthop*, 2016, 8079354.
- Maier, M. W., Streit, M. R., Innmann, M. M., Kruger, M., Nadorf, J., Kretzer, J. P., Ewerbeck, V. & Gotterbarm, T. 2015. Cortical hypertrophy with a short, curved uncemented hip stem does not have any clinical impact during early follow-up. *BMC Musculoskelet Disord*, 16, 371.
- Mazoochian, F., Schrimpf, F. M., Kircher, J., Mayer, W., Hauptmann, S., Fottner, A., Muller, P. E., Pellengahr, C. & Jansson, V. 2007. Proximal loading of the femur leads to low subsidence rates: first clinical results of the CR-stem. *Arch Orthop Trauma Surg*, 127, 397-401.
- Mcguigan, F. X., Hozack, W. J., Moriarty, L., Eng, K. & Rothman, R. H. 1995. Predicting quality-of-life outcomes following total joint arthroplasty. Limitations of the SF-36 Health Status Questionnaire. *J Arthroplasty*, 10, 742-7.

- Mckellop, H., Ebramzadeh, E., Niederer, P. G. & Sarmiento, A. 1991. Comparison of the stability of press-fit hip prosthesis femoral stems using a synthetic model femur. *J Orthop Res*, 9, 297-305.
- Merle, C., Streit, M. R., Volz, C., Pritsch, M., Gotterbarm, T. & Aldinger, P. R. 2011. Bone remodeling around stable uncemented titanium stems during the second decade after total hip arthroplasty: a DXA study at 12 and 17 years. *Osteoporos Int*, 22, 2879-86.
- Monti, L., Cristofolini, L. & Viceconti, M. 1999. Methods for quantitative analysis of the primary stability in uncemented hip prostheses. *Artif Organs*, 23, 851-9.
- Morrey, B. F. 1989. Short-stemmed uncemented femoral component for primary hip arthroplasty. *Clin Orthop Relat Res*, 169-75.
- Morrey, B. F., Adams, R. A. & Kessler, M. 2000. A conservative femoral replacement for total hip arthroplasty. A prospective study. *J Bone Joint Surg Br*, 82, 952-8.
- Ni, G. X., Lu, W. W., Chiu, K. Y. & Fong, D. Y. 2005. Cemented or uncemented femoral component in primary total hip replacement? A review from a clinical and radiological perspective. *J Orthop Surg (Hong Kong)*, 13, 96-105.
- Nogler, M., Polikeit, A., Wimmer, C., Bruckner, A., Ferguson, S. J. & Krismer, M. 2004. Primary stability of a robodoc implanted anatomical stem versus manual implantation. *Clin Biomech (Bristol, Avon)*, 19, 123-9.
- Oldani, C. & Dominguez, A. 2012. Titanium as a Biomaterial for Implants. *Recent Advances in Arthroplasty*. InTech.
- Ong, K. L., Day, J. S., Manley, M. T., Kurtz, S. M. & Geesink, R. 2009. Biomechanical comparison of 2 proximally coated femoral stems: effects of stem length and surface finish. *J Arthroplasty*, 24, 819-24.
- Orlik, J., Zhurov, A. & Middleton, J. 2003. On the secondary stability of coated cementless hip replacement: parameters that affected interface strength. *Med Eng Phys*, 25, 825-31.
- Pancanti, A., Bernakiewicz, M. & Viceconti, M. 2003. The primary stability of a cementless stem varies between subjects as much as between activities. *J Biomech*, 36, 777-85.

- Peeters, C. M., Visser, E., Van De Ree, C. L., Gosens, T., Den Ouden, B. L. & De Vries, J. 2016. Quality of life after hip fracture in the elderly: A systematic literature review. *Injury*, 47, 1369-82.
- Pepke, W., Nadorf, J., Ewerbeck, V., Streit, M. R., Kinkel, S., Gotterbarm, T., Maier, M. W. & Kretzer, J. P. 2014. Primary stability of the Fitmore stem: biomechanical comparison. *Int Orthop*, 38, 483-8.
- Pettersen, S. H., Wik, T. S. & Skallerud, B. 2009a. Subject specific finite element analysis of implant stability for a cementless femoral stem. *Clin Biomech (Bristol, Avon)*, 24, 480-7.
- Pettersen, S. H., Wik, T. S. & Skallerud, B. 2009b. Subject specific finite element analysis of stress shielding around a cementless femoral stem. *Clin Biomech (Bristol, Avon)*, 24, 196-202.
- Pierre Alliez, C. J., Laurent Rineau, Stéphane Tayeb, Jane Tournois, Mariette Yvinec 2014. 3D Mesh Generation. In: *CGAL User and Reference Manual*.
- Pilliar, R. M., Lee, J. M. & Maniopoulos, C. 1986. Observations on the effect of movement on bone ingrowth into porous-surfaced implants. *Clin Orthop Relat Res*, 108-13.
- Pipino, F. 2004. CFP prosthetic stem in mini-invasive total hip arthroplasty. *Journal of Orthopaedics and Traumatology*, 5, 165-171.
- Pipino, F., Molfetta, L. & Grandizio, M. 2000. Preservation of the femoral neck in hip arthroplasty: results of a 13-to 17-year follow-up. *Journal of Orthopaedics and Traumatology*, 1, 31-39.
- Pozowski, A., Scigala, K., Kierzek, A., Paprocka-Borowicz, M. & Kuciel-Lewandowska, J. 2013. Analysis of the influence of a metha-type metaphysical stem on biomechanical parameters. *Acta Bioeng Biomech*, 15, 13-21.
- Raman, R., Kamath, R. P., Parikh, A. & Angus, P. D. 2005. Revision of cemented hip arthroplasty using a hydroxyapatite-ceramic-coated femoral component. *J Bone Joint Surg Br*, 87, 1061-7.



- Rasch, A., Bystrom, A. H., Dalen, N. & Berg, H. E. 2007. Reduced muscle radiological density, cross-sectional area, and strength of major hip and knee muscles in 22 patients with hip osteoarthritis. *Acta Orthop*, 78, 505-10.
- Reddy, J. N. 2006. *An introduction to the finite element method*, New York, NY, McGraw-Hill Higher Education.
- Reggiani, B., Cristofolini, L., Taddei, F. & Viceconti, M. 2008. Sensitivity of the primary stability of a cementless hip stem to its position and orientation. *Artif Organs*, 32, 555-60.
- Reggiani, B., Cristofolini, L., Varini, E. & Viceconti, M. 2007. Predicting the subject-specific primary stability of cementless implants during pre-operative planning: preliminary validation of subject-specific finite-element models. *J Biomech*, 40, 2552-8.
- Reikeras, O. & Gunderson, R. B. 2006. Excellent results with femoral revision surgery using an extensively hydroxyapatite-coated stem: 59 patients followed for 10-16 years. *Acta Orthop*, 77, 98-103.
- Ridzwan, M., Shuib, S., Hassan, A., Shokri, A. & Ibrahim, M. M. 2007. Problem of stress shielding and improvement to the hip implant designs: a review. *J. Med. Sci*, 7, 460-467.
- Rissanen, P., Aro, S., Slati, P., Sintonen, H. & Paavolainen, P. 1995. Health and quality of life before and after hip or knee arthroplasty. *J Arthroplasty*, 10, 169-75.
- Ritter, M. A., Albohm, M. J., Keating, E. M., Faris, P. M. & Meding, J. B. 1995. Comparative outcomes of total joint arthroplasty. *J Arthroplasty*, 10, 737-41.
- Rohlmann, A., Cheal, E. J., Hayes, W. C. & Bergmann, G. 1988. A nonlinear finite element analysis of interface conditions in porous coated hip endoprostheses. *J Biomech*, 21, 605-11.
- Rohlmann, A., Mossner, U., Bergmann, G., Hees, G. & Kolbel, R. 1987. Effects of stem design and material properties on stresses in hip endoprostheses. *J Biomed Eng*, 9, 77-83.
- Ruben, R. B., Fernandes, P. R. & Folgado, J. 2012. On the optimal shape of hip implants. *J Biomech*, 45, 239-46.
- Salaffi, F., Carotti, M., Stancati, A. & Grassi, W. 2005. Health-related quality of life in older adults with symptomatic hip and knee osteoarthritis: a comparison with matched healthy controls. *Aging Clin Exp Res*, 17, 255-63.

- Salemyr, M., Muren, O., Ahl, T., Boden, H., Eisler, T., Stark, A. & Skoldenberg, O. 2015. Lower periprosthetic bone loss and good fixation of an ultra-short stem compared to a conventional stem in uncemented total hip arthroplasty. *Acta Orthop*, 86, 659-66.
- Sawbones. 2017. Femur, Fourth Generation [Online]. Available: <https://www.sawbones.com/products/biomechanical/composite-bones/femur-small-left-4th-generation-composite.html> [Accessed June 14 2017].
- Schileo, E., Taddei, F., Malandrino, A., Cristofolini, L. & Viceconti, M. 2007. Subject-specific finite element models can accurately predict strain levels in long bones. *J Biomech*, 40, 2982-9.
- Schmalzried, T. P. & Callaghan, J. J. 1999. Wear in total hip and knee replacements. *J Bone Joint Surg Am*, 81, 115-36.
- Schmidutz, F., Beirer, M., Weber, P., Mazoochian, F., Fottner, A. & Jansson, V. 2012a. Biomechanical reconstruction of the hip: comparison between modular short-stem hip arthroplasty and conventional total hip arthroplasty. *Int Orthop*, 36, 1341-7.
- Schmidutz, F., Wanke-Jellinek, L., Jansson, V., Fottner, A. & Mazoochian, F. 2012b. Revision of hip resurfacing arthroplasty with a bone-conserving short-stem implant: a case report and review of the literature. *J Med Case Rep*, 6, 249.
- Schmidutz, F., Woiczinski, M., Kistler, M., Schroder, C., Jansson, V. & Fottner, A. 2017. Influence of different sizes of composite femora on the biomechanical behavior of cementless hip prosthesis. *Clin Biomech (Bristol, Avon)*, 41, 60-65.
- Schnurr, C., Schellen, B., Dargel, J., Beckmann, J., Eysel, P. & Steffen, R. 2017. Low Short-Stem Revision Rates: 1-11 Year Results From 1888 Total Hip Arthroplasties. *J Arthroplasty*, 32, 487-493.
- Schulte, K. R., Callaghan, J. J., Kelley, S. S. & Johnston, R. C. 1993. The outcome of Charnley total hip arthroplasty with cement after a minimum twenty-year follow-up. The results of one surgeon. *J Bone Joint Surg Am*, 75, 961-75.
- Schünke, M., Schulte, E. & Schumacher, U. 2015. Thieme atlas of anatomy. General anatomy and musculoskeletal system, New York, Thieme.

- Sharma, A. R., Jagga, S., Lee, S. S. & Nam, J. S. 2013. Interplay between cartilage and subchondral bone contributing to pathogenesis of osteoarthritis. *Int J Mol Sci*, 14, 19805-30.
- Singh, A. P. n.d.-a. Hip Joint Anatomy [Online]. Available: <http://boneandspine.com/hip-joint-anatomy/> [Accessed June 16 2017].
- Singh, A. P. n.d.-b. Hip Osteoarthritis – Causes, Symptoms and Treatment [Online]. Available: <http://boneandspine.com/hip-osteoarthritis-causes-symptoms-and-treatment/> [Accessed June 16 2017].
- Skinner, H. B., Kim, A. S., Keyak, J. H. & Mote, C. D., Jr. 1994. Femoral prosthesis implantation induces changes in bone stress that depend on the extent of porous coating. *J Orthop Res*, 12, 553-63.
- Skoldenberg, O. G., Boden, H. S., Salemyr, M. O., Ahl, T. E. & Adolphson, P. Y. 2006. Periprosthetic proximal bone loss after uncemented hip arthroplasty is related to stem size: DXA measurements in 138 patients followed for 2-7 years. *Acta Orthop*, 77, 386-92.
- Small, S. R., Hensley, S. E., Cook, P. L., Stevens, R. A., Rogge, R. D., Meding, J. B. & Berend, M. E. 2017. Characterization of Femoral Component Initial Stability and Cortical Strain in a Reduced Stem-Length Design. *J Arthroplasty*, 32, 601-609.
- Soballe, K., Hansen, E. S., Brockstedt-Rasmussen, H., Pedersen, C. M. & Bunger, C. 1990. Hydroxyapatite coating enhances fixation of porous coated implants. A comparison in dogs between press fit and noninterference fit. *Acta Orthop Scand*, 61, 299-306.
- Soballe, K., Hansen, E. S., H, B. R., Jorgensen, P. H. & Bunger, C. 1992. Tissue ingrowth into titanium and hydroxyapatite-coated implants during stable and unstable mechanical conditions. *J Orthop Res*, 10, 285-99.
- Sophia Fox, A. J., Bedi, A. & Rodeo, S. A. 2009. The basic science of articular cartilage: structure, composition, and function. *Sports Health*, 1, 461-8.
- Stansfield, B. W. & Nicol, A. C. 2002. Hip joint contact forces in normal subjects and subjects with total hip prostheses: walking and stair and ramp negotiation. *Clin Biomech (Bristol, Avon)*, 17, 130-9.

- Statistisches Bundesamt 2005 to 2015. Fallpauschalenbezogene Krankenhausstatistik (DRG-Statistik). Operationen und Prozeduren der vollstationären Patientinnen und Patienten in Krankenhäusern - Ausführliche Darstellung. Wiesbaden.
- Stolk, J., Verdonschot, N. & Huiskes, R. 2001. Hip-joint and abductor-muscle forces adequately represent in vivo loading of a cemented total hip reconstruction. *J Biomech*, 34, 917-26.
- Streit, M. R., Schroder, K., Korber, M., Merle, C., Gotterbarm, T., Ewerbeck, V. & Aldinger, P. R. 2012. High survival in young patients using a second generation uncemented total hip replacement. *Int Orthop*, 36, 1129-36.
- Stukenborg-Colsman, C. M., Von Der Haar-Tran, A., Windhagen, H., Bougoucha, A., Wefstaedt, P. & Lerch, M. 2012. Bone remodelling around a cementless straight THA stem: a prospective dual-energy X-ray absorptiometry study. *Hip Int*, 22, 166-71.
- Sugiyama, H., Whiteside, L. A. & Kaiser, A. D. 1989. Examination of rotational fixation of the femoral component in total hip arthroplasty. A mechanical study of micromovement and acoustic emission. *Clin Orthop Relat Res*, 122-8.
- Sychterz, C. J., Claus, A. M. & Engh, C. A. 2002. What we have learned about long-term cementless fixation from autopsy retrievals. *Clin Orthop Relat Res*, 79-91.
- Synder, M., Krajewski, K., Sibinski, M. & Drobniowski, M. 2015. Periprosthetic bone remodeling around short stem. *Orthopedics*, 38, S40-5.
- Tahim, A. S., Stokes, O. M. & Vedi, V. 2012. The effect of femoral stem length on duration of hospital stay. *Hip Int*, 22, 56-61.
- Tarala, M., Janssen, D., Telka, A., Waanders, D. & Verdonschot, N. 2011. Experimental versus computational analysis of micromotions at the implant-bone interface. *Proc Inst Mech Eng H*, 225, 8-15.
- Tauber, C. & Kidron, A. 2000. Total hip arthroplasty revision using the press-fit CLS Spotorno cementless stem. Twenty-four hips followed between 1987 and 1998. *Arch Orthop Trauma Surg*, 120, 209-11.

- Thomsen, M. N., Breusch, S. J., Aldinger, P. R., Gortz, W., Lahmer, A., Honl, M., Birke, A. & Nagerl, H. 2002. Robotically-milled bone cavities: a comparison with hand-broaching in different types of cementless hip stems. *Acta Orthop Scand*, 73, 379-85.
- Thorey, F., Hofer, C., Abdi-Tabari, N., Lerch, M., Budde, S. & Windhagen, H. 2013. Clinical results of the metha short hip stem: a perspective for younger patients? *Orthop Rev (Pavia)*, 5, e34.
- Thorey, F., Lerch, M., Kiel, H., Von Lewinski, G., Stukenborg-Colsman, C. & Windhagen, H. 2008. Revision total hip arthroplasty with an uncemented primary stem in 79 patients. *Arch Orthop Trauma Surg*, 128, 673-8.
- Tsertsvadze, A., Grove, A., Freeman, K., Court, R., Johnson, S., Connock, M., Clarke, A. & Sutcliffe, P. 2014. Total hip replacement for the treatment of end stage arthritis of the hip: a systematic review and meta-analysis. *PLoS One*, 9, e99804.
- Vaishya, R., Chauhan, M. & Vaish, A. 2013. Bone cement. *J Clin Orthop Trauma*, 4, 157-63.
- Valle, C. J. & Paprosky, W. G. 2003. Classification and an algorithmic approach to the reconstruction of femoral deficiency in revision total hip arthroplasty. *J Bone Joint Surg Am*, 85-A Suppl 4, 1-6.
- Van Oldenrijk, J., Molleman, J., Klaver, M., Poolman, R. W. & Haverkamp, D. 2014. Revision rate after short-stem total hip arthroplasty: a systematic review of 49 studies. *Acta Orthop*, 85, 250-8.
- Viceconti, M., Monti, L., Muccini, R., Bernakiewicz, M. & Toni, A. 2001. Even a thin layer of soft tissue may compromise the primary stability of cementless hip stems. *Clin Biomech (Bristol, Avon)*, 16, 765-75.
- Viceconti, M., Muccini, R., Bernakiewicz, M., Baleani, M. & Cristofolini, L. 2000. Large-sliding contact elements accurately predict levels of bone-implant micromotion relevant to osseointegration. *J Biomech*, 33, 1611-8.
- Viceconti, M., Pancanti, A., Dotti, M., Traina, F. & Cristofolini, L. 2004. Effect of the initial implant fitting on the predicted secondary stability of a cementless stem. *Med Biol Eng Comput*, 42, 222-9.

- Von Lewinski, G. & Floerkemeier, T. 2015. 10-year experience with short stem total hip arthroplasty. *Orthopedics*, 38, S51-6.
- Weinans, H., Huiskes, R. & Grootenboer, H. J. 1992. Effects of material properties of femoral hip components on bone remodeling. *J Orthop Res*, 10, 845-53.
- Weiss, R. J., Stark, A. & Karrholm, J. 2011. A modular cementless stem vs. cemented long-stem prostheses in revision surgery of the hip: a population-based study from the Swedish Hip Arthroplasty Register. *Acta Orthop*, 82, 136-42.
- Westphal, F. M., Bishop, N., Honl, M., Hille, E., Puschel, K. & Morlock, M. M. 2006. Migration and cyclic motion of a new short-stemmed hip prosthesis--a biomechanical in vitro study. *Clin Biomech (Bristol, Avon)*, 21, 834-40.
- Whiteside, L. A. & Easley, J. C. 1989. The effect of collar and distal stem fixation on micromotion of the femoral stem in uncemented total hip arthroplasty. *Clin Orthop Relat Res*, 145-53.
- Whiteside, L. A., White, S. E., Engh, C. A. & Head, W. 1993. Mechanical evaluation of cadaver retrieval specimens of cementless bone-ingrown total hip arthroplasty femoral components. *J Arthroplasty*, 8, 147-55.
- Whittle, M. 2003. *Gait analysis : an introduction*, Edinburgh ; New York, Butterworth-Heinemann.
- Wilkinson, J. M., Hamer, A. J., Rogers, A., Stockley, I. & Eastell, R. 2003. Bone mineral density and biochemical markers of bone turnover in aseptic loosening after total hip arthroplasty. *J Orthop Res*, 21, 691-6.
- Wittenberg, R. H., Steffen, R., Windhagen, H., Bucking, P. & Wilcke, A. 2013. Five-year results of a cementless short-hip-stem prosthesis. *Orthop Rev (Pavia)*, 5, e4.
- Wolf, O., Mattsson, P., Milbrink, J., Larsson, S. & Mallmin, H. 2010. Periprosthetic bone mineral density and fixation of the uncemented CLS stem related to different weight bearing regimes: A randomized study using DXA and RSA in 38 patients followed for 5 years. *Acta Orthop*, 81, 286-91.

- Woolf, A. D., Erwin, J. & March, L. 2012. The need to address the burden of musculoskeletal conditions. *Best Pract Res Clin Rheumatol*, 26, 183-224.
- Wroblewski, B. M., Siney, P. D. & Fleming, P. A. 2007. Charnley low-friction arthroplasty: survival patterns to 38 years. *J Bone Joint Surg Br*, 89, 1015-8.
- Yamako, G., Chosa, E., Totoribe, K., Watanabe, S. & Sakamoto, T. 2015. Trade-off between stress shielding and initial stability on an anatomical cementless stem shortening: in-vitro biomechanical study. *Med Eng Phys*, 37, 820-5.
- Yamasaki, T., Yasunaga, Y., Mori, R., Hamanishi, M., Shoji, T. & Ochi, M. 2014. The Cementless Spotorno stem in THA: 10 year results. *Hip Int*, 24, 98-102.
- Yan, S. G., Woiczinski, M., Schmidutz, T. F., Weber, P., Paulus, A. C., Steinbruck, A., Jansson, V. & Schmidutz, F. 2017. Can the metaphyseal anchored Metha short stem safely be revised with a standard CLS stem? A biomechanical analysis. *Int Orthop*.
- Zachariah, S. G. & Sanders, J. E. 2000. Finite element estimates of interface stress in the trans-tibial prosthesis using gap elements are different from those using automated contact. *J Biomech*, 33, 895-9.
- Zimmer. 2011. CLS® Spotorno® Hip Stem [Online]. Available: <https://orto.hi.is/skrar/clsspotornostem708.pdf> [Accessed June 14 2017].

## 10. List of figures

Fig. 1: Schematic drawing of a healthy hip joint .....	1
Fig. 2: Schematic drawing of the ligaments around the hip joint.....	2
Fig. 3: Graphical illustration of hip joint arthritis .....	3
Fig. 4: Number of primary and revision hip replacements in Germany .....	4
Fig. 5: Modular structure of a standard hip joint endoprosthesis.....	5
Fig. 6: Graphical illustration of cemented and cementless stems .....	6
Fig. 7: X-ray images of primary THA.....	7
Fig. 8: Examples of the conventional cementless THA stems.....	8
Fig. 9: Examples of short cementless THA stems .....	9
Fig. 10: Classification of the commercially available short stems for THA .....	10
Fig. 11: Difference in the revision rate for patients with different ages .....	11
Fig. 12: Illustration of the relative movement of prosthesis at the bone-implant interface .....	13
Fig. 13: Schematic drawing of osseous integration.....	14
Fig. 14: Schematic drawing of the most important forces on the hip joint .....	15
Fig. 15: Simple scheme of the stress shielding .....	16
Fig. 16: The X-ray images of THA with cementless stems show stress shielding and bone hypertrophy.....	17
Fig. 17: Synthetic composite bone (4th generation, sawbone, left side size L).....	22
Fig. 18: Metha short stem prosthesis.....	23
Fig. 19: CLS standard stem prosthesis .....	24
Fig. 20: Implantations operated under fluoroscopy .....	26
Fig. 21: Sawbones with different femoral head osteotomies according to the stem design .....	27
Fig. 22: Experimental setup for determining the 3D micromotions between the bone and implant interface.....	29
Fig. 23: Flowcharts depicting the preparation and 3D-measurement in the micromotion setup.....	30



Fig. 24: The procedure of revision scenario .....	30
Fig. 25: Measurement points of micromotions .....	32
Fig. 26: Flowcharts depicting the process of creating the homogenized FE models .....	34
Fig. 27: Nodes chosen in the FE model .....	37
Fig. 28: Illustration showing the method of stress analysis in the three FE models .....	39
Fig. 29: 3D-micromotions determined for Metha-Primary stem .....	40
Fig. 30: 3D-micromotions determined for CLS-Primary stem .....	41
Fig. 31: Comparison of 3D-micromotions for the 5 interface points between CLS-Primary and Metha-Primary stems.....	42
Fig. 32: 3D-micromotions determined for CLS-Revision stem.....	43
Fig. 33: Comparison of 3D-micromotions for the 5 interface points between CLS-Primary and CLS- Revision stems .....	43
Fig. 34: Implanted sawbones showing a bone defect in revision.....	44
Fig. 35: 3D relative displacement determined for Metha-Primary stem in the FE model. ....	45
Fig. 36: 3D relative displacement determined for CLS-Primary stem in the FE model .....	46
Fig. 37: Comparison between the 3D relative displacement in FEA and 3D-micromotions in experimental primary SHA .....	47
Fig. 38: Comparison between the 3D relative displacement in FEA and 3D-micromotions in experimental primary THA .....	47
Fig. 39: Mean cortical stress distributions in the three FE models .....	49
Fig. 40: Peak cortical stress distributions in the three FE models.....	50
Fig. 41: Frontal and coronal views of von Mises stress distribution patterns in the three FE models.....	51
Fig. 42: Cross-sectional view of von Mises stress distribution patterns in the three FE models.....	52

## 11. Abbreviations

µm	Micrometer
THA	Total hip arthroplasty
SHA	Short stem total hip arthroplasty
PMMA	Polymethylmethacrylate
LVDT	Linear variable differential transducer
FE	Finite element
FEA	Finite element analysis
FEM	Finite element method
CT	Computed tomography
MRI	Magnetic resonance imaging
3D	Three dimensional
SGFR	Short-glass-fiber-reinforced
CCD	Caput-collum-diaphyseal
BMD	Bone mineral density
DEXA	Dual-energy X-ray absorptiometry
SD	Standard deviation

## **12. Curriculum Vitae**

### **Shuanggen Yan**

Date of birth: 04.11.1987

Place of birth: Wuhu, China

Nationality: Chinese

### **Doctorate (Dr. med.)**

9/2014 - present                      Evaluation of the initial fixation, stress distribution and revision of short stem hip arthroplasty: A biomechanical study and finite element analysis  
Department of Orthopaedic Surgery, Physical Medicine and Rehabilitation, Klinikum Grosshadern, Ludwig-Maximilians-University of Munich, Germany  
Director: Prof. Dr. med. Dipl.-Ing. Volkmar Jansson

### **Medical Physics (M.Sc.)**

09/2013 - 9/2014                      Master of Science in Medical Physics  
Heidelberg University, Germany, PD Dr. Carsten Herskind

### **Study of Human Medicine**

09/2011 - 9/2013                      Master of Science in Medicine (Subject: Orthopaedic)  
The First Affiliated Hospital of Anhui Medical University, China

09/2006 - 9/2011                      Bachelor of Science in Medicine  
Anhui Medical University, China

### **School Education**

09/2003 - 09/2006                      The First High School of Wuwei County

09/2000 - 09/2003                      Junior School Sanxi

09/1994 - 09/2000                      Primary School Changtan

### **Scholarships & Awards**

07/2015 - 07/2017	China Scholarship Council (CSC)
09/2006 - 09/2011	National Encouragement Scholarship
09/2006 - 09/2011	First Class Scholarship of Anhui Medical University

## 13. Publication

### Publication

1. Yan, S. G., Woiczinski, M., Schmidutz, T. F., Weber, P., Paulus, A. C., Steinbruck, A., Jansson, V. & Schmidutz, F. 2017. Can the metaphyseal anchored Metha short stem safely be revised with a standard CLS stem? A biomechanical analysis. Int Orthop. (IF 2.520)

### Vortrag

1. Unterschiede des periprothetischen Knochenremodellings bei verschiedenen Kurzschaftprothesen: Ein systematisches Review  
Florian Schmidutz , Shuan G Yan, Patrick Weber , Arnd Steinbrück , Volkmar Jansson  
DKOU 2017
2. Lässt der Metha Kurzschaft sich sicher mit einem Standard Schaft revidieren? Eine Analyse der biomechanischen Primärstabilität und klinischer Vergleich  
F. Schmidutz, P. Weber, Y. Shuanggen, T. Schmidutz ,M. Woiczinski, V. Jansson  
DKOU 2016
3. Der methaphysär verankerte Metha Kurzschaft kann sicher mit einem CLS Standardschaft revidiert werden: Eine biomechanische Studie  
F. Schmidutz, Y. Shuanggen, M. Woiczinski, T. Schmidutz, P. Weber, V. Jansson  
VSOU 2016
4. Methaphysär verankerte Kurzschaft Implantate können sicher mit einem Standardschaft revidiert werden: Eine biomechanische Studie  
F. Schmidutz, Y. Shuanggen, P. Weber, T. Schmidutz , M. Woiczinski, V. Jansson  
VI. Münchener Symposium 2016

### Poster

1. Lässt sich der Metha Kurzschaft sicher mit einem CLS-Standard Schaft revidieren? Eine biomechanische Analyse der Primärstabilität und klinischer Vergleich  
F. Schmidutz, Y. Shuanggen, P. Weber, T. Schmidutz, M. Woiczinski , V. Jansson  
Endoprothetikkongress Berlin 2017
2. Can the metaphyseal anchored Metha short stem safely be revised with a standard CLS stem? A biomechanical analysis  
F. Schmidutz, Y. Shuanggen, P. Weber, T. Schmidutz, M. Woiczinski , V. Jansson  
European Orthopaedic Research Society (EORS) Munich 2017

## **14. Acknowledgment**

Thank my supervisor Prof. Dr. med. Dipl.-Ing. Volkmar Jansson, Direktor der Orthopädischen Klinik der Ludwig-Maximilians-Universität am Klinikum Großhadern, sincerely giving me the opportunity to perform my Doctorate thesis at his institute and under his supervision.

Grateful thanks go to my co-supervisors PD Dr. med. Florian Schmidutz and Dr.techn. Yan Chevalier for their precious assistances in my project. Their great support, mentorship and guidance have helped me in the successful completion of the doctoral project.

I also want to say thank you to the staffs in the Lab of Biomechanics and Experimental Orthopedics, Dr. rer. biol. hum. Matthias Woiczinski, Dipl.-Ing. Michael Kraxenberger, Dr. biol. hum. Oliver Betz, etc, for their enthusiasms to teach me patiently when I needed help.

I appreciate all the helps from warm-hearted staffs in department of Orthopaedics, Physical Medicine and Rehabilitation in the Grosshadern hospital of the University of Munich.

My appreciation also goes to my family for their continuous support and encouragement at all times in my study and daily life. I especially appreciate China Scholarship Council for her providing scholarship to me for my living and study.